3-31-2017

Phosphodiesterase-8 (PDE8) and the PDE8A-Raf-1 Kinase Signaling Complex Regulate CD4+ T Cell Motility and Autoimmune Inflammation In Vivo

Chaitali Purushottam Basole
University of Connecticut, basole@uchc.edu

Phosphodiesterase-8 (PDE8) and the PDE8A-Raf-1 Kinase Signaling Complex Regulate $CD4^+$ T Cell Motility and Autoimmune Inflammation *In Vivo*

Chaitali Purushottam Basole, PhD

University of Connecticut, 2017

Abstract

The levels of cAMP are regulated by phosphodiesterases (PDE), which are targets for the treatment of inflammatory disorders. The overarching goal of this study was to harness recent successful developments in PDE research for the treatment of experimental autoimmune encephalomyelitis (EAE) and ultimately human autoimmune diseases. We report here that PDE8A exerts its control of T cell function through the Raf-1 kinase signaling pathway. The highly PDE8-selective enzymatic inhibitor PF-04957325 significantly suppresses rolling and adhesion of *in vivo* MOG_{35-55} activated inflammatory $CD4^+$ T effector (Teff) cells while interacting with inflamed brain endothelial cells under shear flow conditions. Recently, PDE8A was shown to associate with Raf-1 creating a compartment of low cAMP around Raf-1 thereby protecting it from protein kinase A (PKA) mediated inhibitory phosphorylation. Disruption of the PDE8A-Raf-1 complex by disruptor peptide (DP) significantly reduces adhesion of Teff cells to endothelial cells. We further observed that disrupting PDE8A-Raf-1 through DP specifically reduces adhesion, spreading and locomotion of Teff cells while interacting with the vascular adhesion molecule ICAM-1. Our investigation of the effect of PDE8 inhibitor on chronic and relapsing-remitting (EAE) *in vivo* indicates suppression of

clinical and histopathological signs of disease. PDE8 inhibitor affects accumulation of $CD4^+$ T cells into the spinal cord. In addition, there is a reduction in pro-inflammatory cytokines TNF-α and IL-17 production in the spinal cord after PDE8 inhibition *in vivo*. Collectively, our studies demonstrate that PDE8A inhibition by enzymatic inhibitors or PDE8A-Raf-1 kinase signaling complex disruptors significantly decreases Teff cell adhesion and migration on endothelial cells, and represents a novel approach to treat autoimmune inflammation *in vivo*.

Phosphodiesterase-8 (PDE8) and the PDE8A-Raf-1 Kinase Signaling Complex Regulate $CD4^+$ T Cell Motility and Autoimmune Inflammation In Vivo

Chaitali Purushottam Basole

B.S Biotechnology, University of Pune, 2008

M.S Biotechnology, University of Pune, 2010

A Dissertation

Submitted in Partial Fulfillment of the

Requirements for the Degree of Doctor of Philosophy

at the

University of Connecticut

2017

APPROVAL PAGE

Doctor of Philosophy Dissertation

Phosphodiesterase-8 (PDE8) and the PDE8A-Raf-1 Kinase Signaling Complex Regulate $CD4^+$ T Cell Motility and Autoimmune Inflammation In Vivo

Presented by

Chaitali Purushottam Basole, B.S., M.S.

Major Advisor

_____

Dr. Stefan Brocke

Associate Advisor

_____

Dr. Robert B. Clark

Associate Advisor

_____

Dr. Paul M. Epstein

University of Connecticut

2017

ACKOWLEDGEMENTS

First and foremost, I want to thank my PhD advisor Dr. Stefan Brocke for all the support and encouragement that he gave me during these past five years. The scientific training that I have received in the laboratory has made my PhD experience productive and stimulating. I am also very grateful to him for his scientific advice, knowledge as well as many insightful discussions and suggestions. Dr. Brocke has also taught me to be better speaker by always helping me practice the talks and by providing feedback before oral presentations at seminars and conferences. I have really enjoyed working on the PDE8 project and being a part of the lab.

I would also like my PhD committee members Dr. Paul Epstein and Dr. Robert Clark. I truly appreciate their support during my dissertation research, and general advice they provided about academic writing, publishing, preparing presentations and career development. I would also like to thank my exam committee members Dr. Laurinda Jaffe and Dr. Guo-Hua Fong for their time and helpful suggestions during the final stages of my PhD.

Many thanks to the fantastic team I have been fortunate to work with over the years. The past and present members of the Brocke lab- Dr. Amanda Vang, Puja Billis, Rebecca Nguyen and Katie Lamothe have contributed immensely towards ongoing projects in the laboratory. I very much appreciate their patience, enthusiasm and willingness to do frequent flow chamber and flow cytometry experiments with me.

I gratefully acknowledge the funding from National Multiple Sclerosis Society, which has helped support our research.

A heartfelt thanks goes out to all of my friends who have provided support, motivation and made my time at UConn Health enjoyable.

Undertaking this Phd has been a truly life changing experience for me, and it would not have been possible without the support and encouragement that I received from my family. My heartfelt thank you to my parents and my dear sister Anagha for always believing in me and encouraging me to follow my dreams.

And finally I truly thank my loving, supportive husband Amod who has been by my side for the past two years and has helped me strive towards my goal. I really appreciate his support during the final stages of my PhD.

TABLE OF CONTENTS

LIST OF TABLES AND FIGURES

Chapter 1

Introduction

1.1 Steps in leukocyte migration into inflamed tissue

Circulating blood leukocytes need to migrate through activated venular walls into the lymphoid organs or the peripheral sites of infection, injury and stress in order to eliminate the inflammatory trigger and contribute to tissue repair. Original leukocyte cascade had three steps: rolling, chemokine triggered integrin activation and integrin dependent arrest. Recently added evidence in integrin activation, post-adhesion events and transendothelial migration has led to an expanded version of the original three step cascade. The updated cascade has the following events: rolling, adhesion strengthening, intraluminal crawling, paracellular/ transcellular migration and migration through the venule basement membrane (*1*).

A. Leukocyte rolling

The first step in leukocyte migration cascade is weak, transient adhesive interactions of circulating leukocytes with endothelial cells in the venule walls. This step is mediated by P select glycoprotein ligand 1 (PSGL-1) expressed on leukocytes and P- and E-selectins expressed on endothelial cells. L and P selectins require shear stress in order to support rolling and adhesion. Rolling cells detach when flow is stopped. Selectins have the catch bond characteristics, which make molecular bonds stronger when pulling force is applied. Shear stress (dyn/cm^2) is defined as the force (dyn) exerted by flowing blood on each unit area of endothelial surface (cm^2). This initial rolling interaction is stabilized by leukocyte microvilli flattening, long tethers at rear end and structures known as slings (*2*). α4β1 integrin and α4β7 integrin also mediate rolling while

interacting with vascular adhesion molecule 1 (VCAM-1) and mucosal vascular addressin cell adhesion molecule 1 (MADCAM-1) respectively. LFA-1 (lymphocyte function antigen 1) in intermediate affinity conformation also can support rolling step. E-selectin, LFA-1 integrin and MAC-1 (αMβ2) integrin mediate slow rolling in which cells roll in venules at a velocity of under 5 μm per second.

B. Leukocyte activation and arrest

Rolling stabilization facilitates engagement of leukocyte chemokine receptors and integrins with endothelial cell chemokines and ligands respectively ultimately leading to leukocyte arrest (*3*). Shear flow applied to the migrating leukocytes can increase leukocyte –endothelial cell contact by deforming the leukocyte and facilitating their exposure to chemokines displayed on endothelial cell surface (*4*). Two major adhesion molecule families important for leukocyte adhesion are β1 and β2 integrins. Leukocyte arrest on inflamed venules requires activation of one of the major integrins- LFA-1 (expressed on all effector leukocytes), VLA-4 (expressed on monocytes, eosinophils, effector T cells and B cells), MAC-1 (expressed on neutrophils and monocytes). Integrins can also be activated via outside - in signaling, independent of chemokines (*5*). Chemokines rapidly regulate integrin avidity by increasing both integrin affinity and valency of ligand binding. Chemoattractants trigger G protein couple receptor (GPCR) activation, which then stimulates inside out signaling leading to integrin activation on leukocytes by triggering complex intracellular signaling network within milliseconds (*6*). Integrin affinity corresponds to conformational changes in individual integrin heterodimer, which leads to decrease in rate of ligand dissociation. Inside out signaling induces transition of integrins from bent to intermediate to high affinity conformation

leading to opening of the ligand binding pocket. Valency corresponds to density of integrins per area of plama membrane involved in adhesion, which can be dependent on lateral mobility and cell surface expression level of integrins.

C. Intraluminal crawling

Post-arrest leukocytes can protrude and undergo trans-endothelial migration via paracellular endothelial cell junctions or crawl on the surface for exit cues. This crawling step is chemokine-GPCR mediated and integrin dependent process (*7*). Chemokine-GPCR mediated signaling lead to Gi protein mediated activation of guanine nucleotide exchange factors (GEFs). This in turn triggers activation of Rho family GTPases and Rap-1 GTPases and their downstream effector molecules leading to conformational activation of integrins and microclustering of ligand occupied integrins at various ventral focal points. Actin cytoskeleton reorganization to generate a protrusive leading edge and contractile uropod at the rear end, integrin recycling at the leading edge, polarized fusion of vesicles containing signaling molecules are the events mediating leukocyte crawling. Leukocytes use numerous millipede- like integrin molecules to scan the activated endothelial surface.

D. Trans-endothelial migration

In order to cross the blood vessel, the leukocytes have to pass through three distinct barriers- endothelial cells, venule basement membrane and pericytes (*5*). Leukocyte migration through endothelial cell take < 2-5 minutes, but penetrating the basement membrane can take between > 5-15 minutes. Leukocytes can cross the endothelium either by passing through the junctions between adjacent endothelial cells (paracellular route) or by passing through the endothelial cells (transcellular route). The paracellular

TEM is the route used by 70-90% leukocytes while the transcellular route is a relatively low frequency event (*8*). However, brain vascular endothelial cells utilize the transcellular route due to the specialized tight junctions, which restricts the paracellular route. Shear flow though restricts the initial recruitment at vascular site, positively regulates leukocyte transendothelial migration (TEM) across endothelium (*9*). Integrin mediated leukocyte adhesion leads to multiple changes in the endothelial cells such as ICAM-1 clustering, concomitant VCAM-1 recruitment to membranous structures, which facilitates leukocyte adhesion and TEM. Binding of leukocytes to their vascular ligands ICAM-1, VCAM-1 triggers downstream signaling in endothelial cells. These events include increase in intracellular Ca^{+2}, reactive oxygen species (ROS) generation, activation of p38 mitogen activated protein kinase (MAPK) pathway, tyrosine phosphorylation of endothelial junction molecules. These events can occur along side activation of RhoA GTPase and its downstream effector molecule Rho activated protein kinase (ROCK), which control actin cytoskeletal machinery as well as endothelial myosin light chain kinase. The breaching of the endothelial cells is regulated by major endothelial cell adhesion molecules: adherens junctions such as cadherins and tight junctions: junctional adhesion molecules (JAM), endothelial cell selective adhesion molecule (ESAM) and claudins. Vesiculo - vacuolar organelles (VVOs) - small membrane associated passageways, or channels formed by endothelial ligands can act as route for leukocyte passage via the transcellular route. Once leukocytes extravasate the endothelial cells, they still need to cross through the pericyte sheath and endothelial cells basement membrane (BM) in order to exit the venular wall. Pericytes are mural cells that form second layer of the venules, and are found in a

discontinuous manner wrapped around endothelial cells and embedded in venule BM. Pericytes express adhesion molecules, chemokines, receptors for pro-inflammatory molecules which aid in the leukocyte trafficking.

Treatment with anti-α4 integrin antibody has been shown to treat EAE and prevent accumulation of leukocytes in the CNS in EAE (*10, 11*). Natalizumab – an antibody against the α4 subunit of VLA-4 reduced the development of brain lesions in MS patients and is now an approved therapy for treating patients with MS (*12, 13*). This suggests that drugs that inhibit migration of inflammatory leukocytes into the CNS can be effective in treating inflammatory disease.

1.2 Role of cAMP and Phosphodiesterases (PDEs) in T cells

cAMP signaling is known to inhibit T cell activation, proliferation and cytokine release (*14-16*). Activation of Gs protein coupled receptors via ligands such as prostaglandins, adenosine, catecholamines and histamines results in accumulation of intracellular cAMP and leads to suppression of immune responses in vitro and in vivo (*17, 18*). PDE are the only known enzymes that are able to hydrolyze and hence maintain spatial and temporal control over formation of cAMP gradients within a cell (*19, 20*). PDEs are divided into 11 different gene families based on their specificity for cAMP or cGMP, structural similarity and mode of regulation (*21*). Specific PDE forms induced in activated lymphocytes are PDE1, PDE3, PDE4, PDE7 and PDE8 (*16, 22-25*). Out of these, PDE3, PDE4B and to a lesser extent PDE7A are the major forms of PDE expressed in activated T cells (*26*). The PDE4 inhibitor - rolipram has been used to ameliorate clinical signs of experimental autoimmune encephalomyelitis (EAE) models

and reduce CNS inflammation when treatment is started after immunization or after onset of disease (*27, 28*). PDE3 inhibitors alone are ineffective at treating Th1 mediated disorders. But PDE4 inhibitor and low doses of PDE3 inhibitors - cilostamide in combination synergistically inhibit T cell proliferation and pro-inflammatory cytokine production of human cells (*26*). PDE7 inhibitors have proved ineffective in suppressing T cell proliferation and mice deficient in PDE7A have functional T cells (*29, 30*). But PDE7 inhibitors when used in combination with PDE4 inhibitors show an additive effect (*31*)**.** These reports suggest that probably there might be other PDEs expressed in T cells that might be important for controlling T cell function. Our previous work has shown that PDE8 is important for chemotaxis of T cells, adhesion of T cells to endothelial cells and breast cancer cell motility (*24, 32, 33*). PDE8 has a very high affinity for cAMP with a km value in the range of 40-150 nM (40 fold higher than that of PDE4) and hence might function at lower cAMP concentrations than PDE4 (*34*). PDE8A is insensitive to inhibition by the non-specific PDE inhibitor IBMX but is inhibited by the PDE inhibitor dipyridimole (DP) (IC_{50} in the range of 4- 9 μM) (*21*).

The similarities in the sequence and structural properties of the catalytic domains of PDEs imply that family specific PDE inhibitors that target the human PDE forms are likely to have the same potency in the corresponding mouse PDE (*35, 36*). We were the first to report the novel PDE8 inhibitor PF-04957325 (*24*). The effect of PDE8 inhibitor on chronic inflammation models has not been tested to date. To date, none of the PDE inhibitors have been approved for MS treatment. Rolipram failed to treat MS patients and also had adverse effects such as emesis at therapeutically relevant doses (*21, 37*).

1.3 Phosphodiesterase 8 (PDE8)

The more recently discovered PDE8 family, encoded by the PDE8A and PDE8B genes, is characterized by high affinity and specificity for cAMP. The human PDE8A gene is located on chromosome 15q25.3 and PDE8B is located on chromosome 5q13.3. PDE8 has high affinity for cAMP (K_M = 40-150 nM). This means that PDE8 is able to metabolize cAMP at basal conditions or in cellular compartments where low levels of cAMP need to be maintained. The human PDE8 lacks the nuclear localization sequence that is present in the mouse PDE8. Thus it may localized in the cytosol or to the membrane due to the presence of sites for myristoylation. Cloning and characterization of cAMP-specific PDE8A and B were first reported in 1998 (*34, 38, 39*). Subsequently, Wang et al. cloned cDNAs representing five full-length human phosphodiesterase (PDE) 8A splice variants (PDE8A 1–5) from testis and T cells (*40*) (Table 1). Five variants have been identified for variants for PDE8B (PDE8B 1-5) (*41*) (Table 2). The PDE8A1 and PDE8A2 isoforms are most abundantly expressed in various tissues. Structurally, PDE8 is hydrophilic protein containing an N-terminal REC domain, a PAS domain, and a C-terminal catalytic domain (Fig. 1). The function of PAS (Per, Arnt and Sim) domain in PDE8 is currently unknown although its role in lower eukaryotic organisms has been identified. The PAS domain is important in protein-protein interaction and small molecule ligand binding. Overexpressed recombinant PDE8A in HEK cells interacts with IκB protein via its PAS domain and this interaction increases the activity the PDE8A *in vitro* (*42*). PDE8A mutants with deleted PAS domains have 6-fold lower activity, which indicates a regulatory role for PAS domains in PDE8A. The REC (Receiver) domain are present exclusively in the human PDE8

gene among all the mammalian PDEs. REC domain are involved in signal transduction in the bacterial two component system. More studies are needed to explore the role of PAS and REC domains in PDE8 regulation. Under elevated cAMP conditions, PDE8A is phosphorylated by PKA on serine 359 and this enhances activity of the enzyme (*43*). cGMP- and cAMP dual substrate PDE3B and cAMP-specific PDE4A, 4B, 4D, 7A1, 7A3 and 8A1 are PDE isoforms expressed in T cells (*15, 23, 24, 44*). Work from Beavo lab has shown that human PDE8A1 mRNA and protein levels is increased in CD3 and CD28 stimulation (*23*). Previous work from our lab has also shown that PDE8A expression in activated $CD4^+$ T cells *in vitro* and *in vivo (24).*

1.4 Compartmentalized signaling

Distinct, non-overlapping intracellular cAMP signaling compartments within a cell comprise of scaffolding proteins, cAMP effector proteins and PDEs. Each of this signaling compartment controls different cAMP regulated functions and targeting PDEs within these unique signaling complexes rather than the targeting the specific PDE gene family will be much more potent and effective treatment option. One example of this is the FAK/RACK1/PDE5D5 direction- sensing complex in invasive cancer cells specifically localizes to nascent integrin adhesions and leading edge of polarizing cells (*45*). PDE8A has been shown to interact with Raf-1 kinase without the need for accessory proteins or lipids and protect it from PKA mediated inhibitory phosphorylation (*46*). Hence we will explore the role of this complex in $CD4^+$ T cells.

1.5 ERK (extracellular signal regulated kinase) signaling pathway

Extracellular signal regulated kinases (ERK) are a part of the mitogen- activated protein (MAP) kinases family. MAP kinases are activated in response to growth factors, integrins, G-protein coupled receptors as well as other receptor tyrosine kinases and thus involves sequential recruitment of the kinases Raf, MEK and ERK (*47*). The Raf family consists of three serine/threonine kinases: A-Raf, B-Raf and C-Raf/Raf-1. Raf is recruited to the membrane by the GTPase Ras and gets activated due to dephosphorylation and phosphorylation events by phosphatases and kinases respectively. Activated Raf further phosphorylates and activates MEK, which in turn phosphorylates and activates ERK. The activated ERK translocates to the nucleus and can phosphorylate a wide range of substrates with divergent functions. B-Raf has been demonstrated to regulate VLA-4 integrin mediated adhesion in human T cells under shear stress. The ERK MAPK pathway has been shown to be important in regulating adhesion, spreading and cell migration (*48, 49*).

1.6 Cross talk between cAMP and ERK signaling pathways

The protein kinase Raf was the first protein identified to be involved in the cross talk between the two signaling pathways (*50*). Raf-1 is inhibited by protein kinase A mediated phosphorylation at Serine 259 (*51*). However elevated cAMP levels can lead to B- Raf activation which in turn activates ERK. Studies indicate that B-Raf mediated activation of ERK occurs via the G protein Rap-1. Protein tyrosine phosphatases (PTP) are able to dephosphorylate and deactivate ERK and hence are another point of cross talk between cAMP and ERK pathways. PKA - mediated phosphorylation of ERK2 docking site of PTP ablates the docking of PTP and thus attenuates the

dephosphorylation of ERK. cAMP phosphodiesterases also are regulated by ERK and PKA. PDE4 long forms possesses two regulatory modules called UCR1 (upstream conserved region 1) and UCR2 located between the N terminal region and catalytic unit. The PDE4 short forms possess only UCR2 whereas PDE4 super short forms consist of a truncated form of UCR2. The UCR1 region contains the PKA serine phosphorylation site. For example: PDE4B, 4C and 4D long forms can be inhibited approximately 80% by ERK mediated phosphorylation at specific motifs located in their catalytic region. This provides a feedback loop where the inhibition of PDE4 by ERK causes a rise in cAMP levels leading to activation of PKA, which then phosphorylates PDE4 to overcome the ERK - mediated inhibition. However, ERK mediated phosphorylation of PDE4 short isoforms leads to PDE4 activation, whereas ERK phosphorylation of PDE4 super short forms has minimal inhibitory effect due to the absence of PKA target sites.

1.7 Exploring PDEs as treatment avenues in inflammatory diseases

Early studies on characterization of PDEs in human lymphocytes had shown them to be excellent targets for producing anti-inflammatory effects with PDE4 the predominant form expressed (*52*). But bringing PDE4 inhibitors into the clinics faced decades of challenges, mostly due to emetic side effects. However, the approval and clinical use of PDE inhibitors for the treatment of major human inflammatory disorders has now finally made tremendous progress over the last 6 years with indications expanding at an almost yearly pace. A potent and selective PDE4 inhibitor, roflumilast, was developed and became the first PDE4-selective inhibitor to be approved. It was approved for

treatment of chronic obstructive pulmonary disease, first in the European Union in 2010, where it is marketed under the name Daxas, and then by the US FDA in 2011, marketed under the name Daliresp (*53, 54*). Subsequently another oral PDE4 inhibitor, apremilast, developed by Celgene and marketed under the name Otezla, was approved by the US FDA in 2014 for the indications of psoriatic arthritis and plaque psoriasis (*55-63*). And in December 2016, another PDE4 inhibitor, crisaborole, developed by Anacor, since acquired by Pfizer, was approved as a topical treatment for atopic dermatitis (*64-70*). There is currently intense further interest and activity in the development of PDE4 inhibitors both for treatment of inflammation as well as other indications. Additionally, selective inhibitors of other PDE gene families are also seeing widespread use for various indications. The PDE5 inhibitors, sildenafil (Viagra), vardenafil (Levitra), tadalafil (Cialis) and avanafil (Strenda) for the indications of erectile dysfunction, pulmonary hypertension and benign prostate hypertrophy, and the PDE3 inhibitors, cilostazol (Pletal) for intermittent claudication and milrinone (Primacor) for heart failure. Hence PDE inhibitors are proving to be of great clinical benefit.

1.8 Hypothesis and Aims of the project

Our overarching goal is to harness recent successful developments in PDE research for the treatment of autoimmune disease. **After decades of research characterized by little progress and disappointing initial clinical results, considerable breakthroughs in PDE inhibitor therapy have finally been achieved.** Using small molecule inhibitors or signaling complex disruptors, the proposed studies will elucidate the role the PDE8 and PDE8A-Raf-1 kinase complex in controlling inflammation and regulating Teff cell functions. This should ultimately lead to the identification of previously unrecognized drugable targets and potential development of novel therapeutic approaches to treat multiple sclerosis (MS) and other inflammatory diseases. **Our central hypothesis is that inhibition of PDE8 expressed in activated Teff cells is capable of suppressing migration of these pathogenic cells into the CNS, while maintaining Treg cell migration and function.** Our goal is to further explore the potential of PDE8A as an anti-migratory therapy to treat T cell mediated diseases. This would have a very significant impact on the treatment of MS and will also define new treatment avenues for this disease. Additionally, we will test whether the known limitations of PDE4 inhibition can be overcome by combination treatment of targeting PDE8 and PDE4 through a combination of signaling disruptors and experimental and approved PDE family selective inhibitors as well as PDE inhibitors with dual specificity. Our work would take advantage of recent major successes of PDE targeted treatments in human inflammatory diseases and successful results of these studies would reinvigorate PDE research in MS and provide novel highly therapeutic treatments for this disease.

Specific Aim 1: **Evaluating the role of PDE8 and the PDE8A-Raf-1 signaling complex in regulating $CD4^+$ T cell motility.**

In this aim we examined the role of PDE8 and PDE8A-Raf-1 complex in controlling T cell adhesion in a functional assay under physiological shear flow conditions using the flow chamber model.

Sub Aim 1a] To study the effect of the PDE8 enzymatic inhibitors and PDE8A-Raf-1 complex disruptor peptide on interaction of activated Teff cells and Treg cells with LPS - activated brain endothelial cells.

In collaboration with Pfizer Inc. our lab was the first to report a potent and novel PDE8 inhibitor PF-04957325, which is now widely used to study PDE8 function [10]. PF-04957325 inhibits PDE8A with an IC50 of 0.0007 μM. This aim was studied using the flow chamber assay which simulates the physiologic shear flow conditions and enables us to monitor the interaction of activated T effector cells (Teff cells) with endothelial cells [14]. In order to distinguish between the effect of the inhibitors or complex disruptors on Teff cells versus Tregs cells, we utilized the *Foxp3gfp*.KI mice (*71*).

Sub Aim 1b] To study the effect of inhibition of PDE8 activity or PDE8A-Raf-1 complex disruption on interaction of integrins expressed on T cells with immobilized vascular ligands *in vitro* using the flow chamber assay

We have investigated whether interaction of the VLA-4 or LFA-1 integrin with their vascular ligands- vascular cell adhesion molecule 1 (VCAM-1) and intercellular adhesion molecule (ICAM-1) respectively is primarily affected by inhibition of PDE8 activity or the PDE8A-Raf-1 kinase complex disruptor.

Specific Aim 2: Studying the role of PDE8 and PDE8A-Raf-1 complex in regulating ERK/MAPK signaling in TCR stimulated $CD4^+$ T cells.

PDE8A has been reported to interact with Raf-1 and protect it from inhibitory phosphorylation by PKA at S259 in HEK cells and also regulate downstream ERK signaling (*46*). In this aim, we have tested whether PDE8 and PDE8-Raf-1 complex regulates ERK signaling using western blot technique. Chapter 3 addresses the answers to the Aims 1 and 2 using the flow chamber assay and western blotting respectively.

Specific Aim 3: To determine the therapeutic potential of targeting PDE8 in treating autoimmune inflammation *in vivo*.

After exploring the PDE8 mediated regulation of $CD4^+$ T cell motility *in vitro*, we have further tested whether targeting PDE8 can suppress EAE clinically and reduce accumulation of inflammatory cells in the CNS. Further we also analyzed whether $CD4^+$ T cells subtypes (Th1/Th17 cells), as well as TNF-α, IL-17, IFN-γ and IL-10 cytokine production is affected by inhibition of PDE8. Chapter 4 addresses the questions in Aim 3 in the EAE model.

Sub aim 3a] To test the effect of the PF-04957325 on treating chronic and relapsing remitting (RR) EAE. MS is a chronic inflammatory demyelinating disease of the central nervous system (CNS). The pathologic features of the disease are by white and grey matter lesions with myelin, oligodendrocyte and neuroaxonal loss (*72*). It is generally accepted that the disease is initiated by breakdown of the blood brain barrier and trafficking of T cells into CNS leading to attack on CNS tissue and formation of lesions (*73, 74*). These MS plaques are characterized by the presence of $CD4^+$ T cells,

$CD8^+$ T cells, B cells and macrophages (*75*). Experimental autoimmune encephalomyelitis (EAE) is the animal model of MS used to study the underlying inflammatory and autoimmune mechanism as well as for evaluation of pharmacotherapies (*12*). EAE can be induced by either active immunization with protein/peptide or by passive transfer of encephalitogenic T cells (*76*). CD4+ T helper type 1 cells (Th1 cells) and the IL-17 producing CD4+ T cells (Th17 cells) are important for disease initiation and inflammation in EAE (*73*). Classical EAE is characterized by ascending tail paralysis beginning at the tail followed by hind limb paralysis and fore limb paralysis. In this aim we explored the therapeutic effect of targeting PDE8 *in vivo* in mice once they show clinical signs of disease.

Sub aim 3b] To test whether targeting PDE8 suppresses accumulation of immune cells and inflammation in the CNS. In order to test whether our hypothesis that PDE8A regulates $CD4^+$ T cell adhesion holds true *in vivo*, we tested whether inhibition of PDE8 in T cell mediated disease leads to suppression of $CD4^+$ T cells into the CNS in a T cell mediated autoimmune disease - EAE. Also since PDE8 is expressed at lower levels in Treg cells compared to Teff cells, hence the treatment might have a selective effect on Teff cells and not Treg cells migration into the CNS. We have done histological analysis of the brains and spinal cord of EAE mice as well as used flow cytometry approaches to evaluate infiltrates accumulating in the after treatment with the PDE8 inhibitor PF-04957325. We have also used flow cytometry to evaluate effect of PDE8 inhibition in Th17 cells, Th1 cells as well as the immunoregulatory IL-10 producing Treg cells.

Sub aim 3c] Assess the effect of the PF-04957325 on peripheral lymphoid organs.

We have done similar flow cytometry analysis of the cervical lymph nodes, draining inguinal lymph nodes and spleen.

Figure 1.1

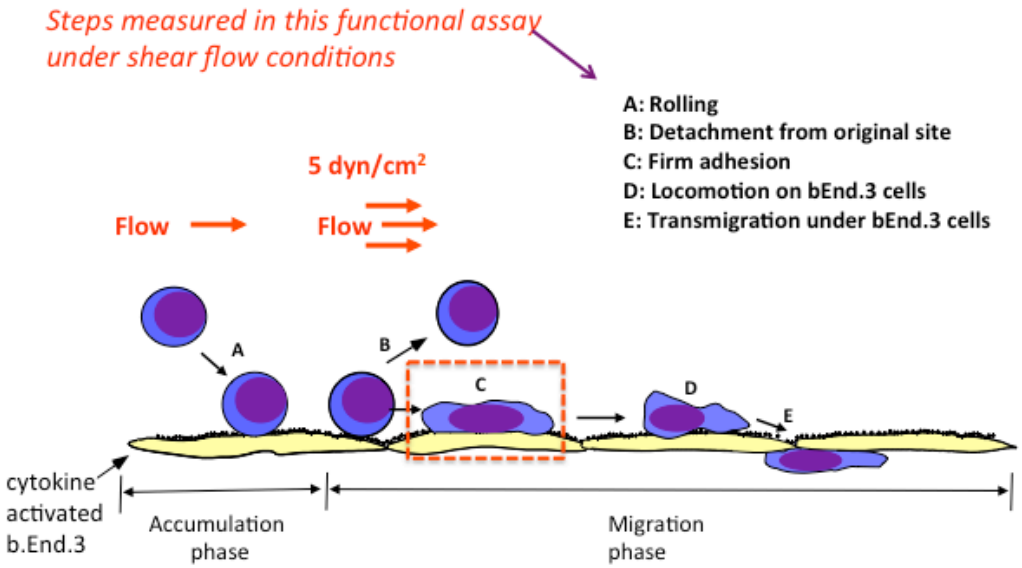

Figure 1.1. Leukocyte recruitment under shear flow conditions in the flow chamber assay (*9*).

Diagram depicts the various steps of T cells interaction with brain endothelial cells under physiological shear flow conditions *in vitro* in the flow chamber assay.

Figure 1.2

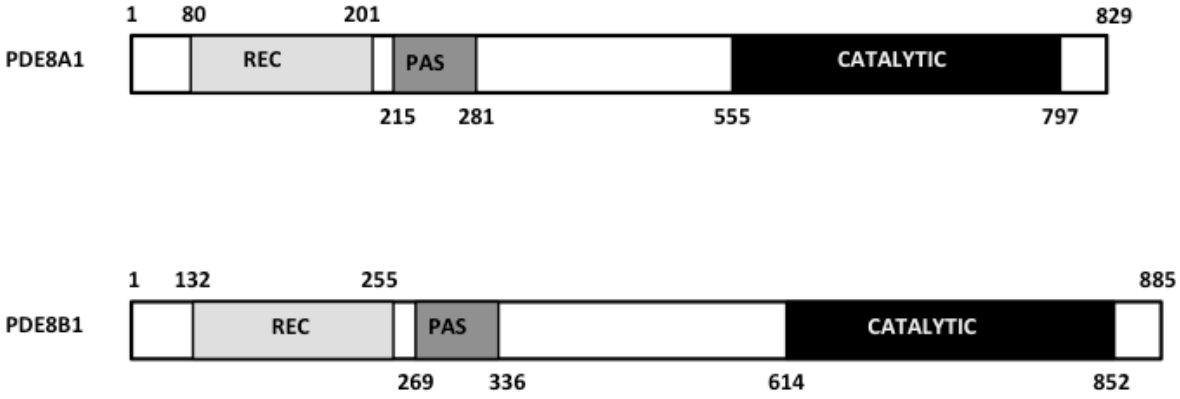

Figure 1.2. Schematic representation of structures of human PDE8A1 and PDE8B1 cDNA (*41*).

Table 1.1 PDE8A splice variants (*40*)

PDE8 splice variant	Amino acid residues	Molecular weight (kDa)	Exons lacking
PDE8A1	829	93.3	
PDE8A2	783	88.3	Exon 8-9, missing PAS domain
PDE8A3	449	51.2	Exons -7-9, lacks PAS domain
PDE8A4	582	66	Exons 7-8, lacks second half of PAS domain
PDE8A5	582	66	Has all 23 exons, Insertion of 198 nucleotides

Table 1.2 PDE8B splice variants (*41*)

PDE8 splice variant	Amino acid residues	Molecular weight (kDa)	Exons lacking
PDE8B1	885	99	
PDE8B2	838	93.7	Exons 8, missing part of PAS domain
PDE8B3	788	88	Exons 8-10, lacks PAS domain
PDE8B4	865	96.8	Exon 2
PDE8B5	830	93	Exon 12, hence missing region between PAS domain and catalytic area.

Chapter 2

Differential expression and function of PDE8 and PDE4 in effector T cells: Implications for PDE8 as a drug target in inflammation

2.1 Summary

Abolishing the inhibitory signal of intracellular cAMP is a prerequisite for effector T (Teff) cell function. The regulation of cAMP within leukocytes critically depends on its degradation by cyclic nucleotide phosphodiesterases (PDEs). We have previously shown that PDE8A, a PDE isoform with 40-100-fold greater affinity for cAMP than PDE4, is selectively expressed in Teff versus regulatory T (Treg) cells and controls $CD4^+$ Teff cell adhesion and chemotaxis. Here, we determined PDE8A expression and function in $CD4^+$ Teff cell populations *in vivo*. Using magnetic bead separation to purify leukocyte populations from the lung draining hilar lymph node (HLN) in a mouse model of ovalbumin-induced allergic airway disease (AAD), we found by Western immunoblot and quantitative (q)RT-PCR that PDE8A protein and gene expression are enhanced in the $CD4^+$ T cell fraction over the course of the acute inflammatory disease and recede at the late tolerant non-inflammatory stage. To evaluate PDE8A as a potential drug target, we compared the selective and combined effects of the recently characterized highly potent PDE8-selective inhibitor PF-04957325 with the PDE4-selective inhibitor piclamilast (PICL). As previously shown, PF-04957325 suppresses T cell adhesion to endothelial cells. In contrast, we found that PICL alone increased firm T cell adhesion to endothelial cells by approximately 20% and significantly abrogated the inhibitory effect of PF-04957325 on T cell adhesion by over 50% when cells were co-exposed to PICL and PF-04957325. Despite its robust effect on T cell adhesion, PF-04957325 was over

two orders of magnitude less efficient than PICL in suppressing polyclonal Teff cell proliferation, and showed no effect on cytokine gene expression in these cells. More importantly, PDE8 inhibition did not suppress proliferation and cytokine production of myelin-antigen reactive proinflammatory Teff cells *in vivo* and *in vitro*. Thus, targeting PDE8 through PF-04957325 selectively regulates Teff cell interactions with endothelial cells without marked immunosuppression of proliferation, while PDE4 inhibition has partially opposing effects. Collectively, our data identify PF-04957325 as a novel function-specific tool for the suppression of Teff cell adhesion and indicate that PDE4 and PDE8 play unique and non-redundant roles in the control of Teff cell functions.

2.2 Introduction

The second messenger cyclic adenosine monophosphate (cAMP) regulates a broad range of biological functions, including the maintenance of immune tolerance (*77*). cAMP controls the immune response mainly through activation of cAMP-dependent protein kinase A (PKA) which suppresses activation and function of effector T (Teff) cells (*16, 18, 20, 77, 78*). Recently, we and others have also determined a role for exchange protein activated by cAMP (Epac) in this process (*79, 80*). Formation of site- and function-specific cAMP gradients and spatially distinct signals within cells critically depend on degradation by phosphodiesterases (PDEs), a family of enzymes that hydrolyze cAMP. As a consequence of selective expression and signaling complex formation of PDEs, cAMP signaling is compartmentalized in cells (*19, 81-83*). This allows specific PDE isoforms to control distinct cellular functions. Altered expression and positioning of particular PDE isoforms may affect cell and tissue function and lead to pathology. While PDE enzymes are encoded by 21 different genes, 11 gene families (PDEs 1-11) are currently noted based on sequence similarities and biochemical properties and functions (*21, 84-87*). Several transcription initiation sites and alternative splicing contribute to the formation of over 100 different forms of PDEs (*21, 84-87*).

Based on the unique roles of individual PDEs, selective PDE inhibition by drugs is considered an attractive approach to modulate cell and tissue function. Due to their importance in governing subcellular temporal distribution of cyclic nucleotides, and their accessibility to potent small molecule inhibitors, PDEs make excellent drug targets, including in diseases associated with chronic inflammation (*88-91*).

PDE4, PDE7 and PDE8 enzymes are cAMP-specific PDEs expressed in T cells (*21*). After many years of preclinical development, two novel PDE4 inhibitors have recently been approved for clinical use in chronic obstructive pulmonary disease (COPD) and psoriatic arthritis (*56, 59, 92-94*). These successes prompted the preclinical development of numerous novel PDE4 inhibitors being tested as potential therapies in a wide range of inflammatory disorders. Since PDEs have different expression and functional profiles in different cell and tissues, a major goal is to selectively inhibit additional PDE families that are expressed in T cells in the hope that distinct and targeted therapeutic activity can be achieved without the side effects associated with PDE4 inhibitors. Previous studies indicated that the high affinity isoforms PDE7A and PDE8A are required for full T cell activation (*15, 23*). The more recently discovered PDE8 family, encoded by the PDE8A and PDE8B genes, is characterized by high affinity and specificity for cAMP. As we and others have shown, PDE8A is important in immune processes such as T cell activation, effector T cell adhesion and chemotaxis (*24, 32, 79*) as well as breast cancer cell motility (*33*). Until recently, pharmacological approaches to studying PDE8 function have been hampered by the lack of suitable inhibitors. Selective inhibitors of PDE8 enzymes were not available and PDE8 is insensitive to the broad methylxanthine based PDE inhibitors such as 3-isobutyl-1-methylxanthine (IBMX). The broad PDE inhibitor dipyridamole (DP) was the only compound known to inhibit PDE8 enzymes, and its inhibition of these enzymes was somewhat weak (IC_{50} = 4-40 μM) (*21*). In 2010, we were the first to report a potent and selective PDE8 inhibitor developed by Pfizer Inc., PF-04957325, that is now widely used to study PDE8 function *in vitro* and *in vivo* (*24, 46, 95-97*). Our work showed that

inhibition of PDE8 with PF-04957325 suppresses two major T cell integrins and firm attachment of effector $CD4^+$ T (Teff) cells to endothelial cells (*24*). Further, treatment of mice with PF-04957325 *in vivo* ameliorates the signs of experimental encephalomyelitis without the side effects associated with PDE4 inhibitor treatment (Basole and Brocke, unpublished results).

To further delineate the specific functions of PDE8 selective inhibition in T cells and to explore the therapeutic potential of targeting PDE8, we probed its function by direct comparison of PDE8 inhibition to a PDE4 selective inhibitor with comparable potency, and to analyze PDE8 expression in immune responses *in vivo* utilizing a bi-phasic murine model of ovalbumin (OVA)-induced allergic airways disease (AAD).

2.3 Results

Selective expression of PDE8A in $CD4^+$ versus $CD4^-$ T cells in inflammation *in vivo*

We previously determined the expression of PDE8A in Teff and Treg cells *in vitro* and *in vivo* after challenge with antigen (*24, 79*). Of note, PDE8B expression has not been detected in T cell populations (*32, 39, 53*). To address the question of whether PDE8 is a potential target for the therapeutic use of selective inhibitors in a T cell mediated inflammatory disease, we analyzed PDE8 expression in lymph nodes of mice challenged with OVA-AAD (*98*). Research over the last three decades has provided evidence that T helper 2 (Th2) $CD4^+$ T cells are a major contributor to the development of AAD in animals and asthma in humans. Using a biphasic ovalbumin (OVA)–induced murine model of AAD (*98*), in which resolution occurs with long-term continuous antigen challenge, we separated HLN cells draining the lung tissue at different time points after AAD induction by OVA aerosol exposure (day 3, 7 and 42) into $CD4^+$ from $CD4^-$ fractions by magnetic bead technique and determined the expression of PDE8A in these cell populations by Western immunoblot. We found that expression of PDE8A protein was higher in $CD4^+$ T cells as compared to the $CD4^-$ LNC population at day 7 and 42 after AAD induction in HLN (Figure 2.1 A, B). This was not seen in ILN cell populations (Figure 2.1 C, D). Collectively, these data suggest that PDE8A protein abundance is higher in the HLN $CD4^+$ T cell population than in the HLN $CD4^-$ cell population at the acute intermediate and later stage of AAD. In contrast, in both HLN and ILN, PDE8A protein expression was lower in $CD4^+$ T cells as compared to the $CD4^-$ LNC population at the early acute stage of AAD on day 3 (Figure 2.1). Of note, this

selective expression pattern was not seen with PDE4B isoforms (data not shown). In contrast to protein expression, the highest of *pde3b, pde4b, pde7a* and *pde8a* genes in the $CD4^+$ T cell fractions from HLN were at day 3 of AAD induction (Figure 2.2). Taken together, overall expression levels of *pde3b*, *pde4b, pde7a* and *pde8a* genes were higher during the acute AAD phase (day 3 or day 7 of the OVA challenge) than at the tolerance (day 42 of OVA challenge) stage of the disease model.

Opposing effects of PDE8 and PDE4 inhibition on T cell adherence to endothelial cells *in vitro*

Functionally, by using the inhibitor DP that inhibits a broad range of PDEs including PDE8 and the recently developed potent and highly PDE8-selective inhibitor PF-04957325 (IC_{50} = 0.0007 μM for PDE8A and < 0.0003 μM for PDE8B), we demonstrated unique effects of PDE8 inhibition on adhesion and chemotaxis of activated T cells (*24*). PDE4 inhibition alone was ineffective in both assay systems. In previous experiments, we repeatedly detected a trend of increase of T cell blast adhesion to endothelial cells and chemotaxis when cells were treated with the highly selective and potent PDE4-selective inhibitor PICL. Therefore, we examined here the effect of combined inhibition of both the PDE4 and PDE8 families which has never been tested. As seen before, DP and PF-04957325 significantly inhibit T cell adhesion in these assays. PF-04957325 had an inhibitory effect on T cell blast adhesion to the endothelial cell line b.End3 by 57% and 29% at 1 μM and 0.1 μM, respectively (Figure 2.3) (*$p<0.05$, **$p<0.001$; one-way ANOVA and Bonferroni t-test). Of note, DP and PF-04957325 were the only compounds that significantly suppressed T cell adhesion. In

contrast, the broad PDE inhibitor IBMX - which does not inhibit PDE8 – only marginally suppressed adhesion of activated T cells to b.End3 cell. Importantly, PICL, a highly potent PDE4 selective inhibitor, reversed the inhibitory effect of PF-04957325 at 1 μM from 57% to 21% when used in combination (Figure 2.3) (*p<0.05; one-way ANOVA and Bonferroni t-test). These results clearly establish opposing effects, including partial reversal, of PDE8 versus PDE4 inhibition on rapid T cell adhesion *in vitro*, a conclusion which is additionally supported by PICL enhancing adhesion to 21% above the DMSO control when acting alone (Figure 3) (*p<0.05; one-way ANOVA and Bonferroni t-test).

Differential potency of PDE8 and PDE4 inhibition on T cell proliferation *in vitro* and *ex vivo*

Our results on adhesion are notable since in proliferation studies, PICL was significantly more efficient at suppressing Teff cell proliferation compared to PF-04957325 indicating a selective effect of PDE8 inhibition on rapid T cell adhesion to endothelial cells. To further probe the selectivity of PDE8 action in the control of T cell function, we examined the single and combined effect of broad and selective inhibitors on purified Teff cell proliferation in response to polyclonal or antigen-specific stimulation through the T cell receptor (TCR) (Figure 2.4). Isolated Teff cells were stimulated with immobilized anti-CD3 mAbs in the presence of broad and selective PDE inhibitors over a range of concentrations alone and in combination in order to establish a dose-response. The PDE4-selective inhibitor PICL was over 100-times more effective in suppressing Teff cell proliferation than PF-04957325 (compare 1 μM PF-04957325 versus 0.01 μM PICL, Figure 2.4). There was a slight additional effect when both inhibitors were combined,

whereas the opposing effects seen in the adhesion assays (Figure 2.3) were not observed in any of the proliferation experiments (Figure 2.4).

Additionally, we tested *in vitro* recall stimulation of T cells from lymph nodes of mice immunized with an encephalitogenic peptide, $MOG_{35-55,}$ of the myelin antigen MOG which is an autoantigen in EAE and MS (*99, 100*). In these assays, in contrast to experiments with anti-CD3 stimulation, antigen presenting cells are present during the entire experiment. As shown in Figure 2.5, proliferation was not inhibited by PF-04957325 application *in vivo* (Figure 2.5 A) or *in vitro* (Figure 2.5 B). In contrast, PICL profoundly inhibited the proliferation in response to MOG_{35-55} *in vitro* (Figure 2. 5B), similar to the effect seen in anti-CD3 responses (Figure 2.4).

2.4 Discussion

PDE enzymes are highly successful drug targets for treating vascular and inflammatory diseases (*85, 91*). The ability to form site- and function-specific cAMP gradients within the cell critically depends on its degradation by PDEs which are pivotal regulators of intracellular cAMP activity (*19, 81-83*). Observations that inhibition of PDE4, an abundantly expressed PDE in T cells, blocks T cell activation and function through elevating cAMP, prompted the development of PDE4 inhibitors as potential immunosuppressive therapies (*21, 92, 93, 101, 102*). After years of research and development of numerous candidate compounds, the FDA approval of the PDE4 inhibitors roflumilast and apremilast in 2011 and 2014 for the treatment of COPD and psoriatic arthritis represent important breakthroughs for the use of PDE inhibitors in the therapy of human inflammatory disorders. Due to the limitations of PDE4 inhibitors set by their narrow therapeutic window, several alternative strategies are pursued to target PDEs in immune diseases. These include the inhibition of different cAMP-specific PDEs, such as PDE7 and PDE8. The recent development of the new PDE8 inhibitor PF-04957325 has helped to identify PDE8 as a novel target for suppression of effector T cell functions due to the important role of the PDE8 family in regulating cAMP signaling in these cells (*91*). After the initial observation that PDE8A is expressed in T cells, several reports documented the role of PDE8 in controlling T cell and cancer cell motility (*23, 24, 32, 33, 79*). Together, PDE7 and PDE8 are now seen as new emerging targets to treat inflammation (*91*). Our data demonstrate for the first time robust PDE8A expression in leukocytes associated with an inflammatory disease *in vivo*, a mouse model of AAD. The preferential expression of PDE8A protein in the $CD4^+$ T cell subset

during the acute AAD stage and its subsequent recession in the non-inflammatory tolerant stage, together with the common assumption that $CD4^+$ Teff cells are a major contributor to the development of AAD in animals and asthma in humans, strengthen the case to further examine PDE8A inhibition in preclinical and clinical studies of inflammatory disorders, including human respiratory airway diseases.

Previously, we failed to detect any suppressive effect of the highly potent PDE4-selective inhibitor PICL on T cell adhesion to activated endothelial cells. In contrast, DP reduced adhesion of T cell blasts by 73% while PF-04957325 reduced adhesion by a maximum of 53%. However, PICL was also very efficient at suppressing proliferation. Thus, our data suggest that a rapid effect on T cell adhesion critically depends on a PDE inhibitor that blocks PDE8 enzymatic activity, while inhibition of Teff cell proliferation is less dependent on blocking the PDE8 isoform. In this present study, we explored the precise action of PDE8 and PDE4 selective inhibition of T cell adhesion by testing inhibitors over a range of concentrations and in combination. In doing so, we found an entirely novel effect of PDE4 inhibition enhancing adhesion of T cells to endothelial cells and opposing the inhibitory effect of PDE8 inhibition. These data suggest distinct signaling pathways utilized by PDE8 and PDE4 in T cells, a hypothesis further supported by the differential action of selective inhibitors of these enzymes in proliferation assays.

At present, it is unknown what accounts for the different effects of selected PDE isoform inhibition during adhesion and proliferation. Regulation of adhesion of leukocytes to

vascular endothelial ligands is a very fast process measured in microseconds (*6*). A possible mechanism may be that DP and PF-04957325 upregulate intracellular cAMP levels more rapidly and efficiently than PDE inhibitors that do not block PDE8, requiring a longer time of action for less efficient PDE inhibitors during Teff cell adhesion (*103*). Since PDE8A is a very high affinity cAMP-specific PDE with a *K*m value ranging from 0.04-0.15 μM, 40-100 times lower than that of PDE4, it is likely to be functioning at lower cAMP concentrations than PDE4 and may thus be involved in the control of intracellular cAMP concentrations at basal levels and in the immediate response to acute increases of cAMP in specific cell regions (*34, 38, 104*). This mechanism would be consistent with our data. Major mechanistic insights into PDE8A signaling came from a recent report that PDE8A associates with Raf-1 to protect it from inhibitory phosphorylation by PKA (*46*). Raf kinases have been shown to regulate integrin α4β1-mediated T cell resistance to shear stress which may explain our observations in T cell adhesion assays (*105*).

We also analyzed the effects of PF-04957325 administration on $CD4^+$ responses in draining lymph nodes 10 days after MOG_{35-55} and CFA immunization. We found no effect of PF-04957325 administered s.c. on $CD4^+$ Teff cell proliferation (Figure 5) or production of IFN-γ or IL-17, nor changes in percentage and numbers of $CD4^+$, $Foxp3^+$ (Treg cells), $\gamma\delta TCR^+$ or Ki-67^+ (proliferating) T cells in the draining lymph nodes of CFA and MOG_{35-55} immunized mice (data not shown). Additionally, in contrast to the PDE4-selective inhibitor PICL, PF-04957325 did not significantly suppress T cell proliferation *in vitro* in response to MOG_{35-55} and showed over 100-times lower efficacy in

suppressing proliferative responses to anti-CD3 stimulation. The different potency of PF-04957325 in assays using whole lymph nodes could indicate a role for costimulation provided by antigen-presenting cells overcoming its moderate anti-proliferative action when isolated Teff cell proliferation were stimulated by anti-CD3 mAb. Overall, our results indicate a non-redundant role for PDE8 in regulating T cell adhesion to vascular endothelium through the cAMP signaling pathway. The data further suggest that PDE8 inhibition, if successful *in vivo* in inflammatory diseases, may selectively target leukocyte motility without exerting global immunosuppressive effects on cytokine production and cell proliferation and thus provide a highly selective therapeutic tool while maintaining the proven characteristics of PDE inhibitors as successful drugs. Taken together, efforts to develop and test selective inhibitors of PDE8 such as PF-04957325 should be undertaken as a means to develop novel therapeutic agents for treatment of inflammatory disorders mediated by activated T cells (*106-110*).

2.5 Materials and Methods

Animals

6-12 week old female C57BL/6 mice were from Jackson Laboratories (Bar Harbor). Female mice are widely used in experimental allergy and autoimmunity models, and we used them to keep consistency with previous studies (*111, 112*). Experiments were performed according to approved protocols at UConn Health (IACUC Protocol number 100794).

Bi-phasic model of OVA-induced AAD

For the induction of OVA-induced AAD mice were: 1) sensitized to 25 μg OVA in the adjuvant alum with 3 intraperitoneal injections, 1 week apart; 2) one week after the last immunization, mice in each group were exposed to 1% aerosolized OVA in physiological saline (one hour/day, 5 days a week until sacrifice) with an estimated inhaled daily dose of 30–40 μg/mouse as described previously (*111, 113, 114*). Groups of mice (5/group) were sacrificed at 3, 7, and 42 days post start of daily aerosolization. Mice sacrificed at 3 and 7 days represent AAD (peak inflammation) and those at 42 days represent resolution of AAD and the development of tolerance. At sacrifice, the lung draining hilar (mediastinal) lymph node (HLN) and peripheral inguinal lymph nodes (ILN) were dissected and further processed as described below. This bi-phasic model enables us to study the expression of PDE8A during and after acute inflammation. Induction of OVA-induced AAD was done by Linda Guernsey.

Myelin oligodendrocyte glycoprotein (MOG) peptide MOG_{35-55}

MOG_{35-55} peptide, corresponding to mouse sequence (MEVGWYRSPFSRVVHLYRNGK) was synthesized and purified by the Yale University Synthesis Facility.

Immunization of mice with MOG_{35-55} peptide

6 - to 12-wk-old mice were immunized with MOG_{35-55} in Complete Freund's Adjuvant (CFA; Sigma-Aldrich), a procedure to induce experimental autoimmune encephalomyelitis (EAE) in C57BL/6 mice, an animal model of multiple sclerosis (MS) (*99*). A total of 200 μg of MOG_{35-55} peptide and 400 μg of killed *Mycobacterium tuberculosis* (Difco Laboratories) was emulsified in CFA and injected s.c. into the footpads of mice.

Cell isolation and activation

In the AAD model, lymph node cells (LNC) from HLN and ILN were processed using $CD4^+$ T cell isolation kits (Miltenyi Biotec) to separate $CD4^+$ from $CD4^-$ cell populations. LNC were also dissected from draining popliteal lymph nodes after s.c. immunization with MOG_{35-55} peptide, an autoantigen recognized by T cells in EAE and MS (*99*). Concanavalin A (Con A) activated mouse splenocytes as a source of T cell blasts were prepared and cultured as described (*24, 32*). Cells were either immediately frozen in appropriate reagents for subsequent qRT-PCR or Western immunoblot analyses or used in proliferation assays as described (*79*).

RNA isolation and cDNA synthesis

RNA from cells was isolated using the RNeasy mini kit and treated with Turbo DNA-free Dnase (Ambion). cDNA was synthesized using Superscript III reverse transcriptase (Invitrogen) (*24, 79*).

Quantitative real-time RT-PCR analysis

Quantitative real-time RT-PCR (qRT-PCR) was performed as described previously (*24, 79*). 10 ng cDNA was amplified by qRT-PCR in a 25µl reaction using SYBR Green PCR Master Mix (Applied Biosystems). Primers were designed using Primer Express software v3.0. Primers were chosen from gene regions common to all known splice variants of a specific gene product. Primer efficiency was verified by slope analysis to be 100% ± 2.5%. qRT-PCR was performed using an ABI 7500 fast system and data analyzed using the Δ^{ct} method (SDS software v3.0). Primer sequences and amplicon sizes were published previously (*24, 79*). Expression data were normalized by calculating the ratio of target gene expression/housekeeping gene *rpl19* expression.

Western immunoblot analysis

Western immunoblot analysis was performed as described previously (*79, 80*)((*53*). Mouse T cells were centrifuged at 300 x g for 5 min, washed twice with ice-cold PBS, and lysed in RIPA buffer with 1:100 protease inhibitor cocktail (Sigma**)**. Protein concentration was determined using a BCA Protein Assay Kit (Pierce). Equal amounts of protein were loaded and run on 10% SDS-PAGE gels. Proteins were then transferred onto Immobilon-P transfer membrane (Millipore). Membranes were blocked

with 5% BSA in Tris-buffered saline for 1 h at room temperature and probed with primary antibodies overnight at 4° C. Specificity and source of antibodies directed against PDE gene families and isoforms were published previously (*79*). After probing, membranes were washed three times with TBS-T buffer, and incubated with horseradish peroxidase-conjugated secondary antibody (Anti-Rabbit IgG-horseradish peroxidase was obtained from GE Healthcare) at a final dilution of 1:5000 and then washed three more times. Proteins were visualized and quantitated with SuperSignal West Femto Maximum Sensitivity Substrate (Pierce) using Syngene G:Box with GeneSnap BioImaging software. Staining with anti-GAPDH antibody (Abcam) was used for loading control and the signal was used for normalization in quantitation by determining the ratio of the target protein band density/GAPDH band density for $CD4^+$ cells divided by the target protein band density/GAPDH band density for the $CD4^-$ cell population.

Adhesion assays

Adhesion assays were performed in 24-well plates with a confluent layer of activated cells of the murine brain endothelium-derived cell line bEnd.3 (ATCC). 100 μM DP, 300 μM IBMX, 1 and 0.1 μM PICL, or PF-04957325 were added to bEnd.3 cells for the last 45 min of TNF-α incubation. T cell blasts or Teff cells were labeled with 5 μM Calcein AM (Molecular Probes) and treated as described above. 7×10^5 pretreated T cell blasts or Teff cells per well were incubated on bEnd.3 cells in RPMI media. After 30 min at 37ºC, non-adherent cells were removed by washing with D-PBS. For analysis, 7×10^5 Calcein AM labeled T cell blasts or Teff cells were used as positive controls.

Fluorescence was read in a Victor 3v microplate reader (Perkin Elmer) with a fluorescein filter set. The percentage of labeled cells resistant to detachment was calculated as total fluorescence of well divided by fluorescence of 7 x 10^5 Calcein AM labeled cells.

Proliferation assays

Isolated Teff cells (5 x 10^4/well) were cultured in round bottom 96-well plates (Costar) in the presence or absence of soluble anti-CD3 mAb (0.7 μg/ml; R&D). PICL (1, 0.1, 0.01 μM), PF-04957325 (1, 0.1, 0.01 μM), alone or in combination, or vehicle control (0.1% DMSO in media) were added at 0 h (*79*). Proliferation of popliteal LNC in reponse to MOG_{35-55} peptide with inhibitors or vehicle control was performed in round bottom 96-well plates (Costar) at a concentration of 2 x 10^5 cells/well. After 48 h, 2 μCi per well of [^{3}H]thymidine (NEN) was added and cells were harvested 16 h later using a semiautomated cell harvester. [^{3}H]thymidine incorporation was determined by scintillation counting.

Statistics

Experimental groups were compared by analyzing data with the Student's unpaired t-test or one-way ANOVA followed by Bonferroni t-test using SigmaStat and GraphPad software. Probability levels for statistically significant differences are indicated by the *p*-value in the figure legend and by corresponding asterisks in the figures (*$p < 0.05$, **$p < 0.001$).

Figure 2.1

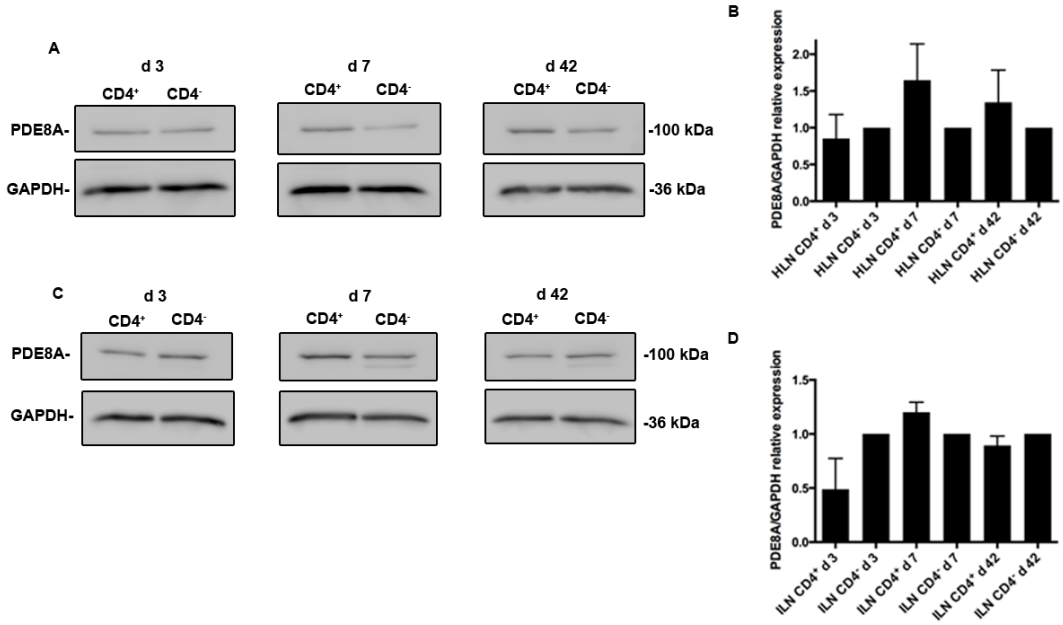

Figure 2.1. Differential expression of PDE8A isoforms in $CD4^+$ and $CD4^-$ leukocyte populations localized in the HLN of mice with OVA-AAD *in vivo*. PDE expression was analyzed by Western immunoblot in *ex vivo* isolated HLN (A, B) and ILN (C, D) cells from mice with AAD. LNCs were separated into $CD4^+$ and $CD4^-$ populations by magnetic bead isolation. A (HLN) and C (ILN) show a comparison of PDE8A protein expression at day 3, 7 and 42 AAD between the $CD4^+$ T cell and $CD4^-$ leukocyte subpopulations and GAPDH as a loading control for each immunoblot. The data shown are immunoblot analyses from pooled LNCs from 5 HLN that were separated into $CD4^+$ and $CD4^-$ populations for each day of the experiments. B (HLN) and D (ILN) show abundance of PDE8A protein determined by immunoblot densitometry and normalized to GAPDH expression. The figure shows the mean + SEM of the quantification of results from HLN samples from day 3, day 7 and day 42 AAD performed in 2 independent

experiments (n = 5 mice per group, 2 groups per day, total n = 30 mice) as the ratio of the target protein band density/GAPDH band density for $CD4^+$ cells divided by the target protein band density/GAPDH band density for the $CD4^-$ cell population.

Figure 2.2

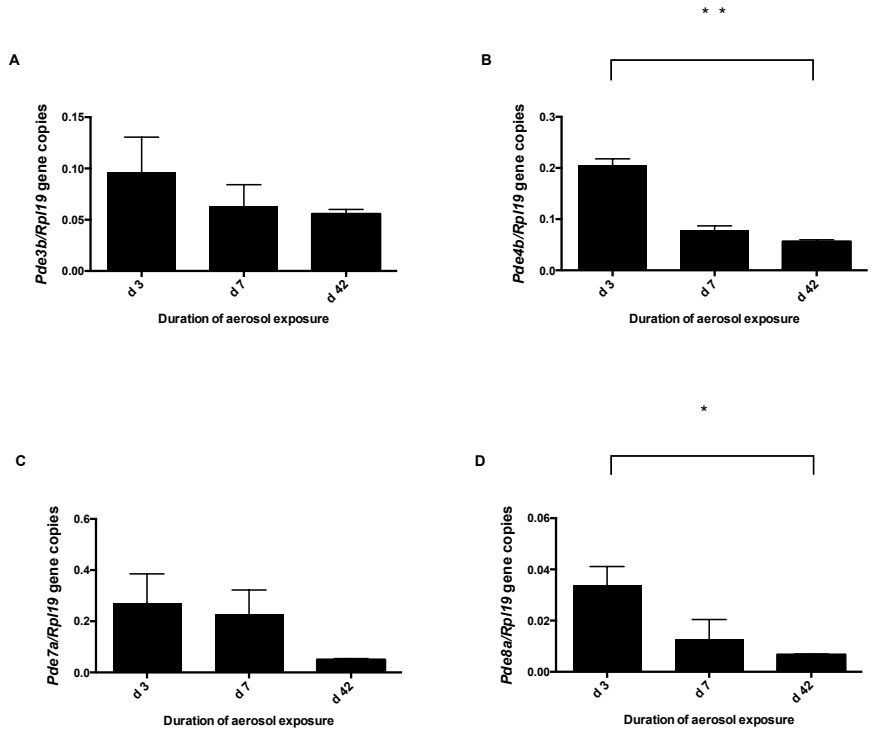

Figure 2.2. *Pde3b*, *pde4b, pde7a* and *pde8a* gene expression in CD4$^+$ T cells localized in the draining HLN of mice at various days of OVA exposure *in vivo*. PDEs were analyzed by qRT-PCR in *ex vivo* isolated HLN cells from mice with AAD separated into CD4$^+$ and CD4$^-$ cell populations. Data are normalized and expressed as the ratio mean + SEM of target gene expression/housekeeping gene *rpl19* expression. Data in (A) show a comparison of *pde3b* gene expression in CD4$^+$ cells of HLN samples from day 3, day 7 and day 42 AAD (n = 3). Data in (B) show *pde4b* gene expression, in (C) *pde7a* gene expression and in (D) expression of *pde8a* in CD4$^+$ cells of HLN in AAD. (n = 5 mice per group, total n = 15 mice; *$p < 0.05$, **$p < 0.001$, unpaired t-test). Experiment performed by Dr. Amanda G. Vang and Rebecca Nguyen.

Figure 2.3

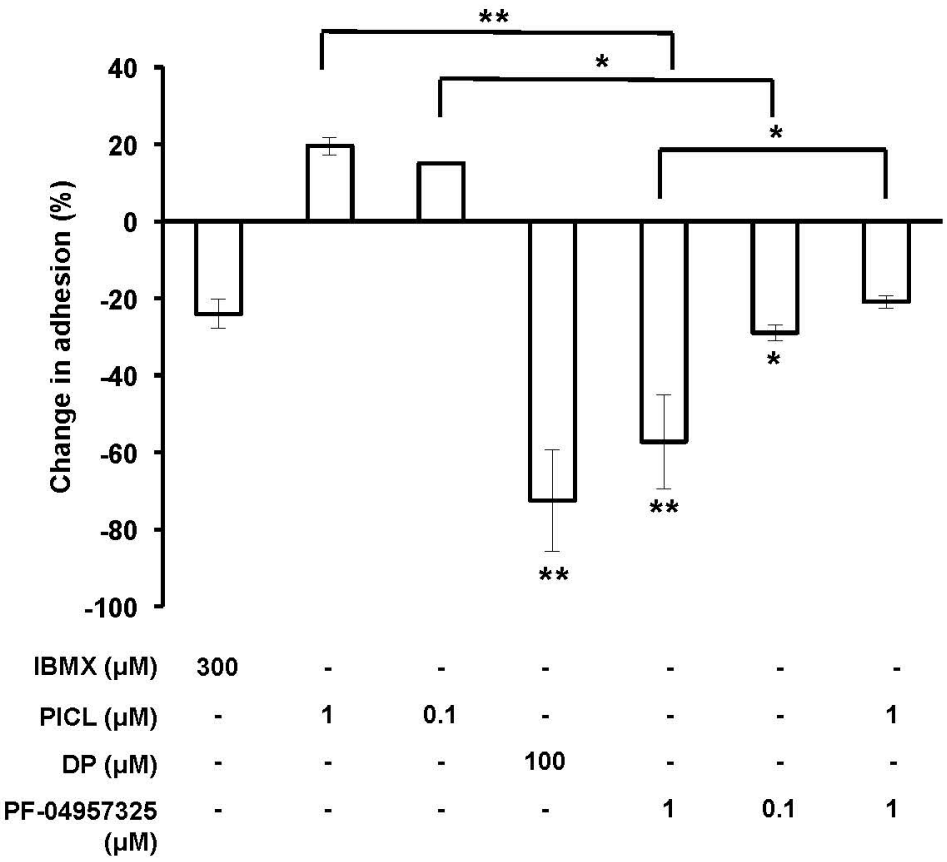

Figure 2.3. Inhibiting PDE8 suppresses Teff cell adhesion to endothelial cells and is reversed by PDE4 inhibition. T cell blasts from C57BL/6 mice and bEnd.3 endothelial cells were incubated alone or in combination with IBMX (300 μM), PICL (1 or 0.1 μM), DP (100 μM) or PF-04957325 (1 or 0.1 μM). Values are normalized to the vehicle condition (0.1% DMSO) and presented as the mean + SEM percentage of T cell blasts resistant to detachment. Data are averages from three to four independent experiments performed in triplicate (*p < 0.05, **p < 0.001, one-way ANOVA and Bonferroni t-test). Experiment performed by Dr. Amanda G. Vang.

Figure 2.4

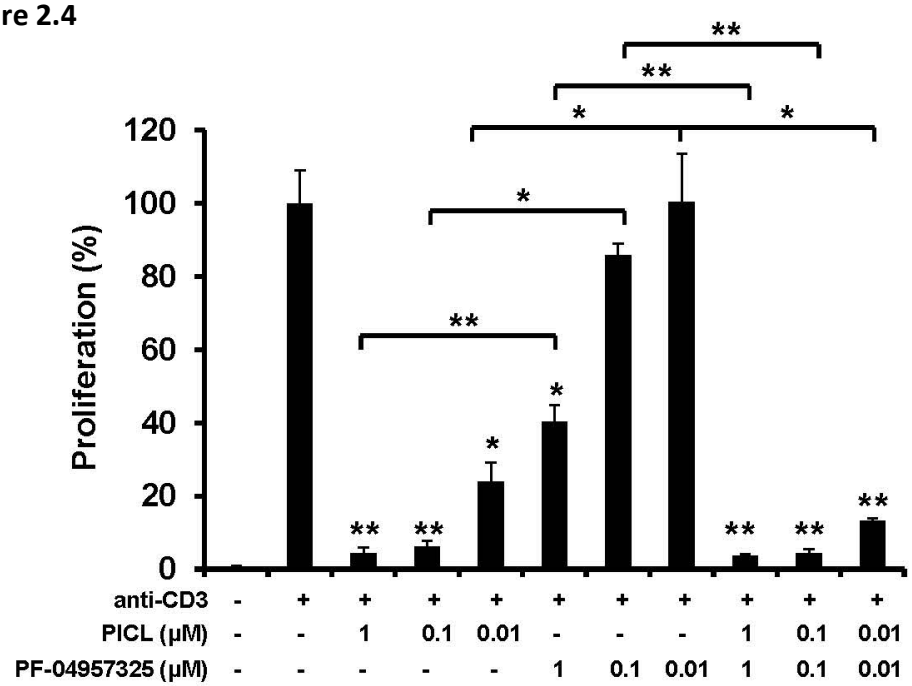

Figure 2.4. Selective inhibition of Teff cell proliferation by PDE4 inhibition *in vitro*. Proliferation of purified $CD4^+CD25^-$ Teff cells exposed to PDE inhibitors. Teff cells (5 x 10^4/well) were cultured with immobilized anti-CD3 mAb or control in the presence of IBMX (300 μM), DP (100 μM), PICL, PF-04957325 alone or in combination, or vehicle control (0.1% DMSO). The extent of proliferation was determined by [^{3}H]thymidine incorporation at 64 h and results are presented as mean + SEM counts per min (cpm). Data are representative of three to five independent experiments performed in triplicate (*p < 0.05, **p < 0.001, comparisons to vehicle were analyzed using a one-way ANOVA and Bonferroni *t*-test). Experiment performed by Dr. Stefan Brocke and Dr. Robert B. Clark.

Figure 2.5

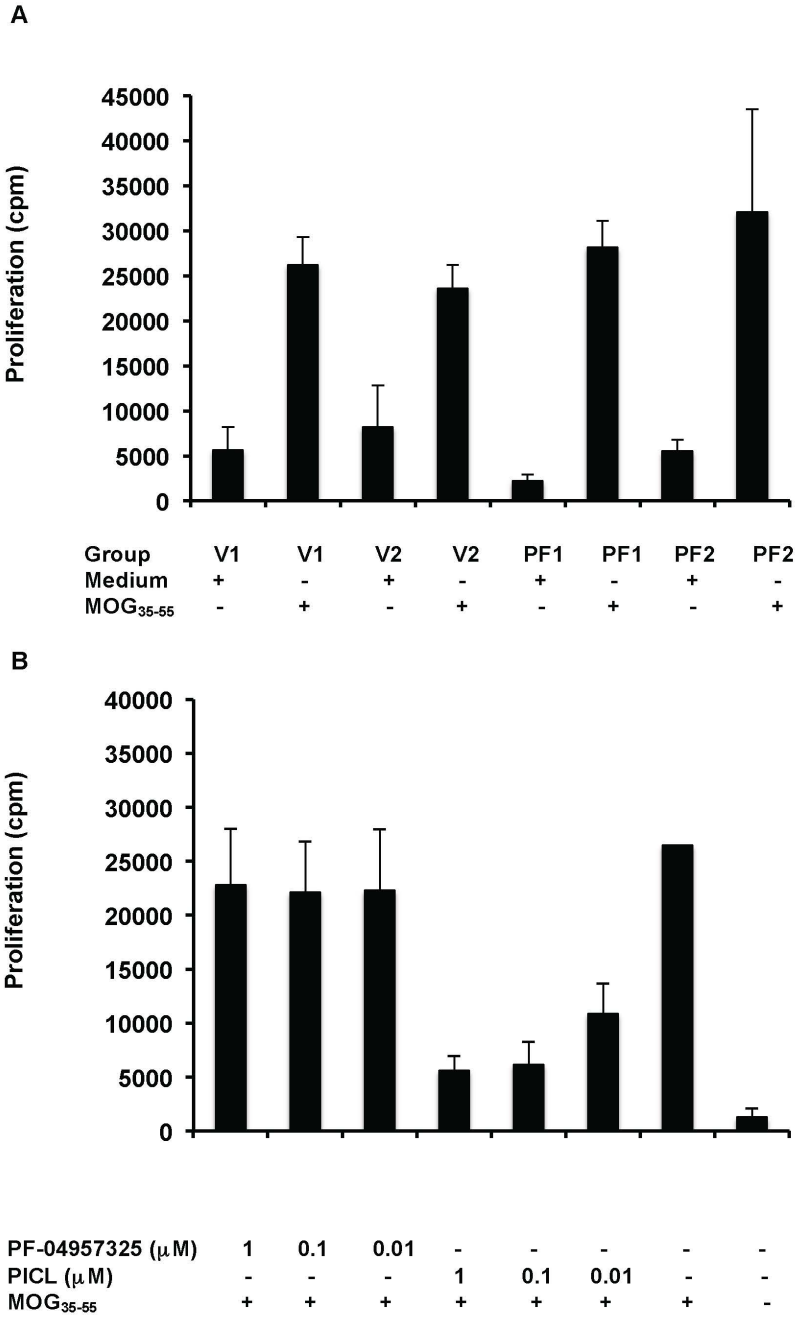
A
Proliferation (cpm)
45000
40000
35000
30000
25000
20000
15000
10000
5000
0
Group V1 V1 V2 V2 PF1 PF1 PF2 PF2
Medium + - + - + - + -
MOG35-55 - + - + - + - +
B
Proliferation (cpm)
40000
35000
30000
25000
20000
15000
10000
5000
0
PF-04957325 (μM) 1 0.1 0.01 - - - - -
PICL (μM) - - - 1 0.1 0.01 - -
MOG35-55 + + + + + + + -

Figure 2.5. PF-04957325 does not suppress T cell proliferation in response to MOG_{35-55} *ex vivo* and *in vitro*. (A) C57BL/6 mice were immunized with MOG_{35-55} and CFA and treated twice daily from day 8-10 by subcutaneous administration of PF-04957325 (PF1, PF2) or vehicle control (V1, V2) (n = 2 mice per group, total n = 4). Each injection contained a dose of 2.5 mg/kg PF-04957325 dissolved in 100 μl vehicle (PF-04957325) or 100 μl vehicle alone (vehicle control). (B). C57BL/6 mice were immunized with MOG_{35-55} and CFA (n = 2). (A, B) Draining popliteal lymph nodes were dissected 10 day after immunization and an *in vitro* proliferation assay was performed under conditions as indicated. MOG_{35-55} (50 μg/ml) was present where indicated (A, B), together with PDE inhibitors *in vitro* as shown (B). Experiment performed by Dr. Stefan Brocke and Dr. Robert B. Clark.

Chapter 3

PDE8 controls $CD4^+$ T cell motility through the PDE8A-Raf-1 kinase signaling complex

3.1 Summary

The levels of cAMP are regulated by phosphodiesterase enzymes (PDEs), which are targets for the treatment of inflammatory disorders. We have previously shown that PDE8 regulates T cell motility. Here, for the first time, we report that PDE8A exerts its control of T cell function through the Raf-1 kinase signaling pathway. To examine T cell motility under physiologic conditions, we analyzed T cell interactions with endothelial cells and ligands in flow assays. The highly PDE8-selective enzymatic inhibitor PF-04957325 suppresses adhesion of *in vivo* myelin oligodendrocyte glycoprotein (MOG_{35-55}) activated inflammatory $CD4^+$ T effector (Teff) cells to brain endothelial cells under shear stress. Recently, PDE8A was shown to associate with V-raf-1 murine leukemia viral oncogene homolog 1 (Raf-1) creating a compartment of low cAMP levels around Raf-1 thereby protecting it from protein kinase A (PKA) mediated inhibitory phosphorylation. To test the function of this complex in Teff cells, we used a cell permeable peptide that selectively disrupts the PDE8A-Raf-1 interaction. The disruptor peptide inhibits the Teff–endothelial cell interaction more potently than the enzymatic inhibitor. Furthermore, the LFA-1/ICAM-1 interaction was identified as a target of peptide mediated reduction of adhesion, spreading and locomotion of Teff cells under flow. Mechanistically, we observed that inhibition of PDE8 and disruption of the PDE8A-Raf-1 complex profoundly alter Raf-1 signaling in Teff cells. Collectively, our studies demonstrate that PDE8A inhibition by enzymatic inhibitors or PDE8A-Raf-1 kinase

complex disruptors decreases Teff cell adhesion and migration under flow, and represents a novel approach to target T cells in inflammation.

3.2 Introduction

Ligand binding to Gs-coupled receptors leads to the generation of the second messenger cAMP following activation of the enzyme adenylyl cyclase. Stimulation of the T cell antigen receptor (TCR) also leads to elevation of cAMP which is known to inhibit T cell proximal signaling, IL-2 production and T cell proliferation (*115*). cAMP exerts these inhibitory effects in T cells through the PKA (cAMP dependent protein kinase) which blocks the MAPK (mitogen- activated protein kinase) and NFAT (nuclear factor of activated T cells) dependent signaling pathways (*116*). The inhibitory action of cAMP is eliminated through the action of phosphodiesterase (PDE) enzymes that hydrolyze cAMP. PDEs 3B, 4A, 4B, 4D, 7A1, 7A3 and 8A1 are the isoforms expressed in T cells (*15, 23, 24, 44*). Raf-1 is an upstream regulator of the mitogen-activated protein kinase (MAPK) – ERK1/2 module, which controls many fundamental biological processes, including T cell proliferation, survival and adhesion (*117-120*). In this pathway Raf-1 phosphorylates and activates MEK1/2, which in turn phosphorylate and activate ERK1/2. ERK has more than 150 known substrates (*117, 120*), which mediate many of the pleiotropic functions of this pathway (*121, 122*). Raf-1 regulation is complex and is still insufficiently understood. Critical events are the dephosphorylation of an inhibitory site, S259, which allows Raf-1 binding to activated rat sarcoma viral oncogene (Ras) and is a prerequisite for further activation. S259 is a target for phosphorylation by cAMP dependent protein kinase A (PKA) (*51, 123, 124*), a family of enzymes whose activity is dependent on local intracellular levels of cAMP. Thus, S259 is the primary target of a complex system of crosstalk between the cAMP and the ERK pathways. A recent report demonstrated that Raf-1 kinase binds to PDE8A in a signaling complex, which acts to

protect Raf-1 from inhibitory phosphorylation by PKA (*43, 46, 125*). Our previous work has shown that PDE8 controls T cell and breast cancer cell motility (*24, 32, 33, 79*). PDE8 is also a target for suppression of myelin oligodendrocyte glycoprotein (MOG_{35-55}) induced experimental autoimmune encephalomyelitis (EAE), a model for multiple sclerosis, *in vivo* (unpublished). Our goal here was to delineate the mechanism by which PDE8 controls distinct categories of T cell motility and determine its selective effect on regulatory and effector components of the T cell immune response.

Our recent work shows that $CD4^+$ T cells isolated from the lung draining hilar lymph nodes have increased PDE8A expression during the acute inflammatory stage in an ovalbumin induced allergic airway disease mouse model (*126*). This further emphasizes the concept of targeting PDE8A in inflammation. Recently, there has been a surge of interest in the cAMP specific PDE8 family of enzymes. PDE8 is expressed widely in human tissue (*127*) with functions in testosterone production (*104*) and lymphocyte adhesion and chemotaxis (*24, 32, 33, 79*). T cell activation induces PDE8A, a cAMP-specific PDE with 40-100-fold greater affinity for cAMP than PDE4 (*23, 32*). This unique feature has led to the suggestion that PDE8 enzymes may have an important role in protecting any associated protein from being affected by fluctuations in basal cAMP concentrations. Compartmentalization of PDE8A in the cell to Raf-1 can regulate Raf-1 phosphorylation on S259, and, in so doing, regulate the cross-talk node whereby cAMP exerts an inhibitory effect on Raf-1 signaling, retarding subsequent ERK phosphorylation and potentially T cell activation (*43, 46*).

Based on these observations, we hypothesized that PDE8A exerts its regulation of T cell function through the Raf-1-ERK signaling pathway. Little is known regarding the specific functions of PDE8A within the immune system, especially whether the control of T cell motility is mediated through different effectors of the canonical Raf-1-ERK signaling cascade. B-Raf has been demonstrated to regulate VLA-4 integrin mediated adhesion in human T cells under shear stress (*105*). Here, we probed the PDE8A-Raf-1 kinase signaling pathway in Teff and regulatory T (Treg) cells, using specific pharmacological tools including PDE8 inhibitors and peptide disruptors of the PDE8A-Raf-1 complex in adhesion assays under flow to assess the molecular regulation of downstream effectors of the PDE8A-Raf-1 complex.

3.3 Results

Differential motility of naive and activated Teff and Treg cells under flow.

Since PDEs and cAMP levels significantly differ between Teff and Treg cells (*79, 128*), we first tested $CD4^+CD25^-$ Teff and $CD4^+CD25^+$ Treg cells under naive and activating conditions for their ability to interact with LPS-activated endothelial cells (ECs) under shear flow. Mouse brain ECs were cultured as a monolayer, stimulated with LPS overnight, and the subsequent adhesive interactions with ECs were measured in the flow chamber assay. Compared to naive Teff cells, naive Treg cells showed 17.8 ± 3.7% higher adhesion (11.1 ± 3.1% vs. 28.9 ± 2.0%, **p=0.0031) (Fig. 1A) while interacting with the EC monolayer. These findings are similar to previous reports indicating that naive Teff cells have lower adhesion potential compared to naive Treg cells (*129*). Activation via their T cell receptor (TCR)/CD3ε led to a 7.7 ± 4.5% (p=0.1287) increase in adhesion in Teff cells (18.8 ± 3.1%) and 13.8 ± 3.9% (**p=0.006) decrease in adhesion of Treg cells (15.1 ± 2.6%) compared to their naive counterparts. Addition of IL-2 along with TCR activation further increased adhesion of Teff cells (24.1 ± 2.4%) by 13.0 ± 4.0% (*p=0.01) and restored adhesion of Treg cells (25.7 ± 7.9%) (p=0.7415). Thus under naive conditions Treg cells are highly motile and activation in the absence of IL-2 led to a decrease in their migratory potential (Fig. 1A). We confirmed these findings using transgenic *Foxp3gfp.KI* mice in which Teff and Treg cells were isolated using a combination of a $CD4^+$ T cell isolation kit and cell sorting by flow cytometry based on GFP expression (Fig. 1B). $Foxp3^-GFP^-$ Teff cells sorted from these mice had significantly lower (5.5 ± 2.0%) TEM potential compared to $Foxp3^+GFP^+$ Treg cells (1.5 ± 0.9% vs. 7.0 ± 2.1%, *p=0.0422) after TCR stimulation (Fig. 1C). $Foxp3^-$

GFP$^-$ Teff cells have a 22.5 ± 9.1% higher detachment compared to Foxp3$^+$GFP$^+$ Treg cells (74.9 ± 6.6% vs. 52.4 ± 5.5%, p=0.0571) (Fig 1D). This differential migratory potential of Teff cells and Treg cells prompted us to study whether PDE8 inhibition using the PDE8 inhibitor PF-04957325 will show a differential effect on motility of Teff versus Treg cells.

PDE8 inhibition at the catalytic moiety leads to decreased adhesion of Teff cells but not Treg cells under shear flow conditions.

We have previously shown that PDE8A is differentially expressed in naive Teff cells versus naive Treg cells (*79*). We now examined whether different expression levels of PDE8A can also be detected in pathogenic T cell populations involved in autoimmune inflammation. Our data show that CD4$^+$CD25$^-$ Teff cells isolated from draining lymph nodes of MOG_{35-55} immunized mice had higher expression of PDE8A and Raf-1 compared to CD4$^+$CD25$^+$ Treg cells (Fig. 2A,B). Next, we used *Foxp3gfp.KI* mice immunized with MOG_{35-55} to determine the effect of PDE8 inhibition on activated, pathogenic T cells. This approach enabled us to visually distinguish Teff and Treg cells and simultaneously measure the effect of inhibitors on Teff and Treg cells within the same experiment. PDE8 inhibition using PF-04957325 led to a significant decrease in adhesion (100.0% vs. 63.3 ± 6.9%, **p=0.0019), and an increase in detachment (100.0% vs. 117.9 ± 7.4%, p=0.0510) of CD4$^+$Foxp3$^-$GFP$^-$ Teff cells compared to vehicle control treatment (Fig. 2C). No significant effect was observed on adhesion (100.0% vs. 108.6 ± 26.1%, p=0.7536) and detachment (100.0% to 105.2± 9.1%, p=0.5850) of CD4$^+$Foxp$^+$GFP$^+$ Treg cells after PDE8 inhibition (Fig. 2D). The observed

difference in PDE8A abundance between Teff and Treg cells could explain the differential effect of PDE8 inhibition on Teff cells vs. Treg cells.

Disruption of PDE8A-Raf-1 kinase signaling complex suppresses Teff and Treg cell adhesion.

PDE8A has been shown to interact with Raf-1 kinase without the need for accessory proteins or lipids and protect it from PKA mediated inhibitory phosphorylation. The Raf family members have been known to regulate adhesion of T cells to vascular ligands (*105*) We next used a cell permeable peptide that disrupts the PDE8A-Raf-1 interaction (*46*) to determine whether this complex regulates $CD4^+$ T cell motility under flow conditions. $CD4^+$ T cells isolated from draining lymph nodes of MOG_{35-55} immunized *Foxp3gfp.KI* mice and endothelial cells were treated with cell permeable disruptor or control peptides for 4 h. Treatment with the disruptor peptide decreased adhesion of $CD4^+GFP^-Foxp3^-$ Teff cells by 43.6 ± 14.3%, (100.0% vs. 56.4 ± 14.3%, *p= 0.0221) and increased detachment by 9.7 ± 6.6% (100.0% vs. 109.7 ± 6.6%, p=0.1919) (Fig.3A) compared to control. We also observed 39.1 ± 24.3% decrease in adhesion of $CD4^+GFP^+Foxp3^+$ Treg cells, but this difference was not significant (100.0% vs. 60.9 ± 24.3%; p=0.1590) and a 7.8 ± 6.0% increase in Treg cell detachment (100.0% vs. 107.8 ± 6.0%, p=0.2417) (Fig. 3B).

Adhesion, spreading and locomotion of Teff cells to ICAM-1 are significantly affected by disruption of PDE8A-Raf-1 complex, but not by PDE8 inhibition at the catalytic moiety.

Next, we assessed whether PDE8 or the PDE8A-Raf-1 kinase complex regulate adhesion via LFA-1 integrin mediated cell tether formation with ICAM-1. For this purpose, we tested interaction of $CD4^+$ T cells on plates coated with recombinant ICAM-1-Fc protein under shear flow conditions. Treatment of $CD4^+$ T cells with PF-04957325 did not lead to significant differences in $CD4^+GFP^-Foxp3^-$ Teff cell mediated transient tethers (100.0% vs. 112.8 ± 53.0%, p=0.8213), firm tethers (100.0% vs. 99.8 ± 9.6%, p=0.9809), spreading (100.0% vs. 66.0 ± 28.8%, p=0.3038), locomotion (100.0% vs. 62.6 ± 29.6%, p=0.2744), detachment (100.0% vs.103.6 ± 2.3%, p=0.1944) (Fig. S1A), or adherence (100.0% vs. 68.6 ± 15.4%, p=0.1120) when ICAM-1 was used as a substrate in flow assays (Fig. 4A). There was also no significant effect of PF-04957325 treatment on $CD4^+GFP^+Foxp3^+$ Treg cell mediated firm tether formation (100.0% vs. 90.0 ± 13.2%, p=0.4916), adherence (100.0% vs. 191.5 ± 83.5%) or detachment (100.0% vs. 88.0 ± 6.7%, p=0.1498) (Fig. S1B). In contrast, treatment with the PDE8A-Raf-1 disruptor peptide led to a significant 52.6 ± 13.3% decrease in $CD4^+GFP^-Foxp3^-$ Teff cell adherence, (100.0% vs. 47.4 ± 13.3%, *p=0.0167), a significant 59.3 ± 4.3% decrease in spreading (100.0% vs. 40.7 ± 4.3%, *** p=0.0002) and a significant 72.7 ± 4.6% decrease in locomotion, (100.0% vs. 27.3 ± 4.6%, ****p < 0.0001) (Fig. 4B), but no significant effect was observed on transient tethers (100.0% vs. 150.8 ± 95.9%, p=0.6240), firm tethers (100.0% vs. 60.3 ± 23.3%, p=0.1634) and detachment (100.0% vs. 106.1 ± 3.6% p=0.1688) of Teff cells when ICAM-1 was used as a substrate (Fig.

S1C). Of note, there was also a significant 43.3 ± 13.1% decrease in adherent cell tethers of $CD4^+GFP^+Foxp3^+$ Treg cells interacting with ICAM-1 (100.0% vs. 56.7 ± 13.1%, *p=0.0299) after treatment with the disruptor peptide (Fig. 4C). No significant effect on firm tether formation (100.0% vs. 65.5 ± 25.3%, p=0.2450) and detachment (100.0% vs. 112.9 ± 9.3%, p=0.2358) of Treg cells was observed (Fig. S1D). These data implicate the LFA-1-ICAM-1 interaction as a target of PDE8A-Raf-1 kinase complex disruption.

$CD4^+$ T cell mediated firm cell tether formation to VCAM-1 is unaffected by disruption of PDE8A-Raf-1 complex and PDE8 inhibition at the catalytic moiety.

To further explore whether the effect of the PDE8 inhibitor or the PDE8A-Raf-1 complex disruptor peptide on adhesion of $CD4^+$ T cells was dependent on the integrin VLA-4, we tested binding of cells to its selective ligand, VCAM-1 under flow (*130*). No significant differences were observed in transient tethers, (100.0% vs. 196.1 ± 81.9%, p=0.2849), rolling (100.0% vs. 87.6 ± 23.8%, p=0.6204), firm tethers (100.0% vs. 134.7 ± 36.6%, p=0.3805), adherence (100.0% vs. 127.9 ± 48.8%, p=0.5881) and detachment (100.0% vs. 99.8 ± 0.6%, p=0.7070) in $CD4^+$ T cell interaction with VCAM-1 after treatment with PDE8 inhibitor (Fig. S2A). Treatment with disruptor peptide did not have any significant effect on transient tethers (100.0% vs. 90.4 ± 22.7%, p=0.6860), firm tethers (100.0% vs. 81.2 ± 13.3%, p=0.2074), adherence (100.0% to 69.5 ± 23.4%, p=0.2402) and detachment (100.0% vs. 102.5 ± 1.7%, p=0.1967). However, there was a significant 56.4 ± 7.3% suppression of rolling (100.0% vs. 43.6 ± 7.3%, **p=0.0015) after treatment

with the disruptor peptide, indicating a selective effect of the peptide on initial loose tethers of T cells to VCAM-1 (Fig. S2B).

Integrin surface expression in $CD4^+$ T cells is not altered by PDE8 inhibition at the catalytic moiety and marginally reduced by disruption of the PDE8A-Raf-1 complex.

α4 and αL integrins as well as CD44 are known cell surface molecules regulating myelin antigen specific Teff cell migration into the central nervous system (*10, 11*) and are targets of drug therapies (*131*). We tested the effect of the PDE8 inhibitor and the disruptor peptide on the surface expression of these adhesion molecules by flow cytometry. PF-04957325 treatment did not significantly alter the mean fluorescence intensity (MFI) of αL integrin (p=0.2608), α4 integrin (p=0.1053) or CD44 (p=0.3675) in $CD4^+Foxp3^-GFP^-$ Teff cells (Fig. S3A) or $CD4^+GFP^+Foxp3^+$ Treg cells (p=0.5396; p=0.0677; p=0.0899, respectively; Fig. S3B). In contrast, there was a small but significant 2830 ± 645.8 unit decrease in the MFI of αL integrin expression (30957 ± 350.1 vs. 28127 ± 542.7, *p=0.0119) and a 259.7 ± 65.19 units decrease in MFI of CD44 expression (3453 ± 55.98 vs. 3194 ± 33.39, *p=0.0164) but not in MFI of α4 integrin (p=0.3814) in $CD4^+Foxp3^-GFP^-$ Teff cells after treatment with the disruptor peptide (Fig. S3A). Disruptor peptide treatment did not significantly alter MFI of αL integrin (p=0.1025), α4 integrin (p=0.8069) or CD44 (p=0.0573) in $CD4^+GFP^+Foxp3^+$ Treg cells. Of note, PF-04957325 and disruptor peptide treatments did not affect the viability of $CD4^+$ T cells (Fig. S4)

PDE8 inhibition at the catalytic moiety significantly suppresses ERK phosphorylation in $CD4^+$ T cells activated by anti-CD3.

To find out whether the effect of the PDE8 and PDE8A-Raf-1 complex inhibition on $CD4^+$ T cell motility directly affects Raf-1 or ERK signaling, we performed assays to determine inhibitory phosphorylation of Raf-1 at S259 and activating phosphorylation of ERK1/2 after treatment and activation through the TCR. ERK1/2 phosphorylation (Thr202/Tyr204) and Raf-1 phosphorylation (S259) was analyzed by Western blot (Fig. 5). We observed no significant effect on Raf-1 phosphorylation (100.0% vs. 104.3 ± 7.2%, p=0.5937), but a significant 36.2 ± 6.8% decrease in ERK1 phosphorylation (100.0% vs. 63.8 ± 6.2%, ***p=0.0002) and a significant 27.9 ± 9.366% decrease in ERK2 phosphorylation (100.0% vs. 72.1 ± 8.6%, *p=0.0125) in $CD4^+$ T cells after 1 h treatment with PF-04957325 compared to the vehicle control (Fig. 5A,B). These results indicate that the PDE8 enzyme regulates in part the ERK1/2 signaling pathway. We also report that inhibition of PDE8 enzymatic activity led to a 71.4 ± 25.8% compensatory increase in PDE8A protein expression, (100.0% vs. 171.4 ± 23.7%, *p=0.0183) (Fig. 5C-D). Augmentation of PDE7A, PDE4B and PDE4D expression after treatment with cAMP elevating agents or gene family specific PDE inhibitors has been reported before (*132, 133*), and we show here that this occurs with PDE8A as well.

Disruption of the PDE8A-Raf-1 complex increases inhibitory Raf-1 phosphorylation and activating ERK1/2 phosphorylation in $CD4^+$ T cells activated by anti-CD3.

Treatment with the PDE8A-Raf-1 disruptor peptide for 4 h followed by 15 min anti-CD3 stimulation, led to a 134.7 ± 59.99% (100.0% vs. 234.7 ± 59.99%, p=0.0549) increase in PKA mediated inhibitory Raf-1 phosphorylation at S259 (Fig. 6A). Additionally, there was a 134.1 ± 57.22% increase at 4 h (100.0% vs. 234.1 ± 50.46%, p=0.0516) in activating ERK1 phosphorylation and a 131.4 ± 64.14% increase at 4 h (100.0% vs. 231.4 ± 56.57%, p=0.0797) in activating ERK2 phosphorylation in $CD4^+$ T cells exposed to the disruptor peptide (Fig. 6B). Since in flow assays the $CD4^+$ T cells were treated with the peptide for 4 h, our data indicate that the major effect of the PDE8A-Raf-1 complex is dependent on Raf-1 signaling independent of the downstream ERK-MAPK pathway. Despite this robust effect on inhibitory Raf-1 phosphorylation, treatment with the PDE8A-Raf-1 disruptor peptide for 4 h leads to an increase of activating ERK1/2 phosphorylation that could be mediated by a large number of effectors acting through ERK during T cell activation (*134*).

3.4 Discussion

Previous work has shown that PDE8A is expressed in activated $CD4^+$ T cells (*23, 24, 32, 135*). Functionally, we have reported that PDE8 regulates T cell motility as inhibition of PDE8 is a non-redundant means to suppress lymphocyte chemotaxis and adhesion (*24, 32, 126*). Moreover, we have recently shown that PDE8A is expressed in breast cancer cell lines and inhibition of PDE8 suppresses breast cancer cell migration (*33*). These previously described roles of PDE8 in cell motility prompted us to mechanistically investigate the specific cell migration categories and molecular signaling complexes that are regulated by PDE8.

PDEs control intracellular cAMP gradients and are positioned in discrete signaling complexes. Much is known about spatial arrangements and specific functions of some PDE isoforms such as PDE4 (*19, 20, 136*). Much of this knowledge has stemmed from the use of disruptor peptides that have no effect on global PDE activity but can discretely displace small pools of tethered PDE from precise microdomains. For example, PDE4D5 forms signaling complexes with signaling and adhesion molecules that regulate spreading of cancer cells (*45*) and endothelial inflammation (*137*). A dearth of information, however, exists for complexes involving PDE8A. A recent study Baillie and colleagues demonstrated the first such PDE8 specific signaling complex (*46*). In this study, we addressed a major gap in the literature by delineating the parts of the mechanism by which PDE8 inhibition acts in T cells, and by investigating the function of the PDE8A-Raf-1 complex in T cells. To analyze T cell migration under physiological conditions, we did motility assays under shear flow conditions. To delineate the role of

PDE8 in different T cell populations involved in pro- and anti-inflammatory immune responses, we subjected polyclonal and antigen-activated Teff and Treg cells to physiological shear stress in flow chamber assays. Our results indicate the higher adhesion and TEM potential of naive Treg cells compared to naive Teff cells. Further activation of these cells with plate bound anti-CD3 led to an increase in migratory potential of Teff cells compared to the Treg cells. Our results indicate that enzymatic inhibition of PDE8 using the specific PDE8 inhibitor, PF-04957325, leads to significant reduction of Teff cell adhesion. In contrast, Treg motility is not profoundly affected by PDE8 inhibition. This differential effect on both the cell populations is consistent with the observed differential expression of PDE8A in Teff cells versus Treg cells where it is considerably more highly expressed in Teff cells. Treatment with the PDE8A-Raf-1 disruptor peptide had a more potent effect on Teff cell adhesion, which suggested the specific involvement of the PDE8A-Raf-1 signaling complex in the control of $CD4^+$ T cell motility beyond a role for the global pool of PDE8 in T cells. In order to dissect the molecular mechanism by which PDE8 and the PDE8A-Raf-1 complex regulate adhesion, we further tested the effect of the enzymatic inhibitor and signaling complex disruptor on interaction of activated $CD4^+$ T cells isolated from lymph nodes of mice immunized with MOG_{35-55}/CFA with endothelial ligands, VCAM-1 and ICAM-1, molecules critically involved in inflammation (*131*). Treatment with the disruptor peptide led to a significant reduction in firm adhesion, spreading and locomotion of Teff cells as well as reduction in firm adhesion of Treg cells while interacting with ICAM-1. Thus PDE8A-Raf-1 signaling complex regulates LFA-1 integrin mediated tether formation while interacting with ICAM-1 vascular adhesion molecules. LFA-1 ICAM-1 interaction is

also necessary in the immune synapse, hence PDE8-Raf-1 kinase complex can also be important in $CD4^+$ T cells and antigen presenting cells interaction. The expression of αL, α4 integrin and CD44 expression in $CD4^+Foxp3^-GFP^-$ Teff cells and $CD4^+Foxp3^+GFP^+$ Treg cells after treatment with PDE8 enzymatic inhibitor was marginally reduced or unaltered suggesting that the effect on adhesion was dependent on cell adhesion molecules activation rather than cell surface expression (Fig. S3A, B) (*138, 139*). Importantly, neither PF-04957325 nor disruptor peptide treatment affected the viability of the cells (Fig. S4).

It is noteworthy that our data suggest a Raf-1 dependent but ERK independent effect of PDE8 inhibition on T cell motility. Previous reports implicate Raf-1 and B-Raf in regulating migration by controlling Rho GTPase mediated downstream signaling which regulates actin cytoskeletal and focal adhesion dynamics (*140, 141*). Our findings further confirm the role of Raf-1 in regulating this process and point towards existence of the novel signaling complex regulating $CD4^+$ T cell motility. Raf-1 is the major downstream effector linking TCR mediated Ras activation to MEK1/2 and ERK1/2 (*134*). However, B-Raf has been identified as the most efficient in interacting with Ras (*142, 143*) and in activating ERK (*144-146*). Importantly, ERK activation and cell proliferation can proceed independently of Raf-1, while Raf-1 can regulate the Rho downstream signaling during cell migration independently of ERK signaling (*141*), highlighting the independent regulation and function of these MAPKs in different signaling pathways. Importantly, in T cells, TCR stimulation can also lead to Ras/Raf-1-independent activation of ERK (*134*). Moreover, findings that PDE8 inhibition has little effect on T cell

proliferation (*24, 126*) indicates an ERK independent action. In contrast, PDE4 inhibition profoundly inhibits cell proliferation and ERK1/2 signaling (*147*), but has little effect on T cell motility (*21, 126*). Taken together, our findings that inhibition of PDE8 and the PDE8A-Raf-1 signaling complex leads to suppression of T cell motility in the absence of marked inhibition of proliferation indicates a novel role for a pool of PDE8A regulating Raf-1 kinase independently of downstream ERK1/2 signaling.

3.5 Materials and Methods

Animals

Female 6-8 weeks old C57BL/6 mice were obtained from Jackson laboratories, Bar Harbor, ME. *Foxp3gfp.KI* knock-in (*Foxp3gfp*.KI) mice were obtained as a gift from Dr. Kuchroo (*148*). Experiments were performed according to approved protocols at UConn Health (IACUC Protocol number 100794-1216).

Chemicals and antibodies

Recombinant mouse VCAM-1/CD106 Fc chimera, recombinant mouse ICAM-1/CD54 Fc chimera were purchased from R&D systems, Minneapolis, MN. The primary antibodies for phospho-p44/42 MAPK (Thr202/Tyr204) (9101; 1:1000), p44/42 MAPK (9102; 1:1000), Phospho-Raf-1 (pSer259) (9421; 1:1000) and Raf-1 (9422; 1:1000) were purchased from Cell Signaling Technology. Anti-GAPDH (ab75834; 1:100,000) and anti-PDE8A antibodies (1:1000) were purchased from Abcam and Scottish Biomedical, respectively. The anti-CD3 antibody was purchased from Biolegend. The secondary antibodies goat anti-rabbit IgG HRP conjugated (1:4000) and chicken anti-rabbit HRP (1:5000) were purchased from Invitrogen and Santa Cruz Biotechnology, respectively. The PDE8A-Raf-1 disruptor peptide (R454–T465; RRLSGNEYVLST) and scrambled control peptide (SYTVRLLGERNS) were synthesized as described (*46*). The PDE8 selective inhibitor PF-04957325 was synthesized by Pfizer Inc., Groton, CT (*24*).

Isolation of Teff cells, Treg cells and $CD4^+$ T cells

$CD4^+CD25^-$ Teff and $CD4^+CD25^+$ Treg cells were isolated from the spleens of C57BL/6 mice using the $CD4^+CD25^+$ Treg Isolation kit (Miltenyi Biotec) as published previously (*135*). $Foxp3^-GFP^-$ Teff cells and $Foxp3^+GFP^+$ Treg cells were sorted based on GFP expression from $CD4^+$ T cells isolated from the spleens of *Foxp3gfp.KI* mice. For the generation of activated pathogenic $CD4^+$ T cells, C56BL/6 or *Foxp3gfp.KI* mice were immunized with MOG_{35-55}/CFA 200 µg s.c. in the footpads (*10, 11*). On d 10 post-immunization, $CD4^+$ T cells were isolated from the draining popliteal lymph nodes (PLN) using the $CD4^+$ T cell Isolation Kit (Miltenyi Biotec).

Cell culture and treatments

Murine brain endothelium derived cell line bEnd.3 (ATCC, Manassas, VA) was cultured in DMEM supplemented with 100 U/ml penicillin, 100 mg/ml streptomycin, 2mM L-glutamine and 10% *f*etal bovine serum as described (*24*). In the flow assays, endothelial cells and $CD4^+$ T cells were treated with 1 µM PF-04957325 PDE8 inhibitor or DMSO vehicle control for 45 min or 1 h, or with PDE8-Raf-1 disruptor peptide or control peptide 10 µM for 4 h. For the flow assay with naive Teff cells or Treg cells, cells were cultured with plate-bound anti-CD3 (10 µg/ml) with or without IL-2 (NIH) (100 Units/ml) for 18 h. For integrin expression analysis, splenic $CD4^+$ T cells isolated from *Foxp3gfp.KI* mice were cultured with plate-bound anti-CD3 (10 µg/ml) for 18 h followed by treatment with PF-04957325 or vehicle control for 1 h or disruptor or control peptide for 4 h. The cells were then pre-incubated with anti-CD16/32 (clone: 2.4 G2, BD Biosciences) for blocking Fcγ III/II receptors followed by surface staining with anti-CD4 eFluor 450 (clone: RM4-5, eBioscience), anti-CD11a BV510 (clone: M17/4, BD Horizon), anti-CD49d PerCp-

eFluor710 (Clone: R1-2, eBioscience), anti-CD44 PE (clone:IM7, BD Pharmingen) antibodies. Events were acquired on LSR II (BD Biosciences). Flow cytometry data were processed on FlowJo software (Tree Star). For the Western blot experiments, $CD4^+$ T cells were treated with the PF-04957325 or the disruptor peptide and respective vehicle or scrambled peptide controls for 1, 2 or 4 h followed by plate-bound 15 min activation with 5 μg/ml plate-bound anti-CD3.

Shear stress (flow) assay

The bEnd.3 cells were stimulated with 1.25 μg/ml LPS for 18 h on d 4 after seeding. The parallel plate flow chamber (Glycotech) was assembled onto the endothelial cell plate and mounted onto the stage of an inverted phase contrast microscope (Nikon Eclipse Ti) (*139*). The $CD4^+$ T cells were treated as described above and then were washed with cation free HBSS and resuspended in binding buffer [HBSS with $CaCl_2$ and $MgCl_2$, 10 mM HEPES (Life Technologies) and 2 mg/ml BSA fraction V (Roche)] at a concentration of 10^6 cells/50 μl binding buffer. The $CD4^+$ T cells were then infused over the endothelial cell layer at a constant low shear rate using a programmable syringe pump (Harvard Apparatus). Once the cells accumulate on the bEnd.3 cells, the shear rate was increased to 5 dyn/cm^2 for the entire 15 min of the assay (migration phase) and a time-lapse video recording was done under phase contrast and GFP illumination settings using Nikon NIS imaging software. The cells and the binding buffer (entire system) were maintained at 37 °C throughout the assay. Motion analysis was done manually on all the T cells that are present in the microscopic field of view. Each T cell was individually tracked starting from the accumulation phase throughout the migration

phase. Only the T cells that were present during the accumulation phase were analyzed. The distinct cell tethers that were examined are defined as follow: cells that detach immediately after application of shear flow were considered to be detached; cells that roll on the endothelial cell surface were rolling; cells that firmly adhere to the endothelial cell surface and remain stationary for at least 1 min were defined as adhesion; cells that form non-stationary adhesion, spread and migrate along the endothelial cell surface were included in the adhesion and locomotion category, cells that undergo TEM were included in the adhesion and TEM category. The number of cells in each category were counted and expressed as percentage of initially accumulated cells during the accumulation phase. For flow assays with immobilized vascular ligands, recombinant VCAM-1 Fc (2 μg/ml) or ICAM-1 Fc (5 μg/ml) (in 20 mg /ml BSA in PBS) was overlaid on protein A pre-coated polystyrene plates overnight at 4 °C. Plates were then washed with PBS three times followed by blocking with 20 mg/ml BSA solution for 2 h at 37 °C. The immobilized vascular ligands coated plates were assembled as lower wall of the flow chamber as mentioned above. The interactions of the $CD4^+$ T cells with the adhesive substrates were manually tracked as mentioned above. The cell tether examined were rolling, transient tether, firm tether, spreading, locomotion and detachment (*138*). Transient tether was defined as cells that stay for less than 4 s after flow starts, firm tether was defined as cells that stay for more than 4 s after flow starts, rolling was defined as cells that persistently rolled for at least 2 s after the flow starts, adherent cells were defined as cells that stay throughout the 15 min shear flow period. Spreading cells were defined as cells that increase their area,

perimeter and also undergo darkening of the edges (*149*). Cells undergoing spreading and migration were included in the locomotion category.

Western blot

$CD4^+$ T cells were centrifuged at 2000 rpm for 5 min, washed twice with ice-cold PBS and lysed using RIPA buffer (Teknova) supplemented with protease inhibitor cocktail (1:100) (Sigma-Aldrich) and phosphatase inhibitor cocktail (1:10) (Roche). The lysates were then centrifuged at 10,000 rpm for 10 min to remove the cells debris. Protein concentration was determined using BCA Protein Assay kit (Pierce). Equal amounts of protein were loaded and run on 10% SDS-PAGE gel. Proteins were then transferred onto a nitrocellulose membrane (Bio-Rad Laboratories). The membrane was blocked for 1 h at room temperature with 5% non-fat dry milk in Tris- buffered saline (Bio-Rad) supplemented with 0.1% tween-20 (Sigma-Aldrich) (TBS-T) before adding the primary antibodies in 5% BSA in TBS-T and incubated overnight at 4 °C. Membranes were washed three times with TBS-T, followed by incubation with horseradish-peroxidase-conjugated secondary antibody (HRP) in 5% non-fat dry milk in TBS-T at room temperature for 2 h and washed 3 more times. Proteins were visualized and quantitated with SuperSignal West Femto Maximum Sensitivity Substrate (Pierce) using Syngene G:Box with GeneSnap BioImaging software. Probing with ERK1/2 and Raf-1 antibody was used for loading control for phospho ERK1/2 and phospho Raf-1 respectively.

Statistical analysis

Experimental groups were compared by analyzing data with Student's unpaired t-test using GraphPad Prism version 7.00 for Mac. Probability levels for statistically significant differences are indicated by the p value in the results and corresponding asterisks in the figures. (*P<0.05, **p<0.002, ***p<0.0002, **** p<0.0001).

Figure 3.1

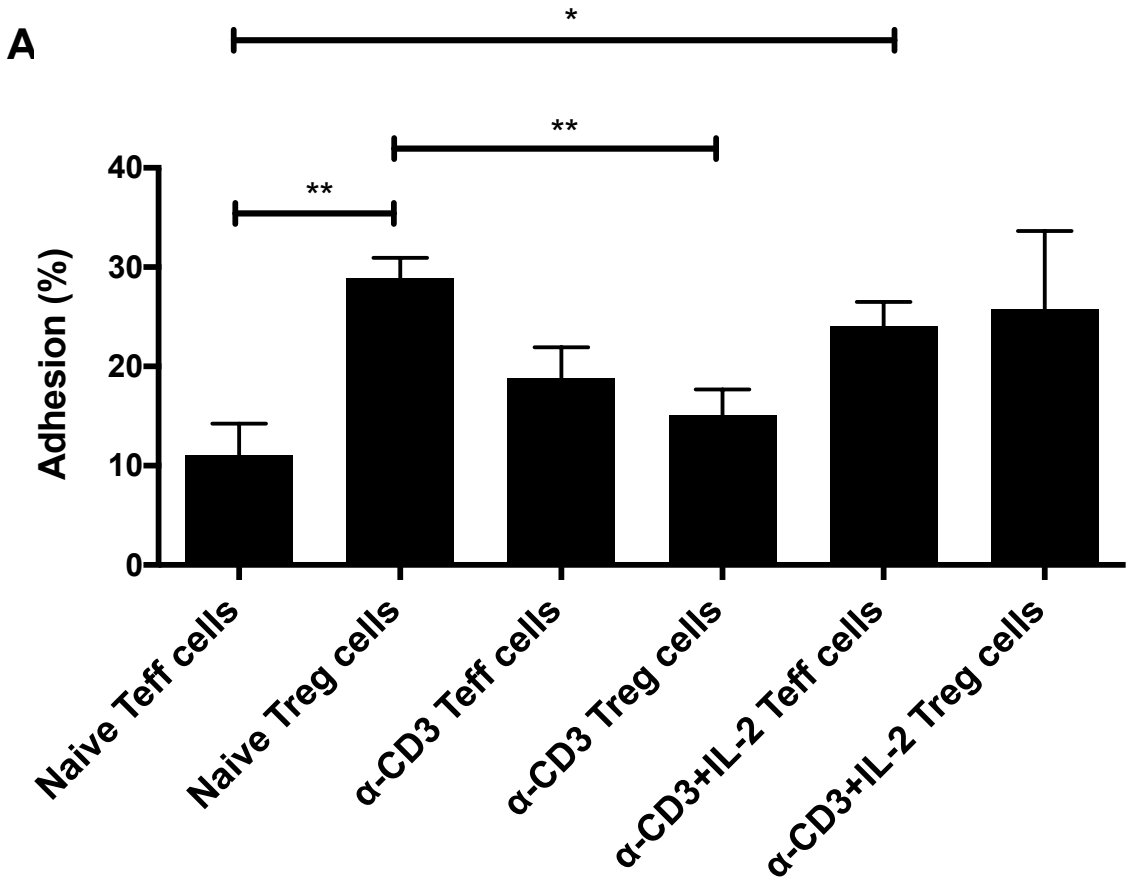
A
*
**
**
40
30
20
10
0
Adhesion (%)
Naive Teff cells
Naive Treg cells
α-CD3 Teff cells
α-CD3 Treg cells
α-CD3+IL-2 Teff cells
α-CD3+IL-2 Treg cells

Figure 3.1

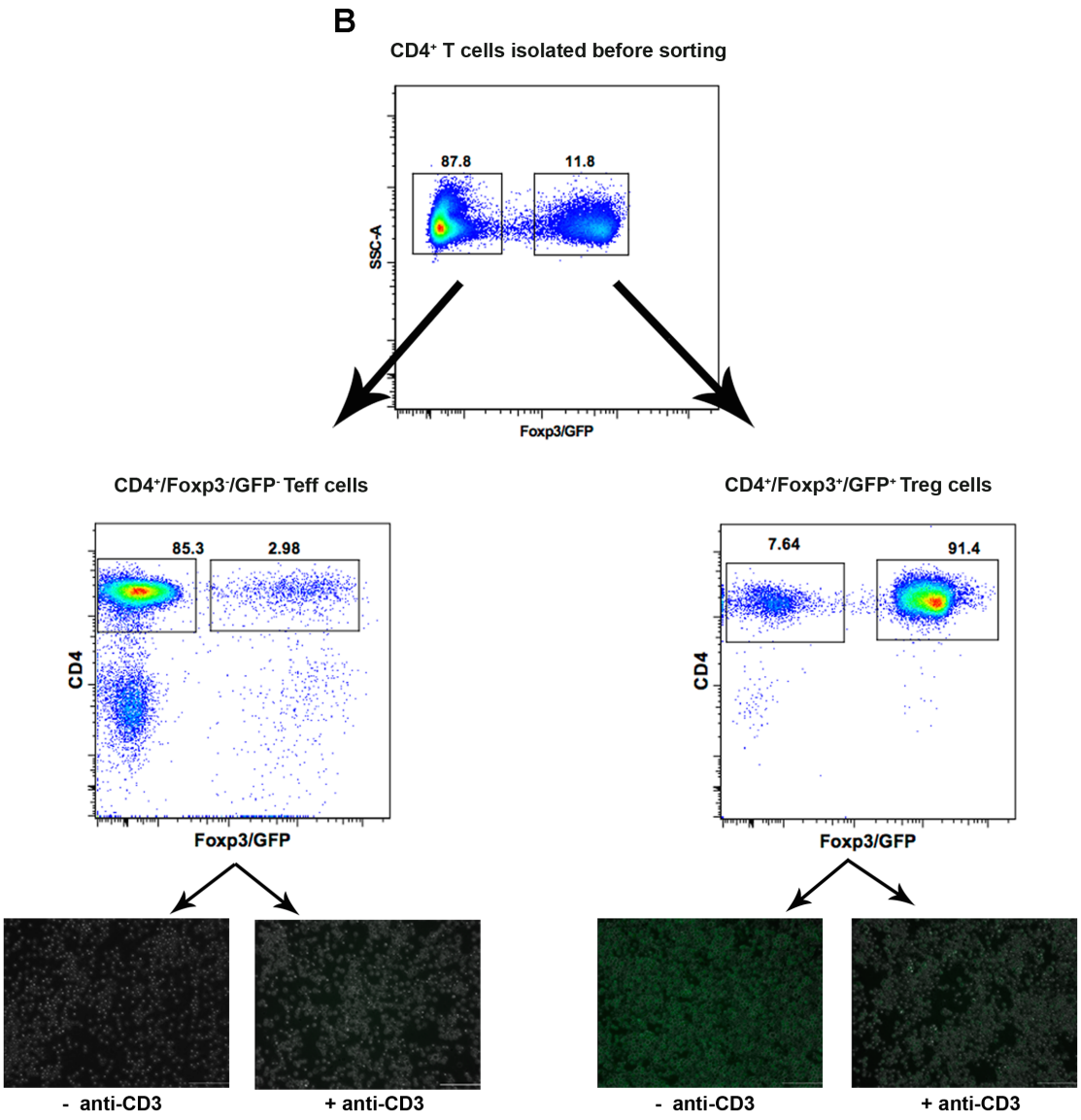
B
CD4+ T cells isolated before sorting
87.8
11.8
SSC-A
Foxp3/GFP
CD4+/Foxp3-/GFP- Teff cells
85.3
2.98
CD4
Foxp3/GFP
- anti-CD3
+ anti-CD3
CD4+/Foxp3+/GFP+ Treg cells
7.64
91.4
CD4
Foxp3/GFP
- anti-CD3
+ anti-CD3

Figure 3.1

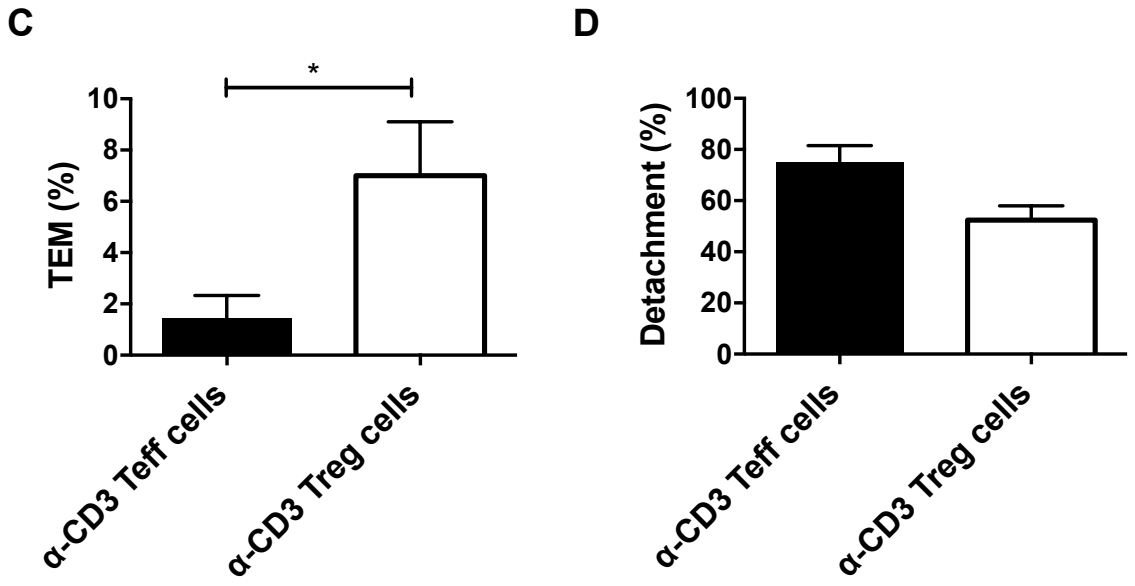

Fig. 3.1: Differential motility of naive and *in vitro* activated $CD4^+$ Teff and Treg cells while interacting with endothelial cell monolayers under shear stress conditions.

(A) Adhesion of $CD4^+CD25^-$ Teff cells and $CD4^+CD25^+$ Treg cells isolated from spleens assayed under shear stress conditions (5 dyn/cm^2); naive (for naive Teff and naive Treg cell flow assays: n=4, 2 independent experiments), anti-CD3 stimulation (for anti-CD3 activated Teff cell assays: n=5, 3 independent experiments; anti-CD3 activated Treg cell assays: n=7, 6 independent experiments) and anti-CD3 + IL-2 (anti-CD3 + IL-2 Teff cell assays: n=7, 3 independent experiments; anti-CD3 + IL-2 Treg cell assays: n=5, 3 independent experiments). (B) Percentage of $Foxp3^-GFP^-$ Teff cells and $Foxp3^+GFP^+$ Treg cells within the $CD4^+$ T cell population isolated from spleens of *Foxp3gfp.KI* mice before and after sorting by flow cytometry. (C) TEM and (D) detachment of anti-CD3 activated $CD4^+Foxp3^-GFP^-$ Teff cells and $CD4^+Foxp3^+GFP^+$ Treg cells sorted based on

GFP expression from *Foxp3gfp.KI* mice under shear stress (flow). ($Foxp3^{-}GFP^{-}$ Teff cell assays: n=4, 2 independent experiments; $Foxp3^{+}/GFP^{+}$ Treg cell assays: n=3, 3 independent experiments.) Data (mean ± SEM) are expressed as percentage out of total cells present in the flow chamber before the start of flow.

Figure 3.2

A

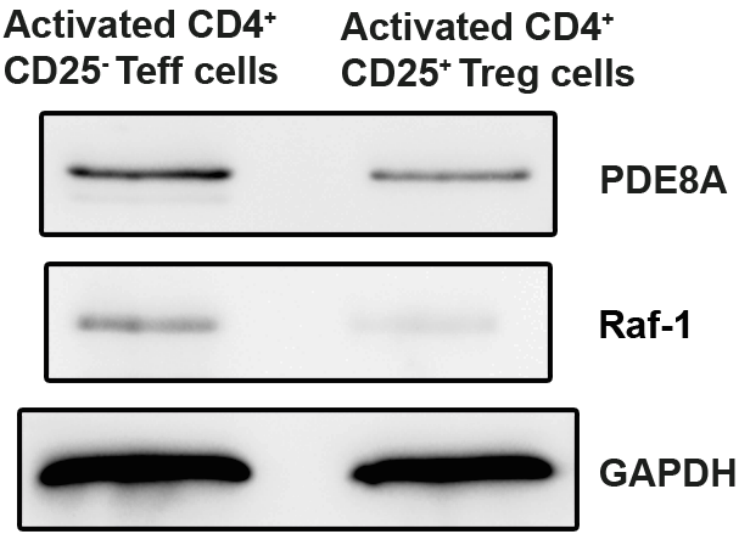
Activated CD4+ CD25- Teff cells
Activated CD4+ CD25+ Treg cells
PDE8A
Raf-1
GAPDH

B

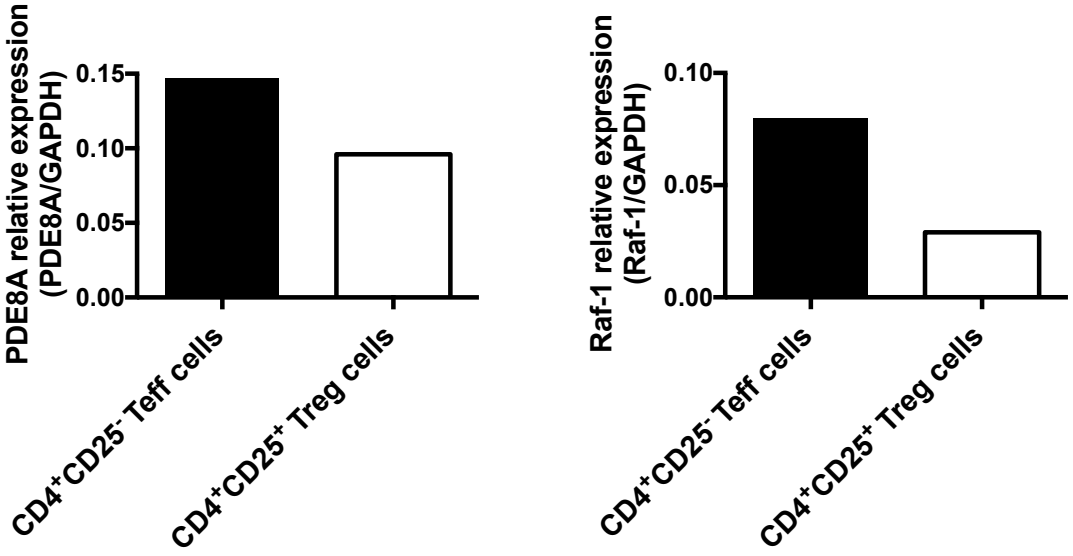
PDE8A relative expression (PDE8A/GAPDH)
0.15
0.10
0.05
0.00
CD4+CD25- Teff cells
CD4+CD25+ Treg cells
Raf-1 relative expression (Raf-1/GAPDH)
0.10
0.05
0.00
CD4+CD25- Teff cells
CD4+CD25+ Treg cells

Figure 3.2

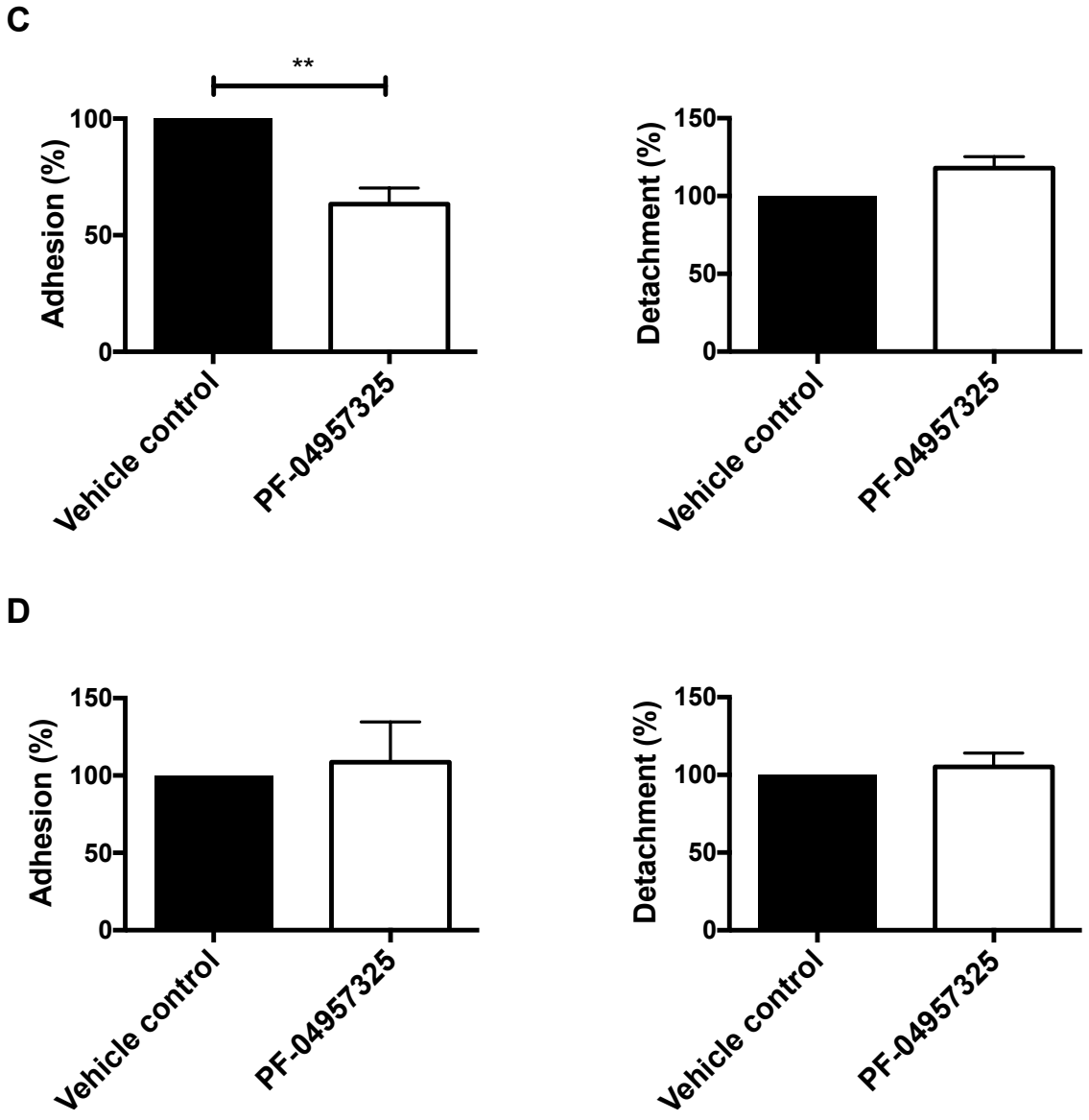

Fig. 3.2: PDE8 inhibition at the catalytic moiety suppresses $CD4^+$ Teff cell motility but not Treg cell motility.

(A) The immunoblot shows PDE8A and Raf-1 expression of *in vivo* MOG_{35-55} activated $CD4^+CD25^-$ Teff and $CD4^+CD25^+$ Treg cells isolated from the draining PLNs. (B) Relative PDE8A expression normalized to GAPDH. Data are from T

cells isolated from lymph nodes of 5 mice. (C, D) LPS activated endothelial cells and MOG_{35-55} primed $CD4^+$ T cells were treated with either vehicle or 1 μM PF-04957325 for 1 h. Adhesion and detachment of $CD4^+Foxp3^-GFP^-$ Teff cells (C) and $CD4^+Foxp3^+GFP^+$ Treg cells (D) were analyzed under shear stress. Data represent mean ± SEM results from 4 independent experiments and are expressed as percentage of total cells that accumulate in the flow chamber before the flow starts. Percentage of cells in each category is normalized to the vehicle condition set at 100 percent.

Figure 3.3

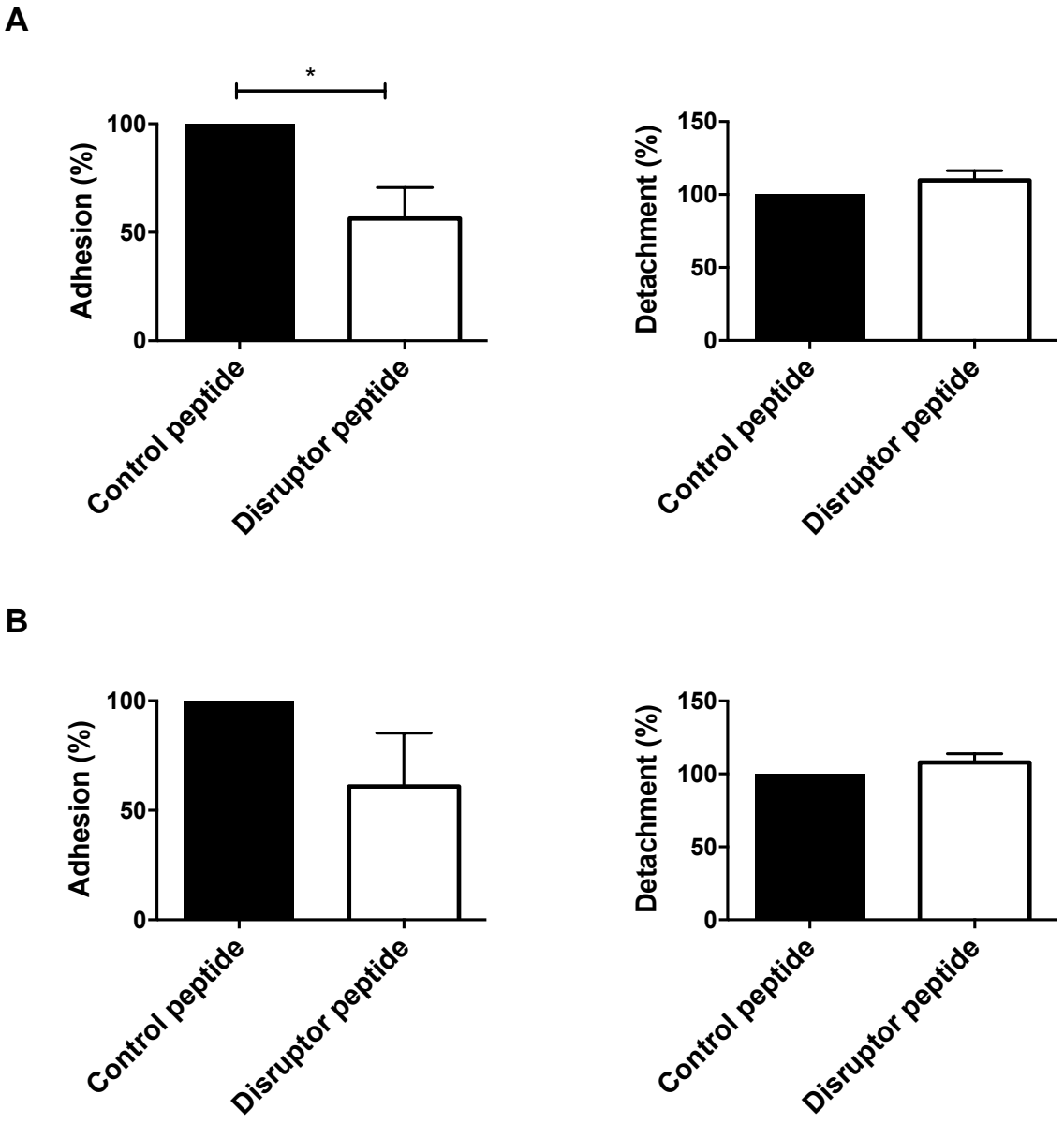

Fig. 3.3: Disruption of the PDE8A-Raf-1 complex suppresses both $CD4^+$ Teff and Treg cell motility.

LPS activated endothelial cells and MOG_{35-55} primed $CD4^+$ T cells were treated with either 10 μM scrambled (control) peptide or disruptor peptide for 4 h. Adhesion and detachment of $CD4^+Foxp3^-GFP^-$ Teff cells (A) and

$CD4^+Foxp3^+GFP^+$ Treg cells (B) were analyzed under shear stress. Data represent mean ± SEM results from 3-4 independent experiments and are expressed as percentage of total cells that accumulate in the flow chamber before the flow starts. Percentage of cells in each category is normalized to the vehicle condition set at 100 percent.

Figure 3.4

A

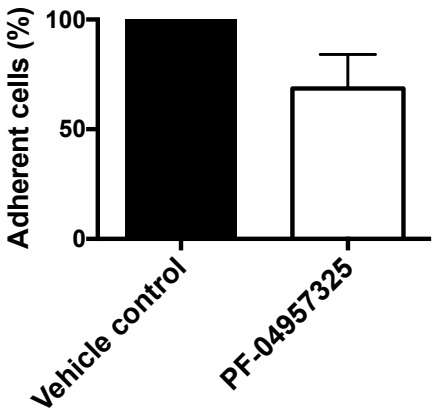
Adherent cells (%)
100
50
0
Vehicle control
PF-04957325

B

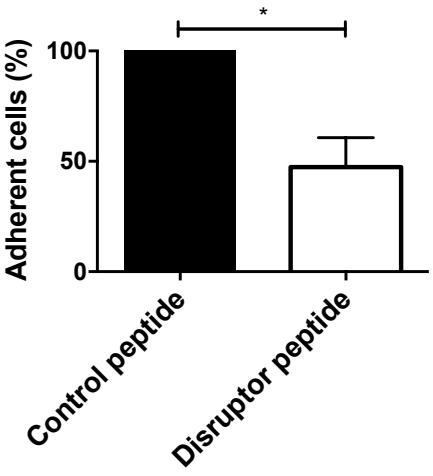
*
Adherent cells (%)
100
50
0
Control peptide
Disruptor peptide

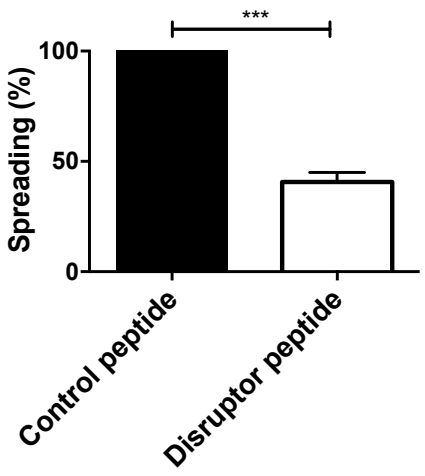
***
Spreading (%)
100
50
0
Control peptide
Disruptor peptide

Figure 3.4

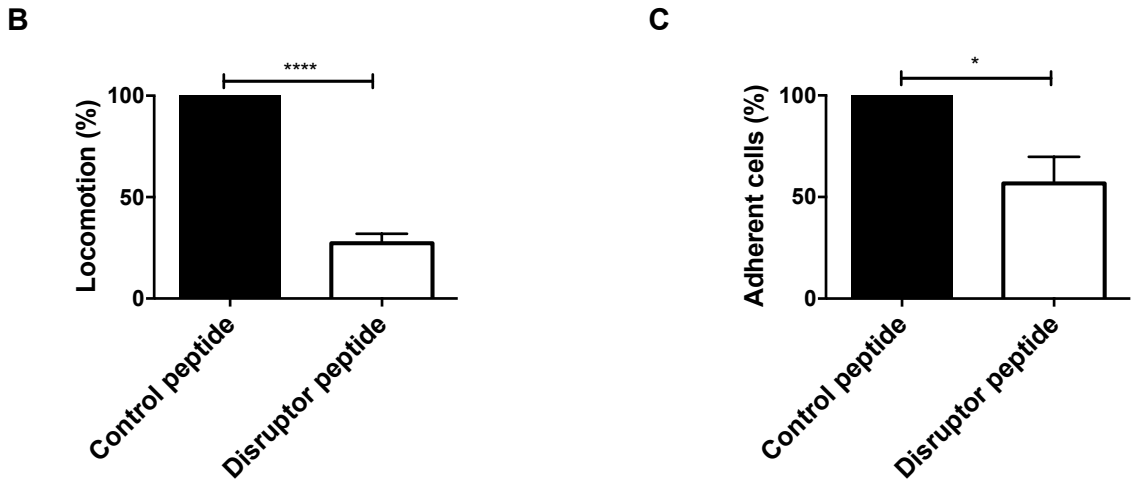

Fig. 3.4: Adhesiveness to ICAM-1 significantly affected by disruption of the PDE8A-Raf-1 complex, but not by PDE8 inhibition at the catalytic moiety. MOG_{35-55} primed $CD4^+$ T cells were treated with vehicle or 1 μM PDE8 inhibitor for 1 h (A) or 10 μM control peptide or disruptor peptide for 4 h (B, C). Spontaneous tethering (adherent cells, spreading or locomotion) of the $CD4^+Foxp3^-GFP^-$ Teff cells (A, B) and $CD4^+Foxp3^+GFP^+$ Treg cells (C) while interacting with high density ICAM-1-Fc (5 μg/ml) were analyzed under flow. Data represent mean ± SEM results from 3 independent experiments and are expressed as percentage of total cells that accumulate in the flow chamber before the flow starts. Percentage of cells in each category is normalized to the vehicle condition set at 100 percent.

Figure 3.5

A

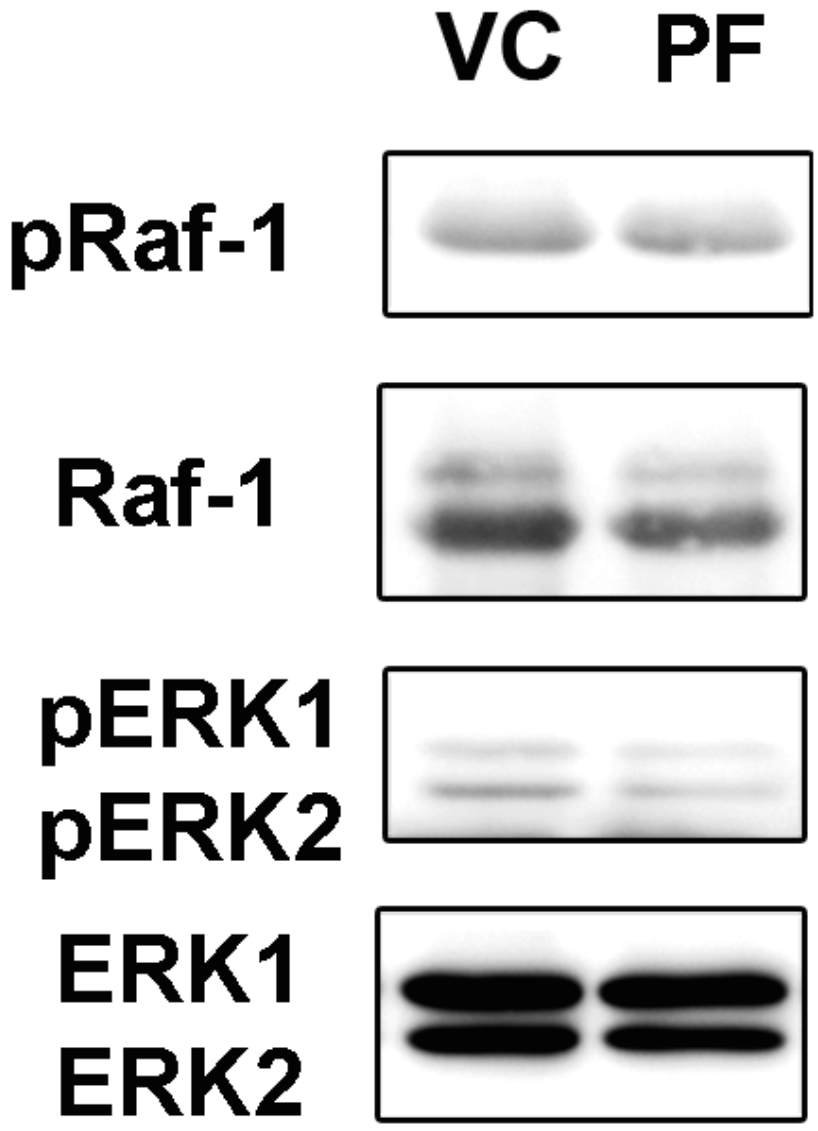

Figure 3.5

B

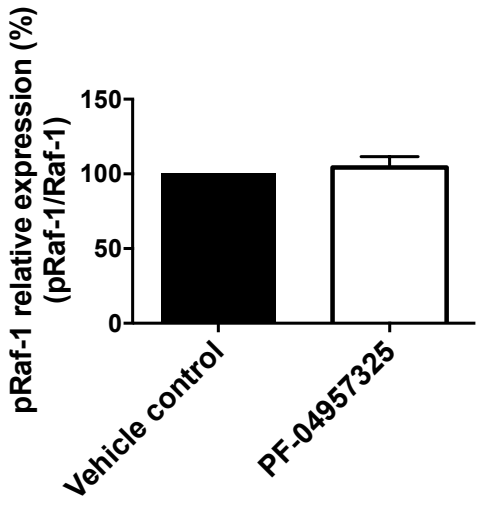
pRaf-1 relative expression (%)
(pRaf-1/Raf-1)
150
100
50
0
Vehicle control
PF-04957325

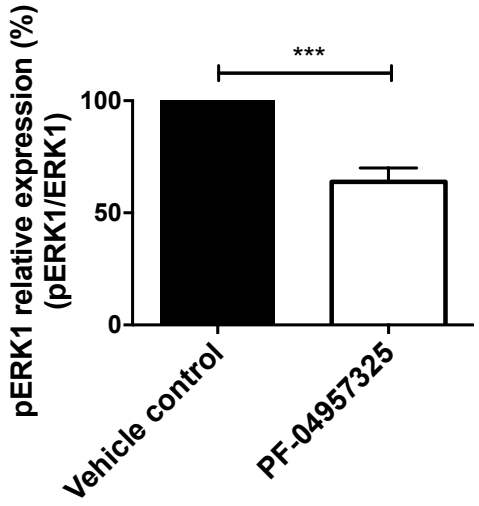
pERK1 relative expression (%)
(pERK1/ERK1)
***
100
50
0
Vehicle control
PF-04957325

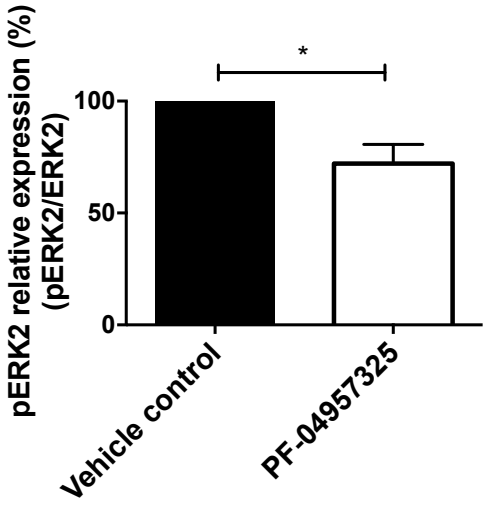
pERK2 relative expression (%)
(pERK2/ERK2)
*
100
50
0
Vehicle control
PF-04957325

Figure 3.5

C

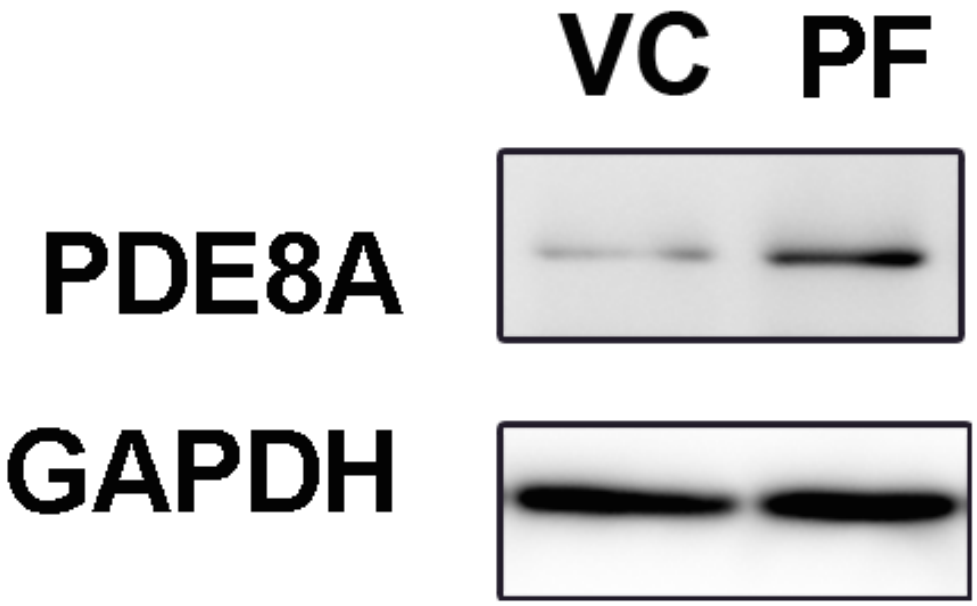
VC
PF
PDE8A
GAPDH

D

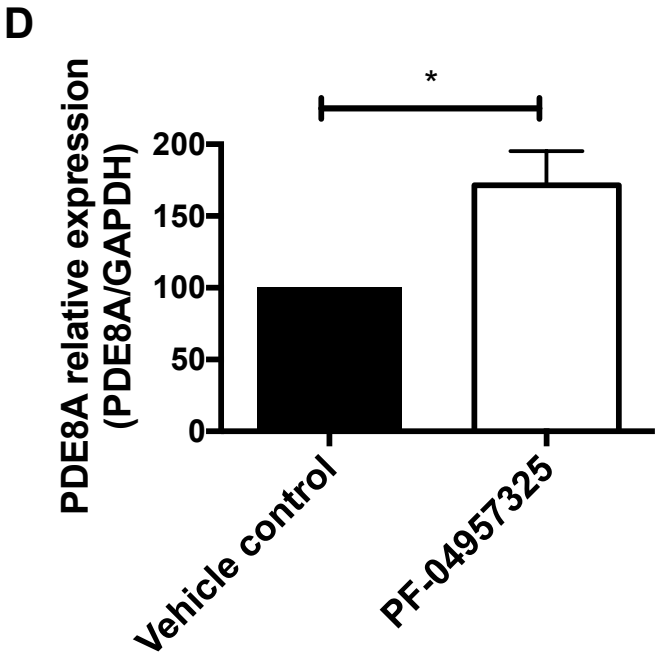
PDE8A relative expression
(PDE8A/GAPDH)
200
150
100
50
0
*
Vehicle control
PF-04957325

Fig. 3.5: Inhibition of PDE8 in $CD4^+$ T cells diminishes ERK1/2 phosphorylation induced by CD3.

MOG_{35-55} primed $CD4^+$ T cells were treated with vehicle or 1 μM PF-04957325 for 1 h followed by anti-CD3 stimulation for 15 min. Cell lysates were then probed for (A, B) phospho Raf-1 (S259), Raf-1, phospho ERK1/2, ERK1/2, (C) PDE8A and GAPDH by Western blot. (B, C) Bands were quantitated by densitometry and data are presented as phospho-Raf-1 (S259) relative to Raf-1, phospho-ERK1/2 relative to ERK1/2 and PDE8A expression relative to GAPDH. Data represent mean ± SEM results from 4 independent experiments (n=7).

Figure 3.6

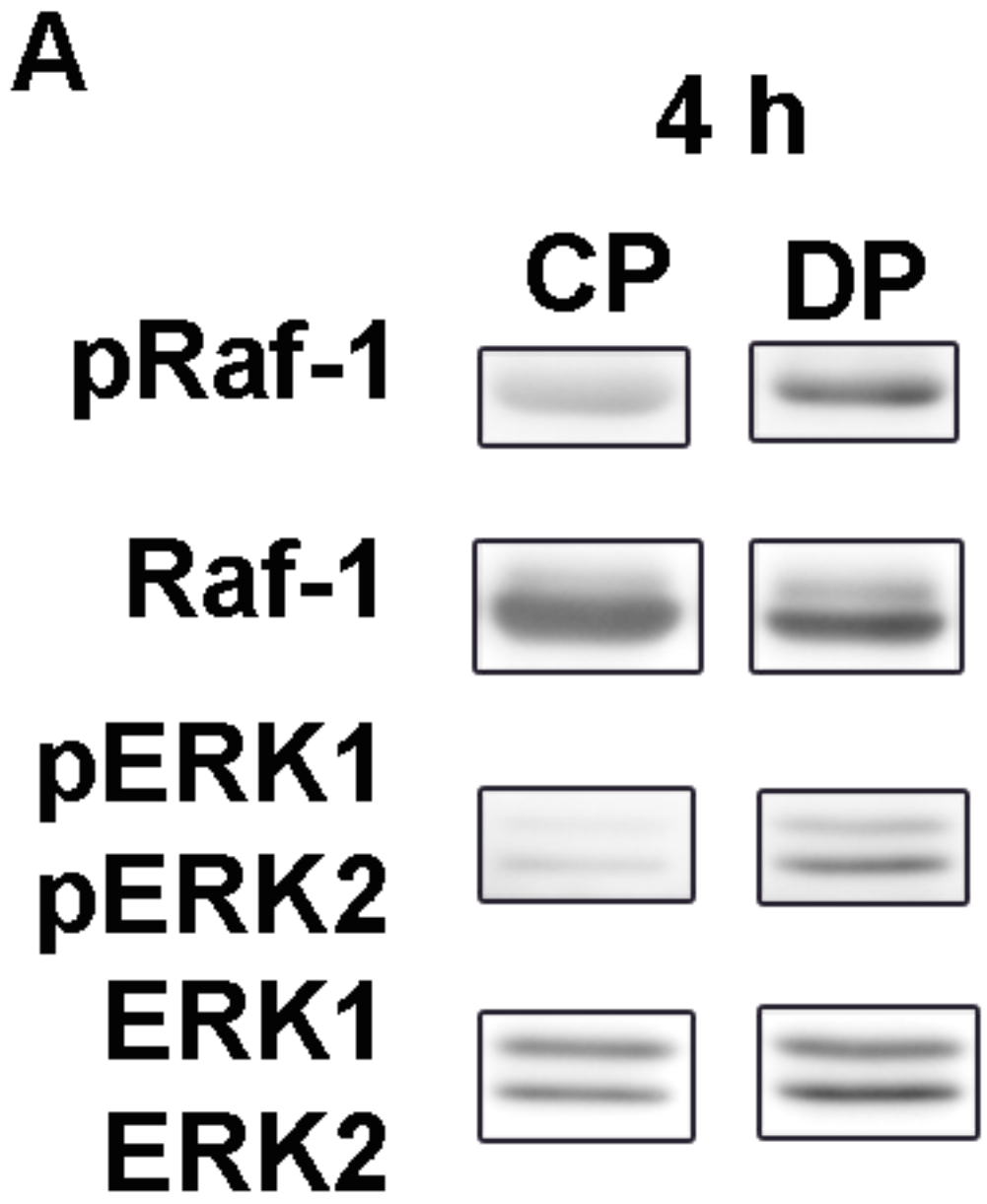

Figure 3.6

B

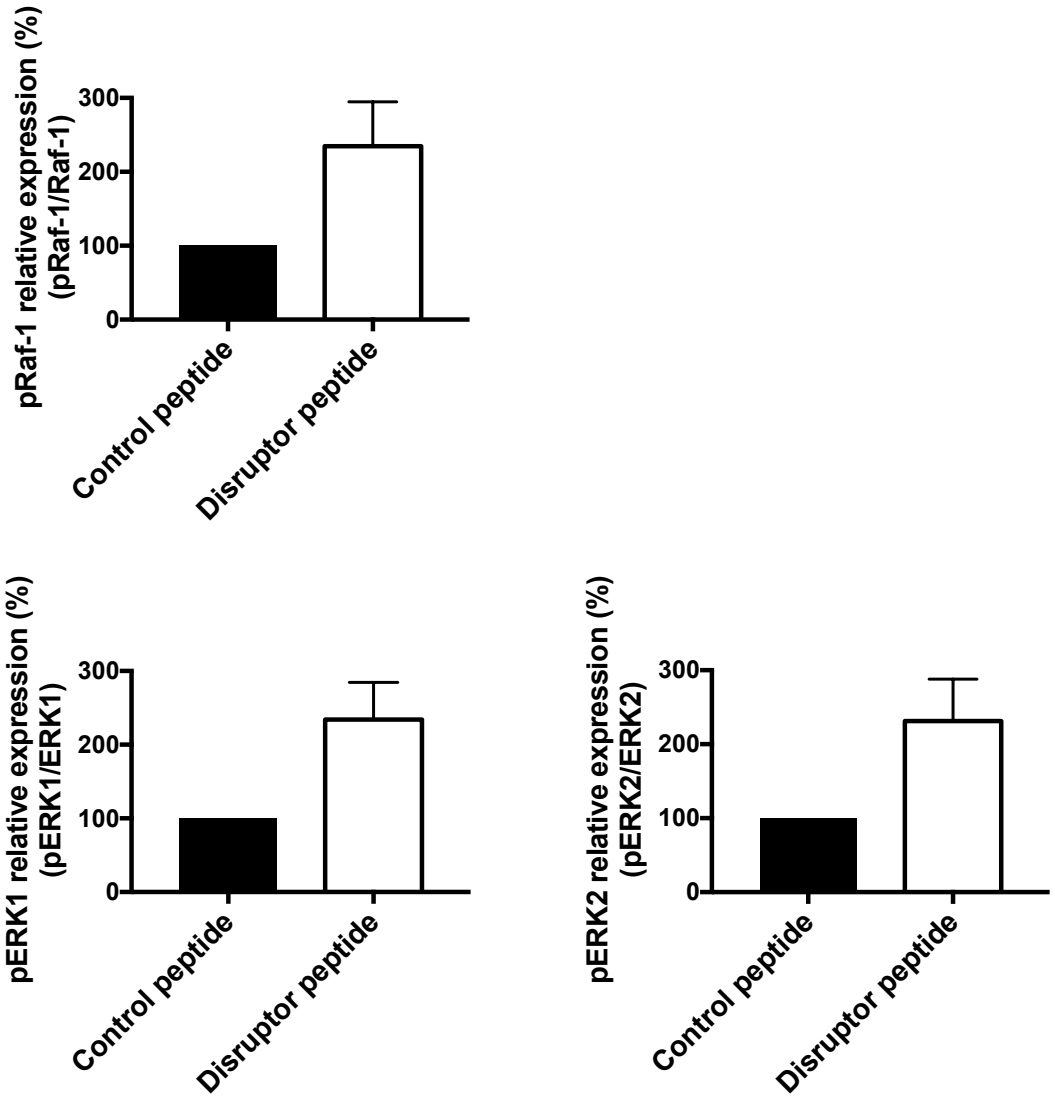

Fig. 6: Disruption of the PDE8A-Raf-1 complex in CD4$^+$ T cells increases inhibitory Raf-1 phosphorylation at serine 259 and increases ERK1/2 phosphorylation induced by CD3.

MOG_{35-55} primed CD4$^+$ T cells were treated with 10 μM control peptide (CP) or disruptor peptide (DP) for 4 h (A) followed by anti-CD3 stimulation for 15 min. Cell lysates were then probed for phospho Raf-1 (S259), Raf-1, phospho ERK1/2

and ERK1/2 by Western blot. (B) Bands were quantitated by densitometry and data are presented as phospho-Raf-1 (S259) relative to Raf-1 and phospho-ERK1/2 relative to ERK1/2 at 4 h. Data represent mean ± SEM from 2 independent experiments (n=5).

Figure 3.S1

A

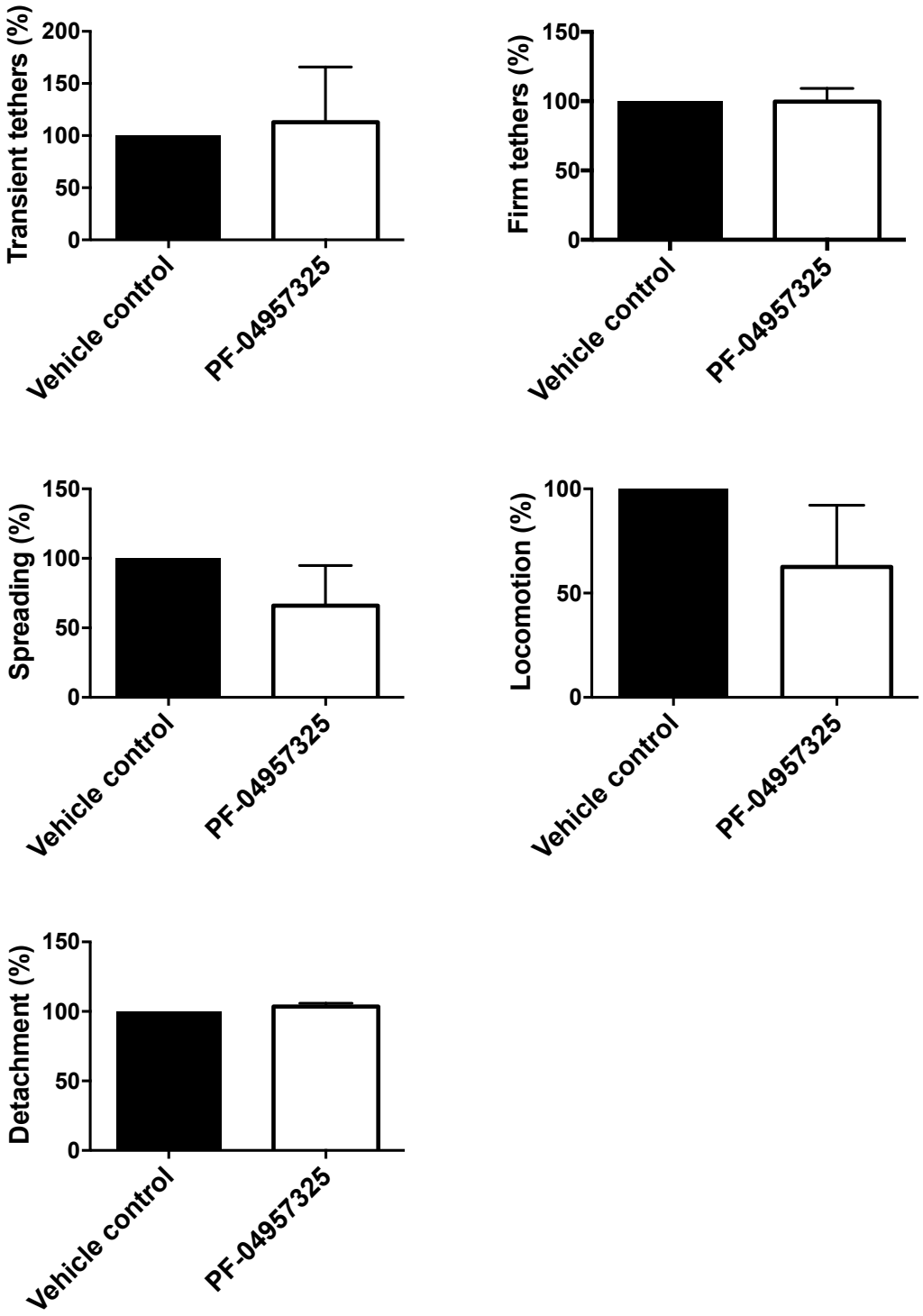
Transient tethers (%)
200
150
100
50
0
Vehicle control
PF-04957325
Firm tethers (%)
150
100
50
0
Vehicle control
PF-04957325
Spreading (%)
150
100
50
0
Vehicle control
PF-04957325
Locomotion (%)
100
50
0
Vehicle control
PF-04957325
Detachment (%)
150
100
50
0
Vehicle control
PF-04957325

Figure 3.S1

B

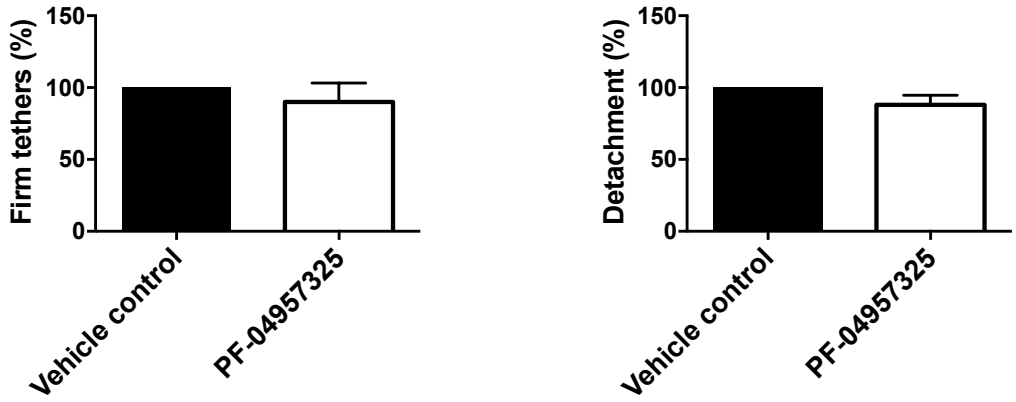

C

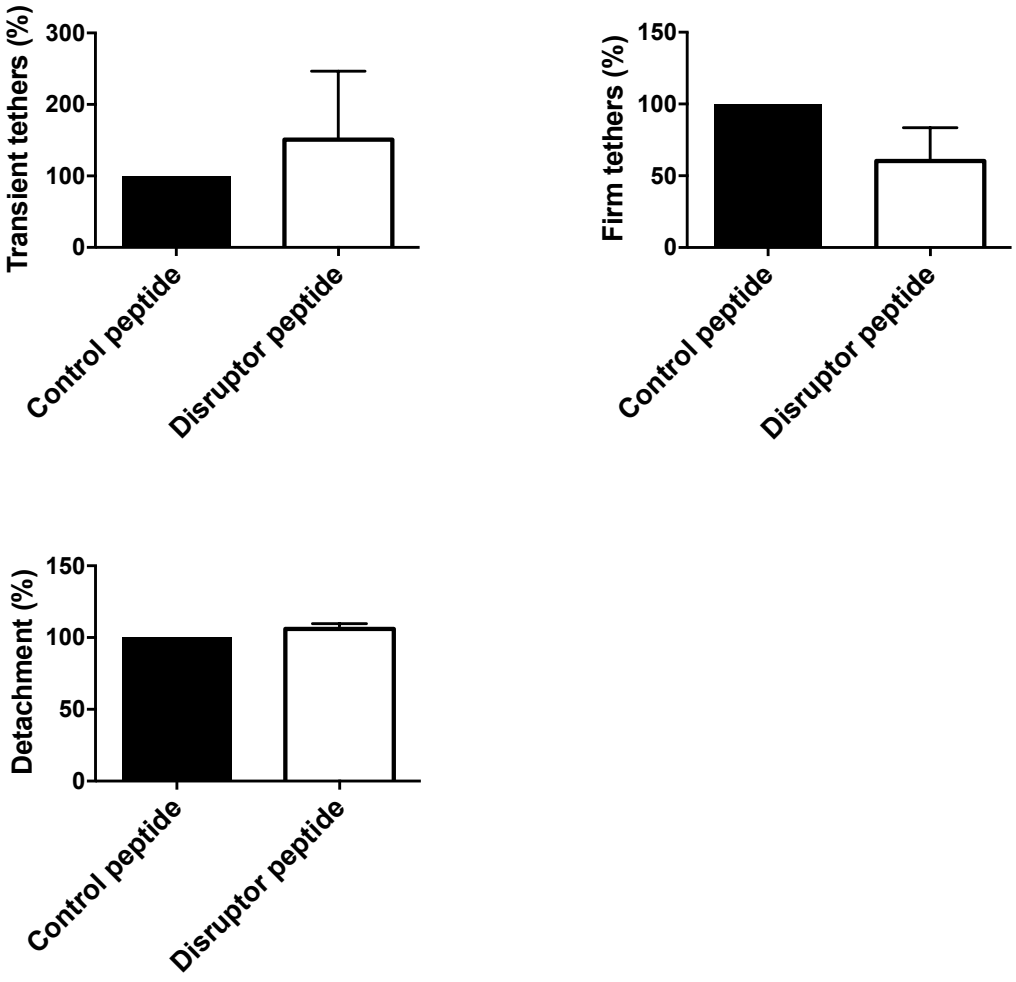

Figure 3.S1

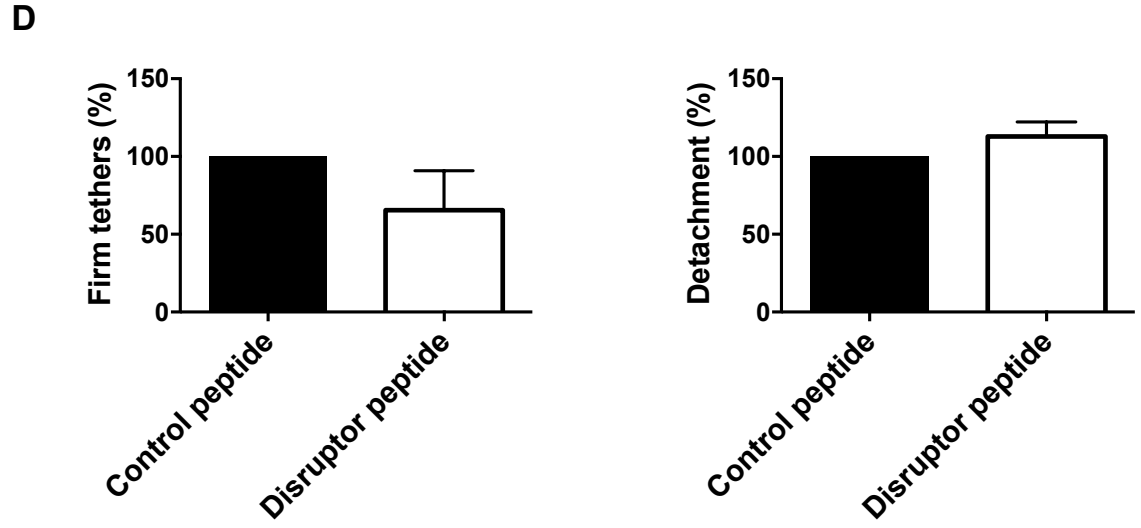

Fig. 3.S1: Adhesiveness to ICAM-1 significantly affected by disruption of the PDE8A-Raf-1 complex, but not by PDE8 inhibition at the catalytic moiety.

MOG_{35-55} primed $CD4^+$ T cells were treated with vehicle or 1 μM PDE8 inhibitor for 1 h (A, B) or 10 μM control peptide or disruptor peptide for 4 h (C, D). Spontaneous tethering (rolling, transient tether, firm tether, spreading, locomotion) and detachment of the $CD4^+Foxp3^-GFP^-$ Teff cells (A, C) and $CD4^+Foxp3^+GFP^+$ Treg cells (B, D) while interacting with high density ICAM-1-Fc (5 μg/ml) were analyzed under flow. Data represent mean ± SEM results from 3 independent experiments and are expressed as percentage of total cells that accumulate in the flow chamber before the flow starts. Percentage of cells in each category is normalized to the vehicle condition set at 100 percent.

Figure 3.S2

A

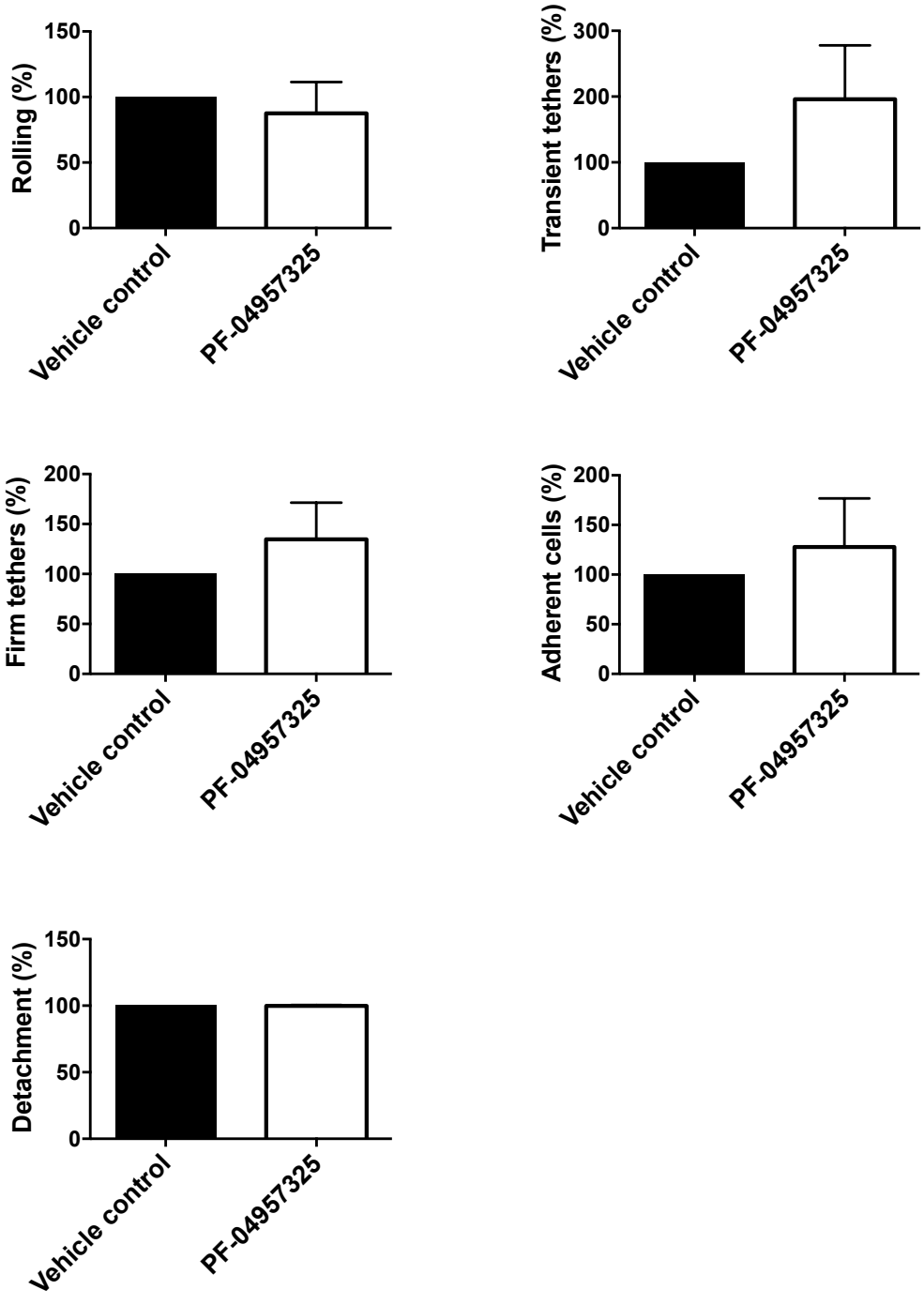
Rolling (%)
150
100
50
0
Vehicle control
PF-04957325
Transient tethers (%)
300
200
100
0
Vehicle control
PF-04957325
Firm tethers (%)
200
150
100
50
0
Vehicle control
PF-04957325
Adherent cells (%)
200
150
100
50
0
Vehicle control
PF-04957325
Detachment (%)
150
100
50
0
Vehicle control
PF-04957325

Figure 3.S2

B

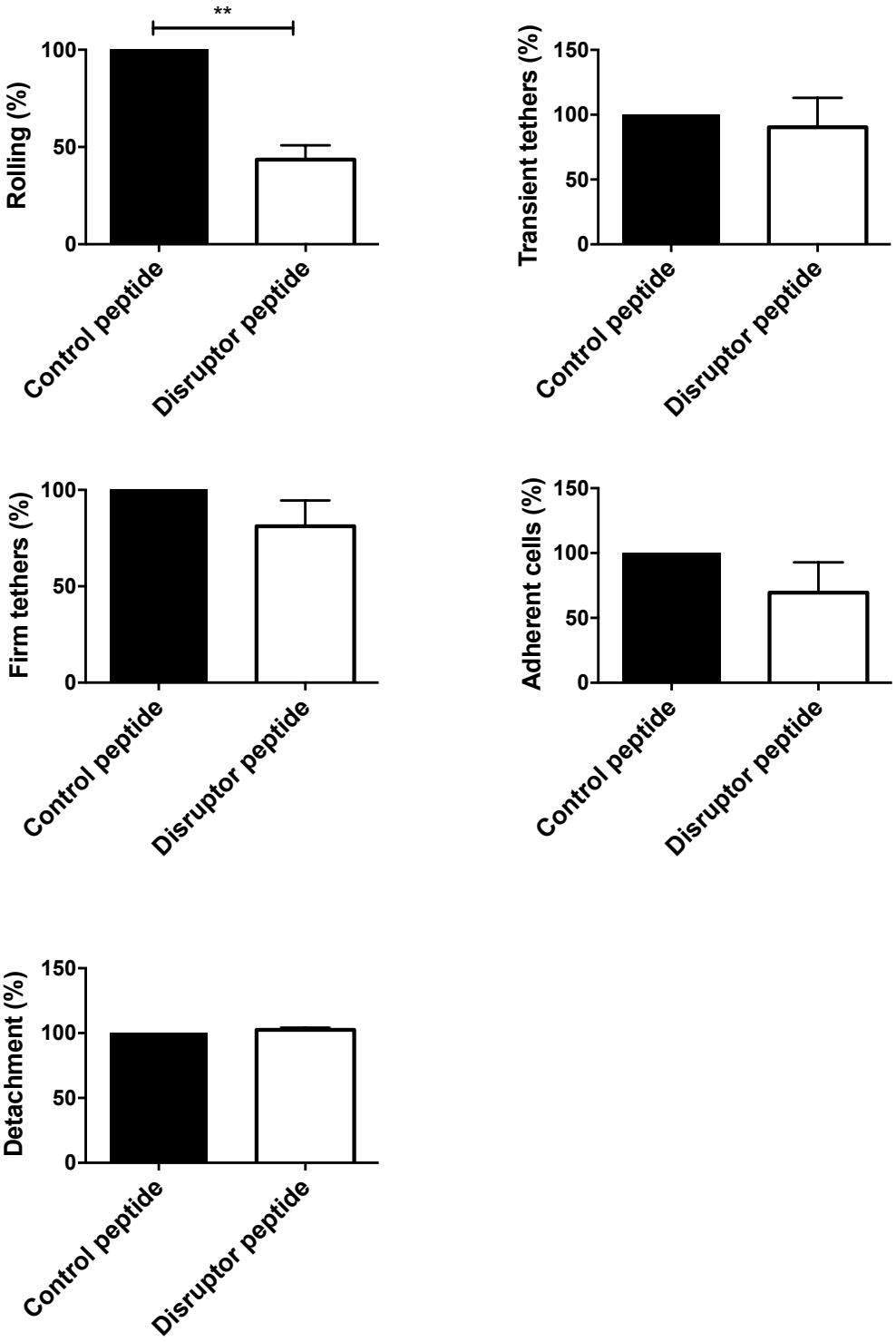
**
Rolling (%)
100
50
0
Control peptide
Disruptor peptide
Transient tethers (%)
150
100
50
0
Control peptide
Disruptor peptide
Firm tethers (%)
100
50
0
Control peptide
Disruptor peptide
Adherent cells (%)
150
100
50
0
Control peptide
Disruptor peptide
Detachment (%)
150
100
50
0
Control peptide
Disruptor peptide

Fig. 3.S2: Firm adhesiveness of $CD4^+$ T cells to VCAM-1 is not affected by PDE8 inhibition at the catalytic moiety or by disruption of the PDE8A-Raf-1 complex.

MOG_{35-55} primed $CD4^+$ T cells were treated with either vehicle or 1 μM PF-04957325 for 45 min (A) or 10 μM control peptide or disruptor peptide for 4 h (B). Spontaneous tethering (rolling, transient tether, firm tether, adherent cells) and detachment of the $CD4^+$ T cells while interacting with high density VCAM-1- Fc (2 μg/ml) were analyzed under shear stress of 5 dyn/cm^2. Data represent mean ± SEM results from 4 independent experiments and are expressed as percentage of total cells that accumulate in the flow chamber before the flow starts. Percentage of cells in each category is normalized to the vehicle condition set at 100 percent.

Figure S3

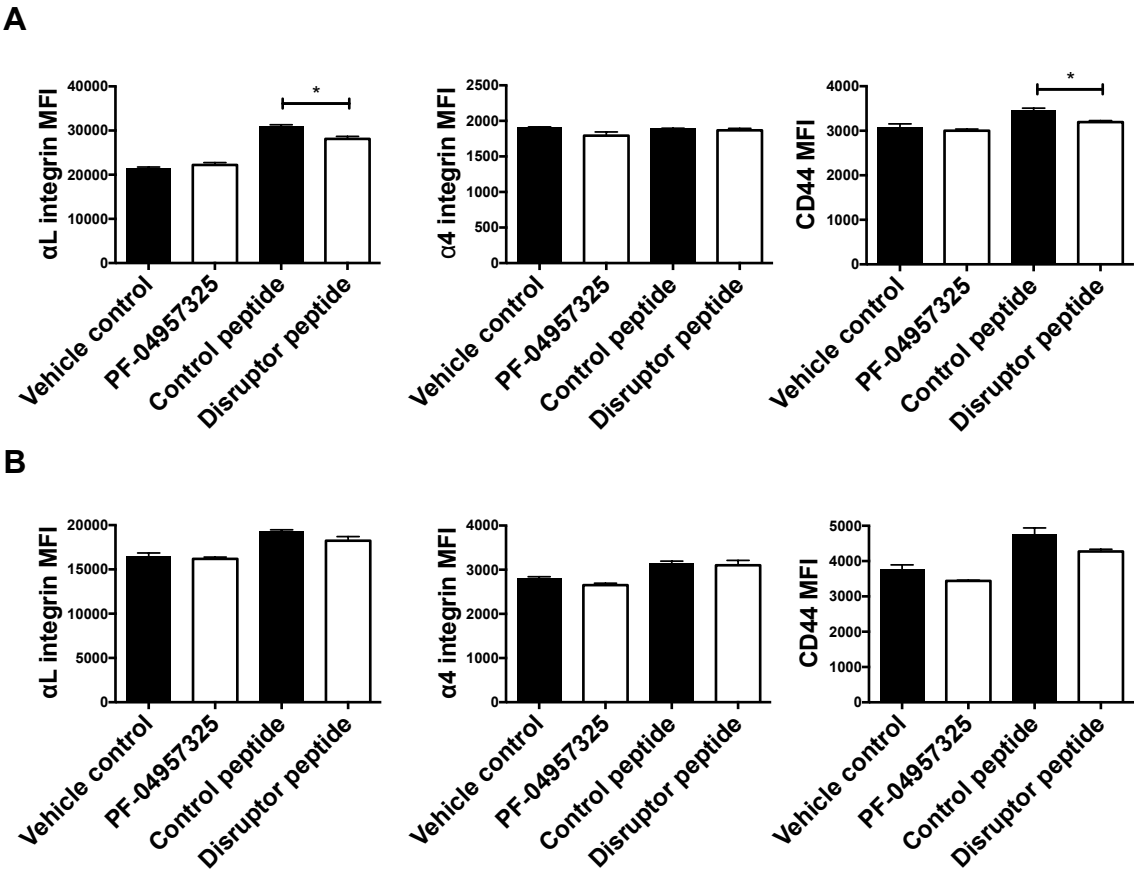

Fig. S3: Integrin surface expression is not altered by PDE8 inhibition at the catalytic moiety and marginally reduced by disruption of the PDE8A-Raf-1 complex.

$CD4^+$ T cells isolated from spleens of *Foxp3gfp.KI* mice were treated with plate-bound anti-CD3 (10 µg/ml) for 18 h followed by treatment with vehicle or 1 µM PF-04957325 for 1 h or 10 µM control peptide or PDE8A-Raf-1 disruptor peptide for 4 h. Expression of αL integrin, α4 integrin, and CD44 was evaluated by flow cytometry. Data show MFI of the αL^+, $\alpha 4^+$ and $CD44^+$ cells within the $Foxp3^-GFP^-$ Teff cell (A) and $Foxp3^+GFP^+$ Treg cell populations (B). Data represent mean ± SEM results from 1 experiment (n=3).

Figure S4

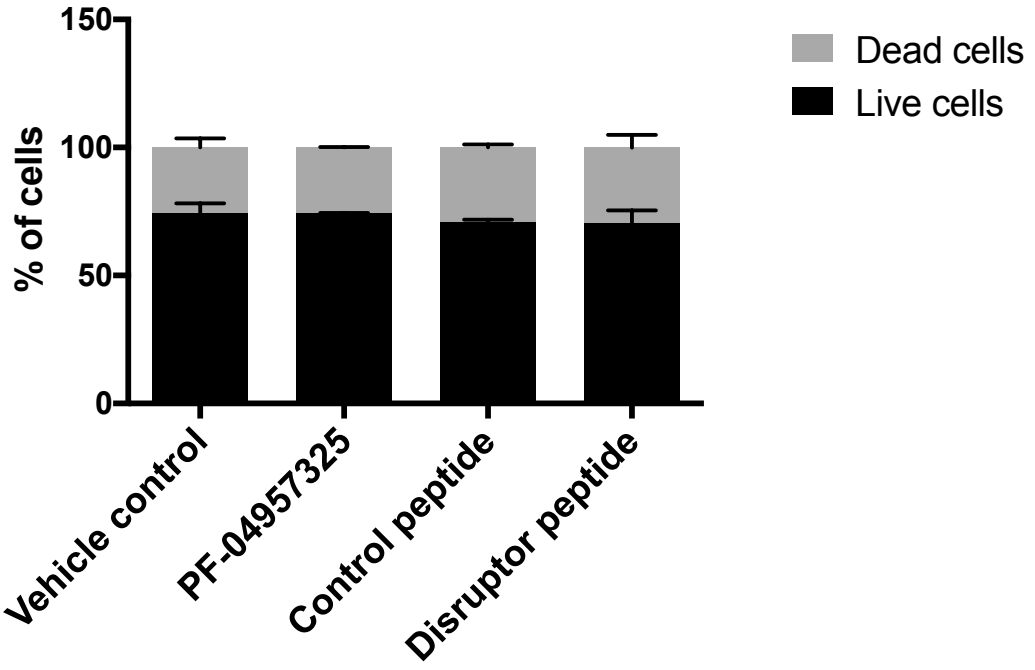

Fig. S4: Inhibition of PDE8 or disruption of the PDE8A-Raf-1 complex does not affect viability of $CD4^+$ T cells.

The viability of the $CD4^+$ T cells after treatment was assessed using the trypan blue assay. The graphs represent the percentage of live and dead cells within each treatment group. Data represent mean ± SEM results from 1 experiment (n=3).

Chapter 4

Targeting Phosphodiesterase-8 (PDE8) suppresses accumulation of immune cells to the central nervous system in experimental autoimmune encephalomyelitis

4.1 Summary

Phosphodiesterases have been used as targets for treatment of inflammatory, diseases with two PDE4 inhibitors recently approved for treatment of psoriasis/psoriatic arthritis and COPD. We have previously demonstrated PDE8 and PDE8A-Raf-1 kinase complex mediated regulation of MOG_{35-55} activated $CD4^+$ effector T cell adhesion and locomotion under shear flow conditions. In this paper, we have explored treatment with PDE8 specific inhibitor in a T cells mediated disease model-experimental autoimmune encephalomyelitis (EAE). We report a suppression of clinical signs of disease after treatment with PDE8 inhibitor PF-04957325 in chronic and relapsing-remitting EAE. Further, there is reduction in infiltrates in the CNS as observed by histology and counting mononuclear cells isolated from spinal cord. Additionally, the PDE8 inhibitor treatment induces a relative increase in anti-inflammatory phenotype by increasing the percentage of IL-10 producing $CD4^+$ T cells and reducing encephalitogenic Th1, Th17 cells in the CNS. Our study demonstrates the importance of targeting PDE8 in autoimmune inflammation model without affecting the immunoregulatory Treg cells.

4.2 Introduction

cAMP is a known regulator of physiological functions in a cell and is a known target for regulating immune responses and inflammation (*77*). Extracellular ligand binding to G protein coupled receptors (GPCRs) lead to cAMP synthesis via activation of adenylyl cyclase and convertion of ATP to cAMP. Activation of T cells lead to a transient upregulation of cAMP levels, which is then degraded by phosphodiesterase enzymes (*150*). PDE are the only known enzymes that are able to hydrolyse and hence maintain spatial and temporal control over formation of cAMP gradients within a cell (*19, 20*). PDEs are divided into 11 different gene families based on their specificity for cAMP or cGMP, structural similarity and mode of regulation (*21*). Specific PDE forms induced in activated lymphocytes are PDE1, PDE3, PDE4, PDE7 and PDE8 (*16, 22-25*). Out of these PDE3, PDE4B and to a lesser extent PDE7A are the major forms of PDE expressed in activated T cells (*26*). PDE4 inhibitor - rolipram has been used to ameliorate clinical signs of EAE models and reduce CNS inflammation when treatment is started after immunization or after onset of disease (*27, 28*). PDE3 inhibitors alone are ineffective at treating Th1 mediated disorders. But PDE4 inhibitor and low doses of PDE3 inhibitors - cilostamide in combination synergistically inhibit T cell proliferation and pro-inflammatory cytokine production of human cells (*26*). PDE7 inhibitor have proved ineffective in suppressing T cell proliferation and mice deficient in PDE7A have functional T cells (*29, 30*). But PDE7 inhibitors when used in combination with PDE4 inhibitors show an additive effect (*31*)**.** These reports suggest that probably there might other PDEs expressed in T cells that might be important for controlling T cell function. Our previous work has shown that PDE8 is important for chemotaxis of T cells and

adhesion of T cells to endothelial cells (*24, 32*). PDE8 has a very high affinity for cAMP with a km value in the range of 40-150 nM (40 fold higher than that of PDE4) and hence might function at lower cAMP concentrations than PDE4 (*34*). PDE8A is insensitive to inhibition by non-specific PDE inhibitor IBMX but is inhibited by the PDE inhibitor dipyridimole (DP) (IC_{50} in the range of 4- 9 μM) (*21*). Work from our lab has shown that only treatment with dipyridamole inhibits chemotaxis of concanavalin A activated splenocytes (*32*). Whereas, inhibition of PDE3, PDE4 or PDE7 did not affect chemoattractant induced migration of cells. Since dipyridamole also inhibits PDE8, this was the first evidence that PDE8 might be an important regulator of migration. Broad PDE inhibitor Dipyridamole treatment at high doses (100 mg/kg-300 mg/kg) on day 7 or day 20 post EAE induction leads to reduction in disease severity and reduction in microglial reactivity (*151*).

PDE8A is expressed in activated $CD4^+$ T cells and we have proven that it regulates adhesion of MOG_{35-55} activated $CD4^+$ effector T cells to inflamed brain endothelium. PDE8A forms a complex with Raf-1 kinase and protects it from cAMP effector protein PKA mediated phosphorylation. We have previously shown that disruption of PDE8A-Raf-1 kinase complex also inhibits MOG_{35-55} activated $CD4^+$ effector T cells to inflamed brain endothelium under shear flow conditions (Basole et al., under review). PDE4 inhibitors increased adhesion of CD4 T cells, and when added along with PDE8 inhibitor reduced the suppression of adhesion. This indicates that PDE8 and PDE4 regulate different pools of cAMP in $CD4^+$ T cells and hence regulate different cAMP mediated functions. Our previous studies have demonstrated that PDE8 does not effect T cells

proliferation, ex vivo cytokine production but specifically targets motility of $CD4^+$ T cells. We have also shown that PDE8 is expressed at higher levels in acute inflammatory stage compared to the tolerant stage in lung draining hilar lymph nodes in a Ovalbumin induced allergic airway disease model (*126*). This evidence points towards the need for targeting PDE8 in inflammatory diseases. Further, our findings that PDE8 is expressed at higher levels in naive and MOG_{35-55} activated effector T cells (Teff cells) compared to regulatory T cells (Treg cells) and PDE8 inhibition specifically affects Teff cell adhesion and not Treg cell adhesion, indicates that this can be a beneficial treatment for specifically targeting pathogenic Teff cells. Our current study explores targeting PDE8 in vivo in EAE using a highly specific PDE8 inhibitor (IC_{50} for PDE8A = 0.0007 μM, PDE8B < 0.0003 μM, other PDE isoforms >1.5 μM) which was first reported in our publication (*21*).

4.3 Results

Therapeutic effect of treatment with the PF-04957325 in active EAE and adoptive transfer EAE

To examine whether PDE8 mediated regulation of $CD4^+$ T cell motility has implications *in vivo*, we tested effect of PF-04957325 on a T cell mediated disease. Active EAE was induced in C57BL/6 mice using MOG_{35-55}/CFA. Mice with a grade 1 or grade 2 clinical disease were then treated with PF-04957325 or vehicle control s.c thrice daily for 10 days from day 13 to day 22. We observed a clinical suppression of disease in the PF-04957325 treated group compared to mice in the vehicle treated group (Fig. 4.1A, ***p=0.0007). However, mice in the PF-04957325 group again increased in disease severity once the treatment was stopped. After testing the inhibitor in chronic disease model, we next tested the effect of treatment with PF-04957325 in a relapsing-remitting disease model. Disease was induced in SJL mice by injecting them with $PLP_{139-151}$ activated lymph node cells. Mice were treated during the second relapse of disease from day 41 to day 50. Mice treated with PF-0495732 had reduced the severity of disease compared to mice treated with vehicle control (Fig. 4.1B, ***p=0.0004). For continuous drug delivery, we implanted osmotic pumps filled with PF-04957325 or vehicle control into the subcutaneous cavities of active or RR-EAE mice with grade 1 or 2 disease. These pumps are designed to release the drug once they are in the body cavity at a flow rate of 0.5 µl/h for 14 days. In the active EAE model, PF-04957352 treated mice had amelioration of clinical disease during the treatment period (day 12 to day 26) compared to the vehicle treated mice (Fig. 4.1C, ****p<0.0001). After the 14 d treatment period, the osmotic pumps were removed and the clinical scores of the mice

were monitored daily. As observed earlier once the treatment was halted, mice in the PF-04957325 treated group had clinical disease similar to mice in vehicle treated group. In the RR-EAE model, mice were implanted with the pumps on day 21 after the first relapse. Mice in the PF-04957352 treated group had a suppression of clinical disease compared to vehicle control treated mice (Fig 4.1D, ****p<0.0001). Although the treatment did not prevent occurrence of the third relapse, but the there was reduction in disease severity of the relapse.

Treatment with the PF-04957325 suppresses infiltrates in the spinal cord and brain

To test whether inhibition of PDE8 *in vivo* reduced accumulation of cells in the CNS, we treated grade 1 or 2 EAE mice with vehicle control/PF-04957325 for 4 d. Hematoxylin and eosin (H&E) staining of the brain and spinal cord sections on day 4 post treatment were performed in order to obtain a quantitative assessment of the infiltrates in the CNS (Fig 4.2A-B). There was significant reduction in infiltrates in the brain meninges (* p=0.0339), spinal cord parenchyma (* p=0.0245) and additive meningeal and parenchymal infiltrates (** p=0.0052) after treatment with PF-04957325 (Fig. 4.2C). We also counted the SC MNCs isolated from EAE mice treated with PF inhibitor for either 4 days or 6-13 days using the trypan blue assay. There was a non-significant decrease in total number of MNCs accumulated in the spinal cord after 4 d treatment (0.701×10^6 vs. 0.549×10^6; p=0.5203). 6-13 d treatment leads to a reduction in total number of MNCs accumulated in the SC (0.663×10^6 vs. 0.222×10^6; p=0.0783) (Fig. 4.3A), however this reduction was not significant. At the 4 d treatment timepoint, there was an

increase in sequestration of cells in the cervical (1.663×10^6 vs. 4.2×10^6; **p=0.0035), inguinal lymph nodes (5.053×10^6 vs. 9.533×10^6; p=0.1128) as well as in the spleen (76.043×10^6 vs. 131×10^6; p=0.3223) (Fig. 4.3B-D). We observed a slight non-significant decrease in the cells in the cervical (1.636×10^6 vs. 1.251×10^6; p=0.4397) and inguinal lymph nodes (1.331×10^6 vs. 0.947×10^6; p=0.4631), whereas a slight non-significant increase in the total number of cells in the spleen (66.366×10^6 vs. 72.985×10^6; p=0.7416) after 6-13 d treatment. Thus short treatment leads to sequestration of cells in the peripheral lymphoid organs and slight decrease in cell infiltrates in the spinal cord. 6-13 d treatment further decreases cell infiltrates in the spinal cord while equalizing the cell number in the periphery.

Treatment with the PF-04957325 suppresses CD4 effector T cell accumulation in the spinal cord but does not affect Treg cells accumulation

In order to effect if $CD4^+$ T cells accumulation into the spinal cord was being affected by the treatment, we did a detailed FACS analysis on the MNCs isolated from the spinal cord of EAE mice after 4 d and 6-13 d treatment (Fig. 4.4A).

PDE8 inhibition *in vivo* does not change the percent and total number of $CD4^+$ T cells, $CD4^+/Foxp3^-$ Teff cell accumulating in the spinal cord after 4 d treatment (Fig. 4.4B-C). On the contrary, after 6-13 d treatment we observed a decrease of the total number of $CD4^+$ T cells (1.21×10^5 vs. 2.13×10^4, p=0.0597) and $CD4^+/Foxp3^-$ Teff cells (1.02×10^5 vs. 1.72×10^5, p=0.0535), although the decrease was not statistically significant. There wasn't a significant effect on percent and total number of $CD4^+/Foxp3^+$ Treg cells infiltrating in the spinal cord (Fig. 4.4D). The selective effect of the PDE8 inhibition on

Teff cells and not Treg cells is consistent with our previous observations that PDE8 inhibition affects MOG_{35-55} activated Teff cell adhesion and not Treg cell adhesion *in vitro* under shear flow conditions (Basole CP et al., under review). To assess whether PDE8 inhibition in vivo was affecting the proliferation of cells in the spinal cord, we analyzed percent and total number of Ki-67^+ cells within the Teff and Treg cell populations. 4 d treatment does not affect the percent and total number of Ki-67^+ cells within the Teff cells (Fig. 4.4E) and Treg cells (Fig. 4.4F) populations. But there is a significant decrease in total number of Ki-67^+ Teff cells in the spinal cord after 6-13 d treatment (3.03×10^4 vs. 6.42×10^3, **p=0.0049).

Treatment with the PF-04957325 suppresses pro-inflammatory cytokine production and induces IL-10 production in the spinal cord

In order to assess the effect of PDE8 inhibition on inflammation in the spinal cord and periphery, we analyzed the pro-inflammatory and anti-inflammatory cytokine synthesis after PMA-ionomycin stimulation post 4 d and 6-13 d treatment with PF-04957325. 4 d treatment leads to significant reduction in percentage (82.5% to 70.43%; p=0.0248) and total number (0.78×10^5 vs. 0.26×10^5; *p=0.0297) of TNF-α^+ producing $CD4^+$ T cells in the spinal cord (Fig. 4.5A). There wasn't any significant differences in the percentages and total number of IL-17, IFN-γ, IL-17+/IFN-γ^+ production (Fig. 4.5B-D) in $CD4^+$ T cells after 4 d treatment. 6-13 d treatment, there was a non-significant decrease in percent of IL-17 producing $CD4^+$ T cells in the spinal cord. However there wasn't any effect on IFN-γ, IL-17^+/IFN-γ^+ production in $CD4^+$ T cells. In addition, 6-13 d treatment showed similar TNF-α synthesis in the $CD4^+$ T cells and $CD11b^+$ monocytes in the spinal cord.

Since we observed a clinical suppression of disease after long term treatment, we tested whether there were any changes in IL-10 production in $CD4^+$ T cells (Fig. 4.6). There was 4.44% increase in percent (14.03% to 18.47%; p=0.3603) and significant decrease in total number (2.96×10^3 vs. 1.37×10^3, *p=0.0388) of IL-10 producing $CD4^+$ T cells. There was only a 1.296% increase in IL-10 production in the $CD11b^+$ monocytes (2.042% vs. 3.338%; p=0.2723)

Relative increase in Treg cells in the spinal cord compared to pathogenic $CD4^+$ T cells after treatment

There is a significant increase in $Foxp3^+$/Tregs cells compared to TNF- α producing $CD4^+$ T cells in the spinal cord following PF-04957325 treatment as observed by the decrease in TNF-α to Treg ratio (4.6 vs. 1.99; *p=0.0174) (Fig. 4.7A). In addition, there was also a relative increase in Treg cells in the spinal cord compared to Th1 and Th17 cells (Fig. 4.7B-D), although this increase was not statistically significant.

Effect of PDE8 inhibition on peripheral immune response: There was a significant increase in total number of $CD4^+$ T cells, Teff cells, Treg cells as well as B cells in the cervical lymph nodes after 4 d treatment with PF-04957325 compared to vehicle control treated mice (Fig. 4.8A-D). We also analyzed *ex vivo* cytokine production after PMA/Ionomycin stimulation and found that there was significant increase TNF- α producing $CD4^+$ T cells (Fig. 4.8E). In the spleen, there was significant increase in the total number Teff cells after PDE8 inhibition compared to vehicle treated EAE mice (Fig 4.8F). In the draining inguinal lymph nodes, there was also significant decrease in the

pathogenic Th17, TNF- α producing $CD4^+$ T cells and TNF- α producing $CD11b^+$ monocytes (Fig 4.9A-C). Thus PDE8 inhibition in vivo leads to sequestration of the pathogenic T cells in the periphery within the lymph nodes and spleen. We assessed IL-10 production in the cervical lymph nodes and spleen after 6-13 d treatment. There wasn't much difference in the percentage and total number of IL-10 producing $CD4^+$ T cells and $CD11b^+$ monocytes in the cervical lymph nodes and the spleen (Fig 4.10A-D).

4.4 Discussion

Early studies on characterization of PDEs in human lymphocytes had shown them to be excellent targets for producing anti-inflammatory effects with PDE4 the predominant form expressed (*52*). But bringing PDE4 inhibitors into the clinics faced decades of challenges, mostly due to emetic side effects. However, the approval and clinical use of PDE inhibitors for the treatment of major human inflammatory disorders has now finally made tremendous progress over the last 6 years with indications expanding at an almost yearly pace (*53-70, 152*). There is currently intense further interest and activity in the development of selective inhibitors of additional PDE gene families to target inflammation. Our study shows that inhibition of PDE8 in both chronic and RR EAE disease models suppresses clinical disease, although this effect lasts only long as the inhibitor is administered *in vivo*. This can be due to short half life of the inhibitor and reversible type of inhibitor. Effectiveness of inhibitors also depends on whether inhibitors act reversibly or irreversibly. Most inhibitors are reversible, hence they bind to the enzyme through non-covalent bonds and act on ATP binding site or catalytic site. In this case, the cells can recover their enzymatic activity quickly. With irreversible inhibitors, forming covalent with the enzyme and thus have increased biochemical efficiency of target disruption, reduced sensitivity toward pharmacokinetic parameters and increased duration of action that outlasts pharmacokinetics of the compound (*153*).

We have tried to elucidate the mechanism by which PDE8 inhibits cell migration into the CNS by treating EAE mice for either 4 d or 6-13 d timepoint. 4 d treatment leads to accumulation of the pathogenic $CD4^+$ T cells in the lymph nodes and spleen. The exact

mechanism of blocking lymphocyte egress from the lymph nodes after PDE8 inhibition is unknown. Long term treatment blocks $CD4^+$ T cell infiltration into the spinal cord possibly by affecting integrin mediated adhesion of $CD4^+$ T cells to the vascular endothelial cell of the blood brain barrier. Once these $CD4^+$ T cells enter the spinal cord, their reactivation might also be blocked since. We have shown previously that disruption of PDE8-Raf-1 complex suppresses adhesion by affecting LFA-1 integrin mediated cell tethers with ICAM-1. Since LFA-ICAM-1 is crucial part of T cell activation at the immunological synapse, it is possible that *in vivo* $CD4^+$ T interaction with antigen presenting cells is affected. This might explain the reduction in total number of Th17 cells and proliferating $CD4^+$ T cells observed in the spinal cord. The inhibitor has selective effect in the CNS as we did not see any effect on cytokine production in the periphery after 6-13 d treatment. MS patients who receive Natalizumab (Tysabri) treatment (a monoclonal antibody against α4 integrin subunit of α4β1 integrin) are at risk of progressive multifocal leukoencephalopathy (PML) due to impaired immune surveillance (*154*). Since PDE8 is not the major PDE expressed in $CD4^+$ T cells, inhibition of PDE8 may not lead to profound effect on immune surveillance. Additionally, due to the short on and off rates and their oral availability, PDE inhibitors can be dosed very efficiently and quickly removed from the circulation should side effects emerge.

Selective effect of PDE8 inhibition on Teff cells infiltration in the spinal cord and not Treg cell infiltration will be beneficial treatment option in autoimmune diseases. Previous reports indicate that treatment with PDE4 inhibitor significantly improves Treg cell mediated suppression of Th2 response in allergic airway disease (*155*). PDE4 inhibitor

Rolipram at therapeutically relevant doses leads to side effects such as emesis and also did not reduce the lesions in the brain of MS patients (*37*). PDE inhibitors are now emerging to be important targets for treating inflammatory diseases, with PDE4 inhibitor Apremilast (Otezla) now being approved for treatment of psoriasis and psoriatic arthritis. Combined treatment with PDE8 and lower doses of PDE4 inhibitor might be better treatment option since it improves patient compliance and might increase the Treg cell infiltrates in the CNS as well as increase their suppressive capacity. The recent paper from Hoffman and colleagues have discovered a dual PDE4/8 inhibitor BC8-15 (IC_{50} for PDE8A and PDE4 is 0.28 μM and 0.22 μM respectively) (*97*). Effect of this inhibitor on clinical suppression of disease and leukocyte infiltration of T cells in the CNS in the EAE model needs to be tested in the future.

4.5 Materials and Methods

Animals

Female 4-6 weeks old C57BL/6 and SJL mice were obtained from Jackson laboratories (Bar Harbor, ME) and were used for the autoimmunity studies. Experiments were performed according to approved protocols at UConn Health (IACUC Protocol number 100794).

Peptides for EAE induction: MOG_{35-55} peptide corresponding to mouse sequence (MEVGWYRSPFSRVVHLYRNGK) was purified by the Yale University Synthesis Facility and Hebrew University. $PLP_{139-151}$ corresponding to sequence (HSLGKWLGHPDKF) was synthesized peptide synthesis facility at Hebrew University (*156*)**.**

Induction of Active EAE: Four to six week old mice were immunized with MOG_{35-55} in Complete Freund's Adjuvant (CFA; Sigma-Aldrich) as previously described by us (*99*). A total of 200 µg of MOG_{35-55} peptide and 400 µg of killed *Mycobacterium tuberculosis* (Difco Laboratories) was emulsified in CFA and injected s.c. into the flanks of mice. The mice were also injected with 200 ng Pertussis toxin (Biological Laboratories Inc.) i.p on day 0 and day 2 post- immunization.

Induction of Adoptively transferred EAE: Female donor SJL mice were immunized with 200 µg $PLP_{139-151}$ and 400 µg of killed *Mycobacterium tuberculosis* emulsified in CFA and s.c injected into the flanks. Day 10 post immunization, the draining inguinal

lymph nodes were harvested and made into a single cell suspension. Cells were washed in RPMI media with 1% L-glutamine, 1% penicillin/Streptomycin and HEPES. LNCs were stimulated with 10 µg /ml $PLP_{139-151}$ at a concentration 2 million cells/ml in tissue culture media (RPMI media with 1 % L-glutamine, 1 % penicillin/Streptomycin, HEPES, 10 % heat inactivated serum and 1 % 5 x 10^{-3} M 2–mercaptoethanol) for 4 d. LNCs are detached from the well, counted and washed with PBS. Each recipient mouse is injected with 22-30 million cells in 200 µl PBS i.p.

Clinical Evaluation of EAE: Mice will be scored daily according to a non-linear grading scale from 1-5 as follows: 0, no disease; 1, tail weakness; 2,hind limb paresis/marked slowing of righting; 3, complete paralysis of hindlimbs; 4, severe forelimb weakness/paralysis; 5, moribund or dead (*99, 157*). The cumulative disease index (CDI) will be obtained by summing the daily average disease scores of each experimental group from the first day after beginning of treatment. A mean of these daily disease scores (MDD) will be calculated over the entire treatment period based on the number of treatment days. (*158*)

Treatment: The PDE8 selective inhibitor PF-04957325 was synthesized by Pfizer Inc., Groton, CT (*24*). Mice with a grade 1 of grade 2 disease were treated with PF-04957325 (2 mg/ml) 10 mg/kg/dose or vehicle control s.c injections twice daily for 4-13 days for short term histology or FACS experiments. For long term treatment experiments were either injected s.c thrice daily for 10 d (10 mg/kg/dose) or were implanted s.c with mini-

osmotic pumps filled with PF-04957325 (22 mg/ml) (15.5 mg/kg/day) or vehicle control for 14 d. Mice were scored and weighed daily during and after the treatment was over.

Histology of brain and spinal cord: Mice were sacrificed by intra-cardiac perfusion with 20 ml cold PBS under isoflurane narcosis. Brain and spinal cord were extracted and fixed by immersion in 10% phosphate buffered formalin, paraffin embedded and sectioned (6-7 μM). Three longitudinal sections spanning the entire length of the spinal cord, three cross-sections at different levels in the spinal cord, and four to five sections of brain and brain stem were stained with hematoxylin and eosin (H&E) for each animal (*99*). Total number of inflammatory foci (over 10 mononuclear cells) per visual field in the brain and spinal cord were quantified in meninges & parenchyma by an expert double blinded and not aware of the treatment group of the mice (*99, 159*).

Flow cytometry staining: Mice were sacrificed by intra-cardiac perfusion with 20 ml cold PBS under isoflurane narcosis. Spinal cord is enzymatically digested by incubation with Collagenase D (Roche Diagnostics) and DNase I (Sigma) at 37°C for 45 minutes. Mononuclear cells are isolated by passing through a cell strainer followed by percol gradient (70%/37%) centrifugation (*148, 160*). Total number of mononuclear cells isolated from the spinal cord is determined by trypan blue exclusion method. Teff cells and Treg cells characterization: Mononuclear cells are first stained with cell surface molecules CD3, CD4, CD8, CD49d/α4 integrin and CD11a/αL integrin from E-Bioscience. Intracellular staining is done with transcription factor Foxp3 from E-Bioscience (*160*). Percentage of cells, absolute number of cell and MFI are determined

while analyzing FACS data. In addition we will do a similar analysis of the T cell populations in the regional cervical lymph nodes, spleen and inguinal lymph nodes. Cytokine staining: Mononuclear cells are first treated with phorbol 12-myristate 13-acetate (PMA) (Sigma), Ionomycin (Sigma) and brefeldin A (Sigma) in order to induce synthesis of cytokines for 4 hours at 37°C. The cells are then permeabilized and fixed with the BD bioscience buffers followed by intracellular staining with TNF-α (eBioscience), IL-17 (BD Biosciences) and IFN-γ (Biolegend) antibodies (*160, 161*). For IL-10 staining: After PMA/Ionomycin/BFA stimulation,the cells will be stained for surface markers and fixed with 4% PFA. Next day, cells are permeabilized using BD permeablization buffer followed by intracellular staining with IL-10 (clone: JES5).

Statistical Analysis: Treatment effects were assessed by comparing the mean daily disease scores of both experimental groups using the nonparametric Wilcoxon 2 sample analysis/ Mann-Whitney *U* test using GraphPad Prism. For comparison of total number of cells, proliferation, cytokine analysis unpaired t test was used.

Figure 4.1

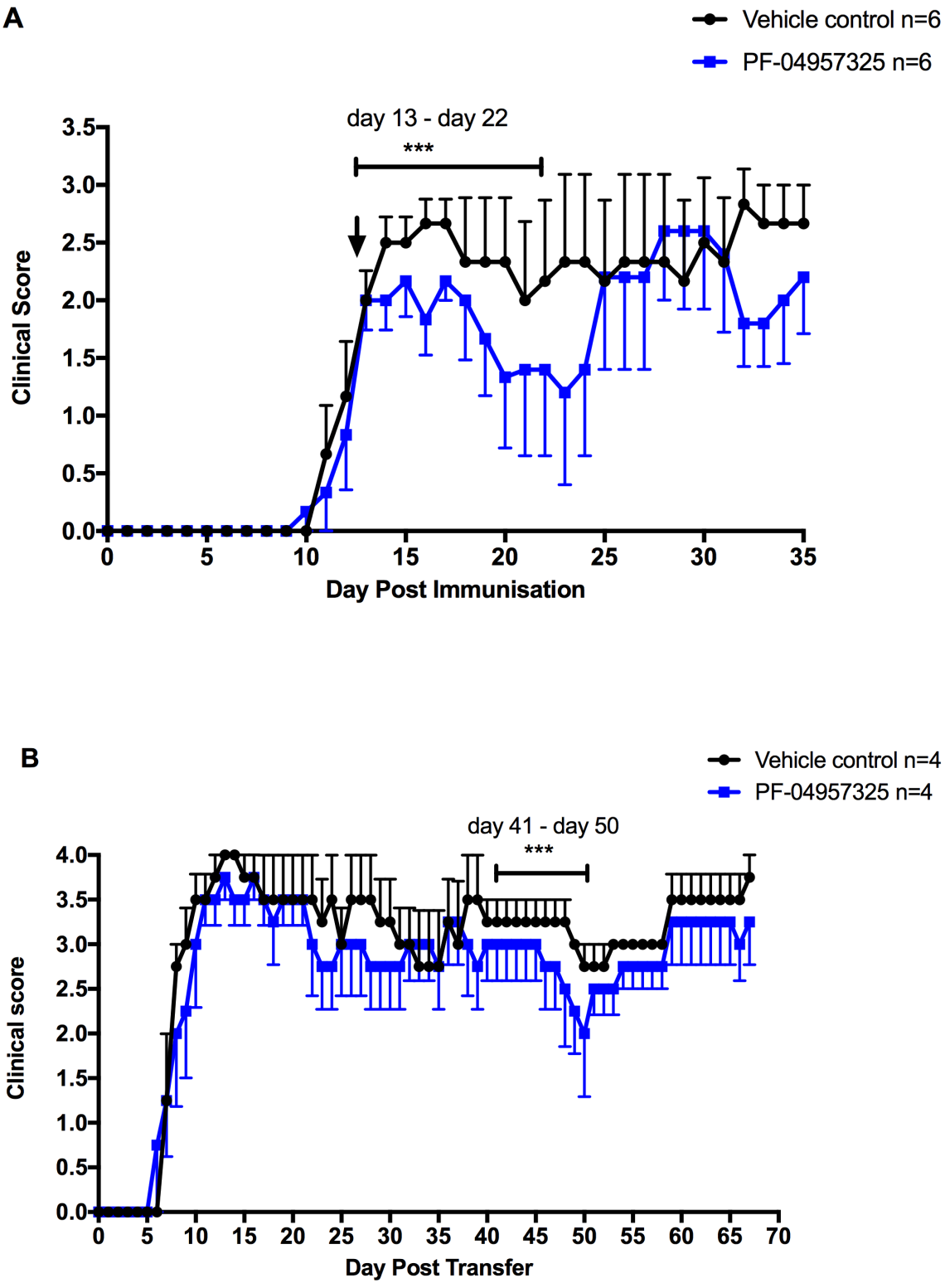
A
Vehicle control n=6
PF-04957325 n=6
day 13 - day 22
***
Clinical Score
Day Post Immunisation
B
Vehicle control n=4
PF-04957325 n=4
day 41 - day 50
***
Clinical score
Day Post Transfer

Figure 4.1

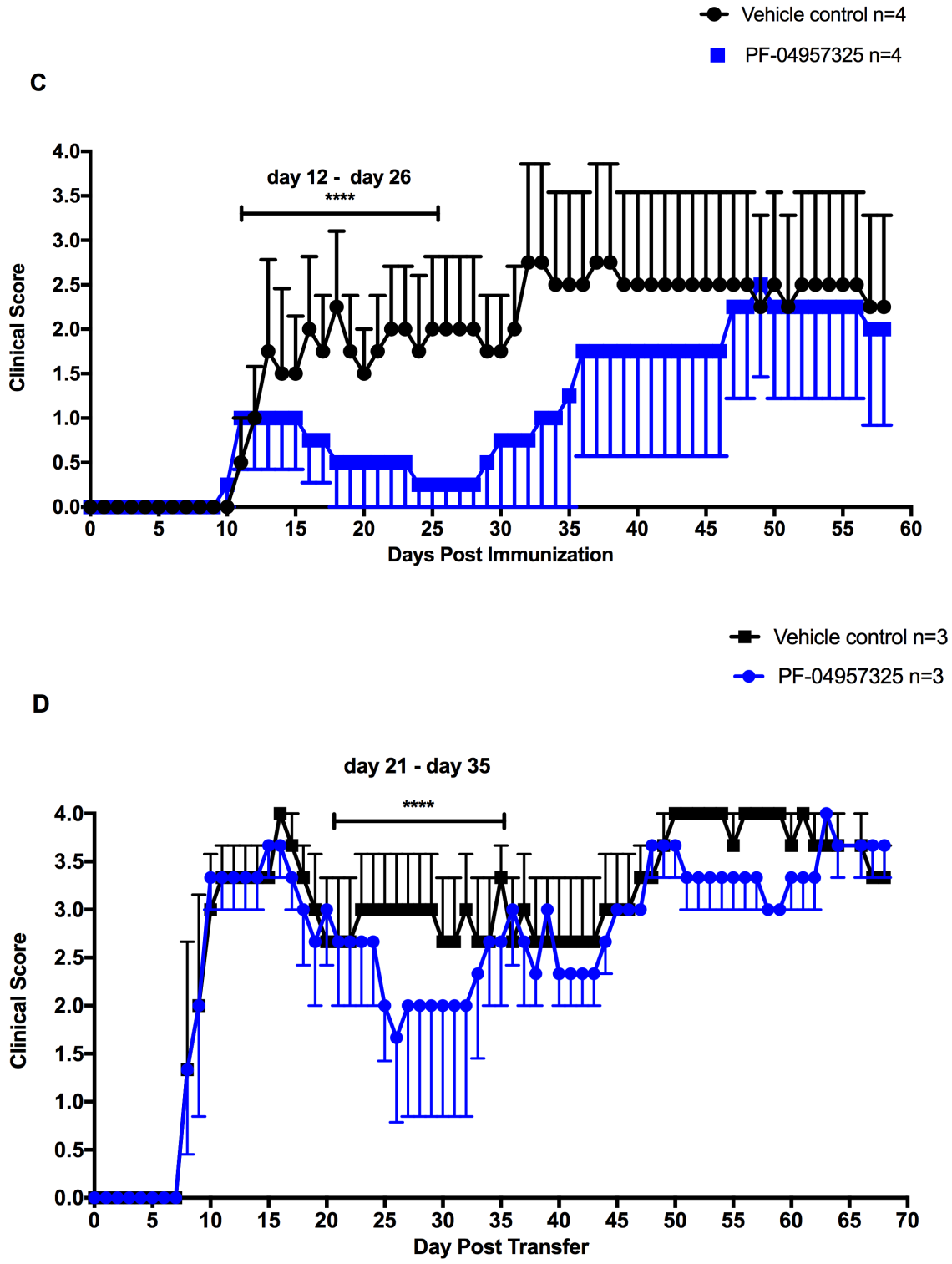
Vehicle control n=4
PF-04957325 n=4
C
day 12 - day 26
****
Clinical Score
Days Post Immunization
Vehicle control n=3
PF-04957325 n=3
D
day 21 - day 35
****
Clinical Score
Day Post Transfer

Figure 4.1. Treatment with the PDE8 enzymatic inhibitor ameliorates disease in EAE mice. (A) C57BL/6 mice with chronic EAE treated with PF-04957325 10 mg/kg/dose or vehicle control s.c 3 times from day 13 to day 22. Data represents mean scores (mean ± SEM) per day for 6 mice per group. (B) SJL mice with relapsing remitting EAE were treated with 10 mg/kg/dose or vehicle control s.c 3 times each day from day 41 to day 50. Data represents mean (mean ± SEM) of 4-5 mice in each group. (C) C57BL/6 EAE mice were implanted with mini-osmotic pumps filled with either PF-04957325 (15.5 mg/kg/day) in vehicle or vehicle (50 % DMSO and 50 % PBS) on day 12 post-immunization. The pumps are designed to deliver the drug for 14 d. The pumps were removed at day 28 post-immunization. Data represent the mean scores (mean+SEM) per day for 4 mice in each treatment group. $p<0.0001$ between d12-d26 treatment days, $p<0.0001$ between d27-d46, $p<0.0.01$ between d47-d58 post-treatment. (D) SJL mice were implanted with mini-osmotic pumps filled with either PF-04957325 (15.5 mg/kg/day) in vehicle or vehicle (50% DMSO and 50% PBS) on day 21. The pumps are designed to deliver the drug for 14 d. The pumps were removed at day 38 post- immunization. Data represent the mean scores (mean+SEM) per day for 3 mice in each treatment group. $p<0.0001$ between d21-d35 treatment days, $p<0.05$ between d36-d49, $p<0.0001$ between d50-d60 post-treatment. P value was calculated using Mann-Whitney non-parametric test.

Figure 4.2

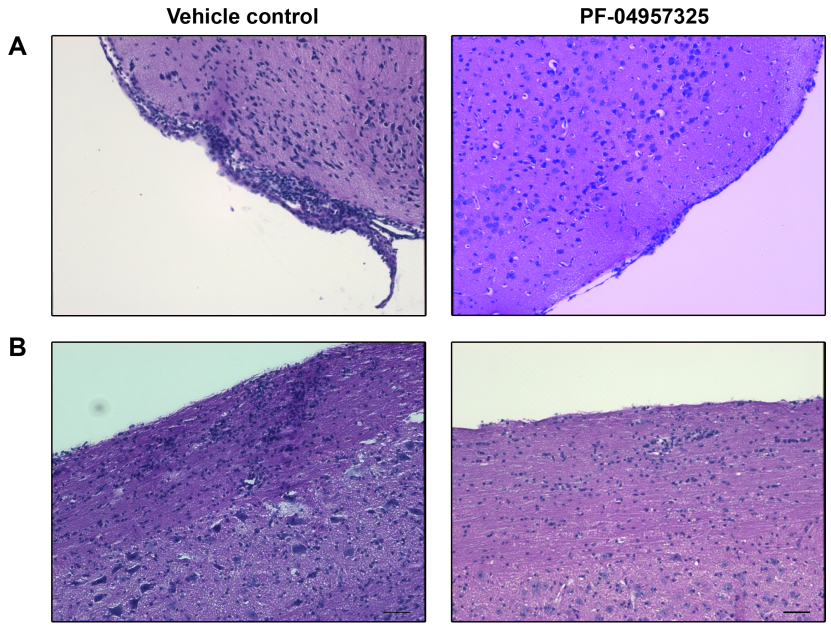
Vehicle control
PF-04957325
A
B

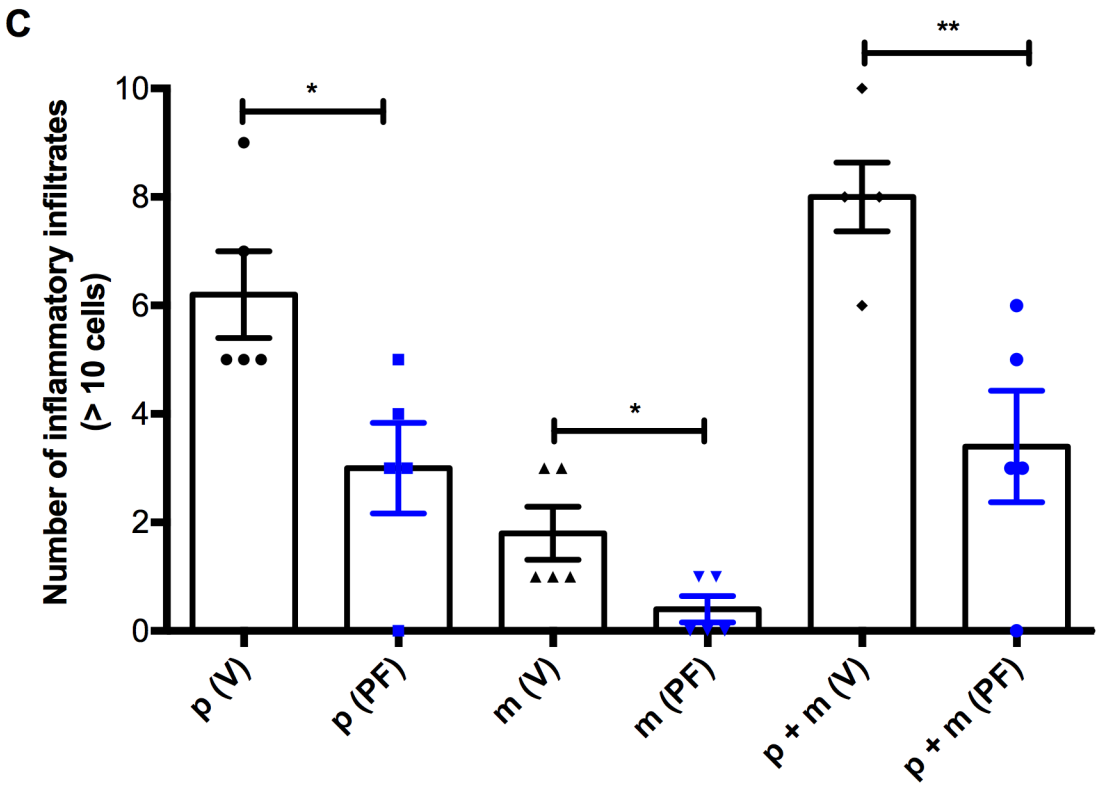
C
Number of inflammatory infiltrates (> 10 cells)
10
8
6
4
2
0
*
*
**
p (V)
p (PF)
m (V)
m (PF)
p + m (V)
p + m (PF)

Figure 4.2. Treatment with PF-04957325 suppresses infiltration of cells into the brain and spinal cord. EAE mice were treated with vehicle control or PF-04957325 from day 10 to day 13 (4 d) followed by isolation of brain and spinal cord for histology. H/E images of the brain (A) and spinal cord (B) sections of vehicle control (grade 4) and PF-04957325 (grade 2) treated mice at 10X. (C) Graph represents the inflammatory foci present in the spinal cord parenchyma (p) and brain meninges (m) based on H/E sections. (n=5)

Figure 4.3

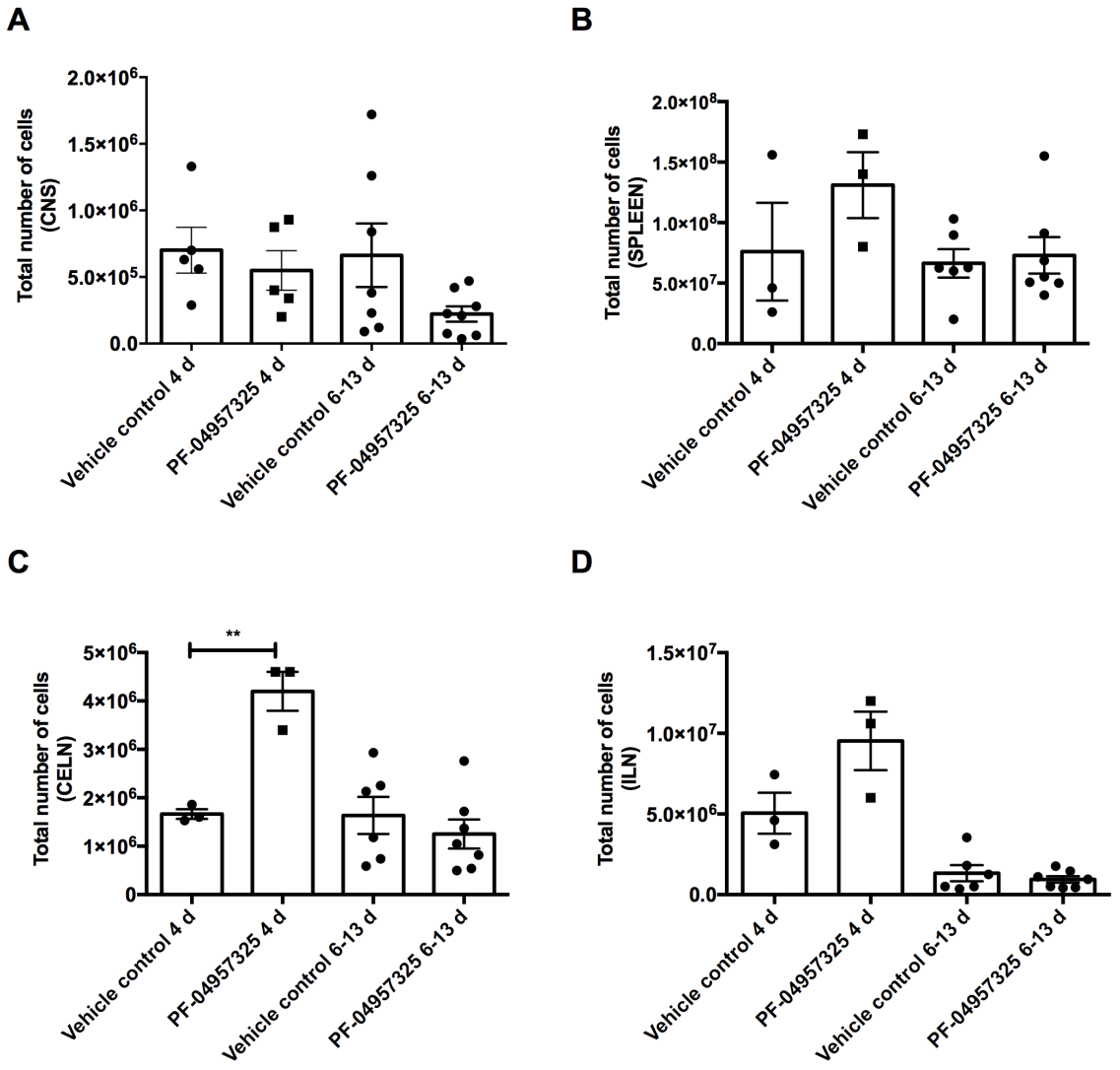

Figure 4.3. Treatment with PF-04957325 suppresses infiltration of cells into the spinal cord. EAE mice with grade 1-3 disease were treated with PF-04957325 or vehicle control either twice daily for 4 d or thrice daily for 6-13 d. Data represents the total number of cells in the spinal cord (A), spleen (B), cervical lymph nodes (C) and draining inguinal lymph nodes (D) counted by trypan blue assay (n=3-7).

Figure 4.4.

A

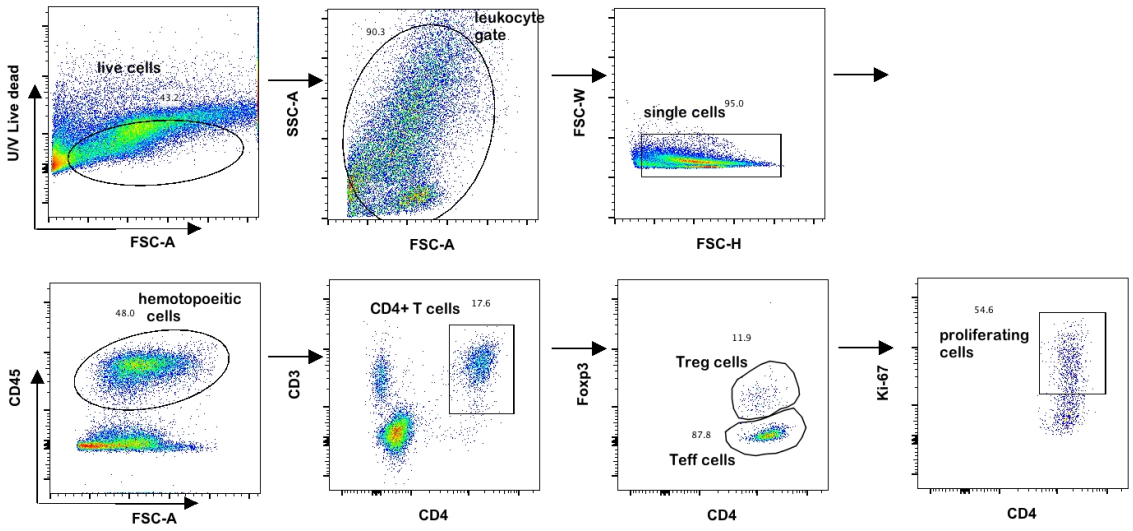

B

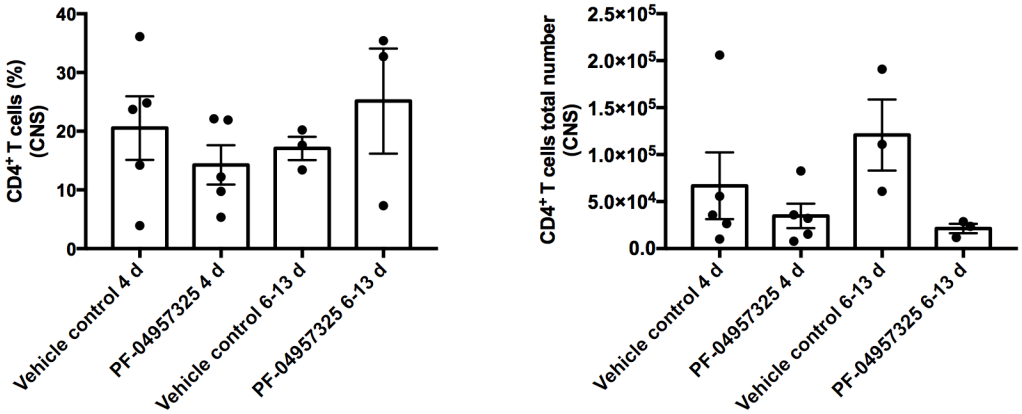

C

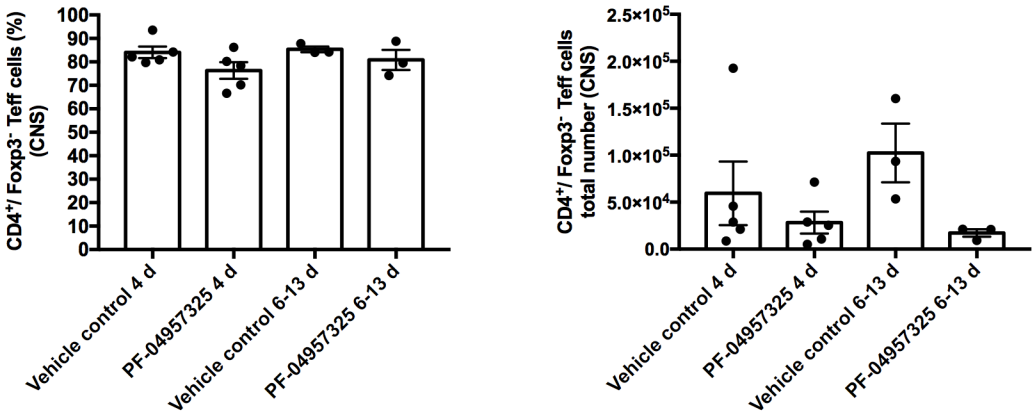

Figure 4.4

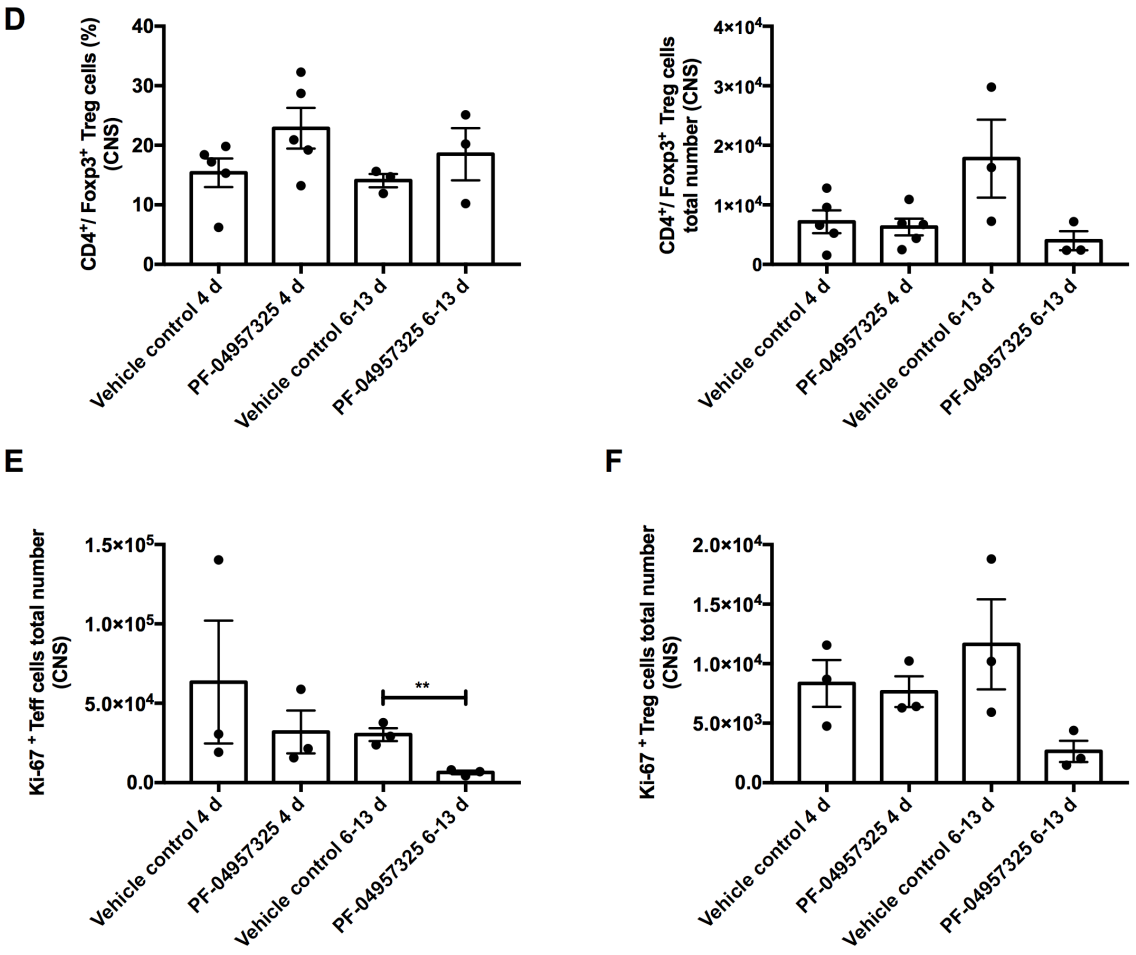

Figure 4.4. Treatment with PF-04957325 suppresses $CD4^+$ T cells and Teff cells accumulation into the spinal cord. (A) Detection of $Foxp3^+$ Treg cells, $Foxp3^-$ Teff cells and Ki-67^+ Teff and Treg cells by flow cytometry in spinal cord mononuclear cells of EAE mice treated with vehicle control or PF-04957325.Data represents percent and total number of $CD4^+$ T cells (B), $Foxp3^-$/Teff cells (C), $Foxp3^+$/Treg cells (D), $Foxp3^-$/Ki-67^+ Teff cells (E), $Foxp3^+$/Ki-67^+ Treg cells (F) analyzed by flow cytometry. (n=3-5)

Figure 4.5
A

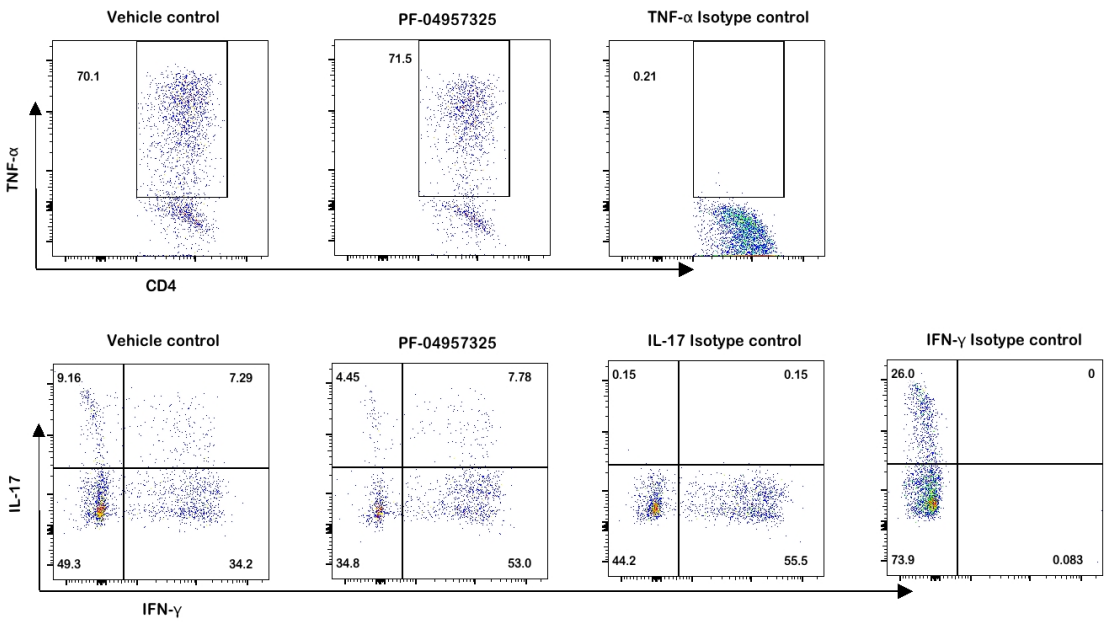

B

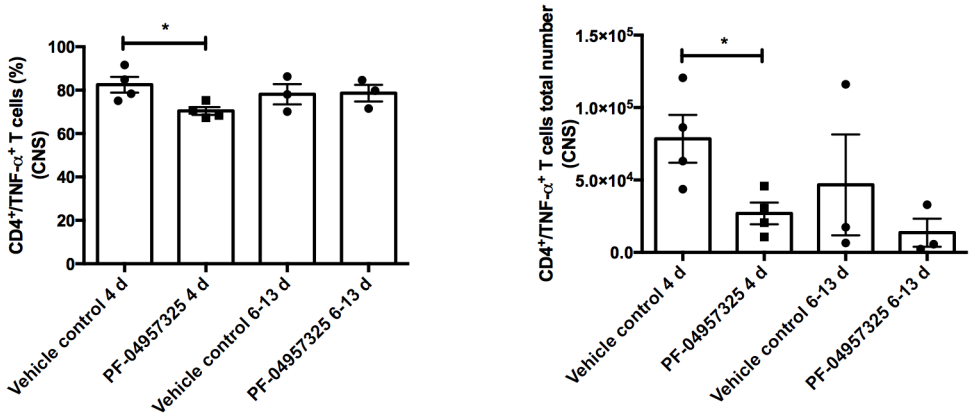

C

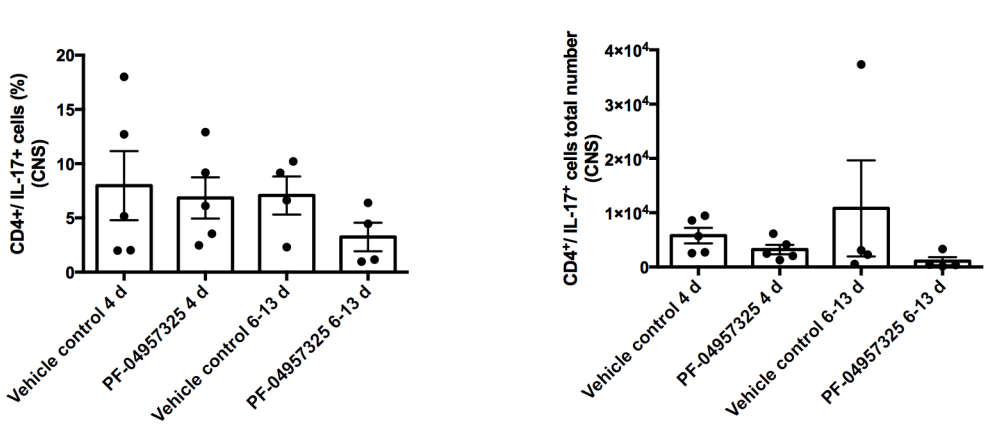

Figure 4.5

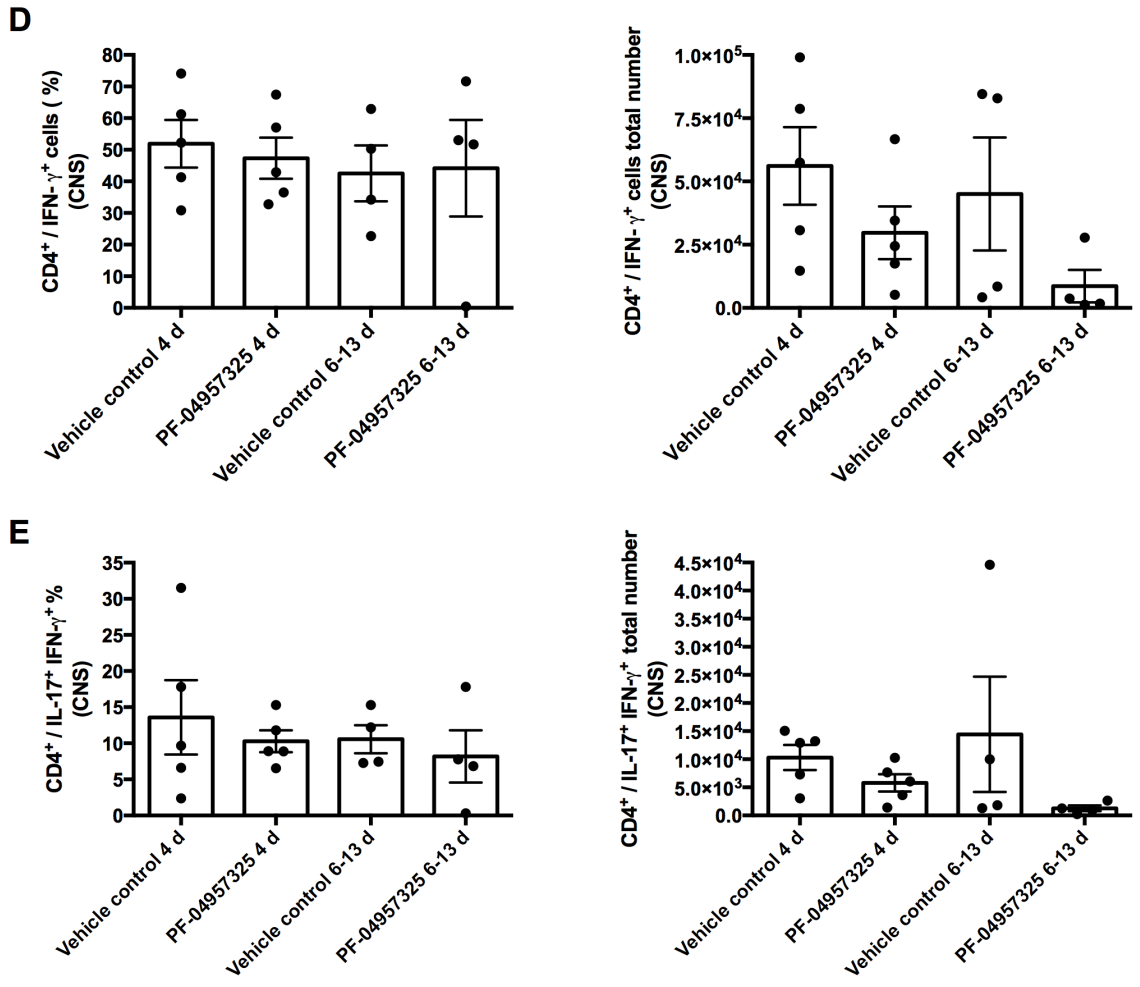

Figure 4.5. Treatment with PF-04957325 decreases the Th1 and Th17 cells in the spinal cord. (A) Detection of TNF-α^+, IL-17$^+$ and IFN-γ^+ CD4$^+$ cells after *ex vivo* restimulation with PMA/Ionomycin by flow cytometry in spinal cord mononuclear cells of EAE mice treated with vehicle control or PF-04957325. Representative dot plots show CD4$^+$ T cells that are positive for TNF-α^+ (above), IL-17 (x-axis) and IFN-γ^+ (y-axis). Data represents percent and total number of TNF-α^+ (B), IL-17$^+$ (C) and IFN-γ^+ (D) and IL-17$^+$ IFN-γ^+ (E) CD4$^+$ cells.

Figure 4.6
A

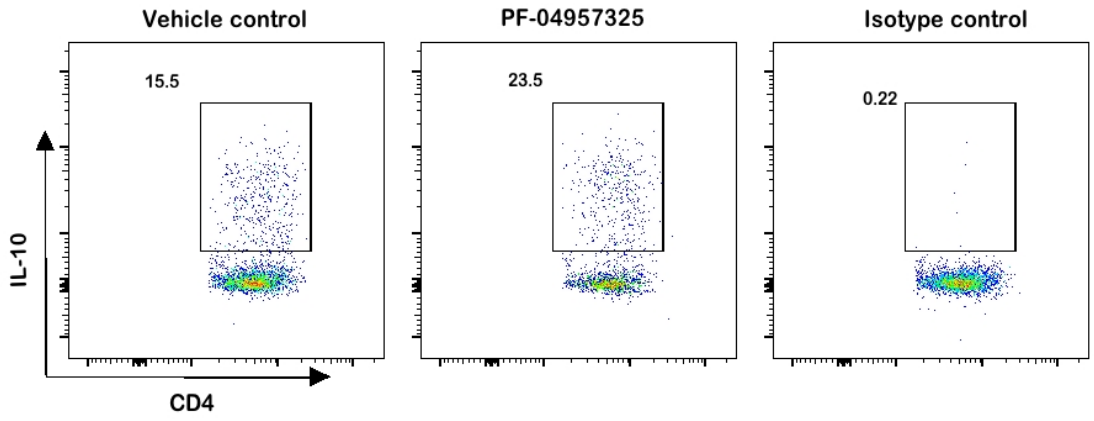

B

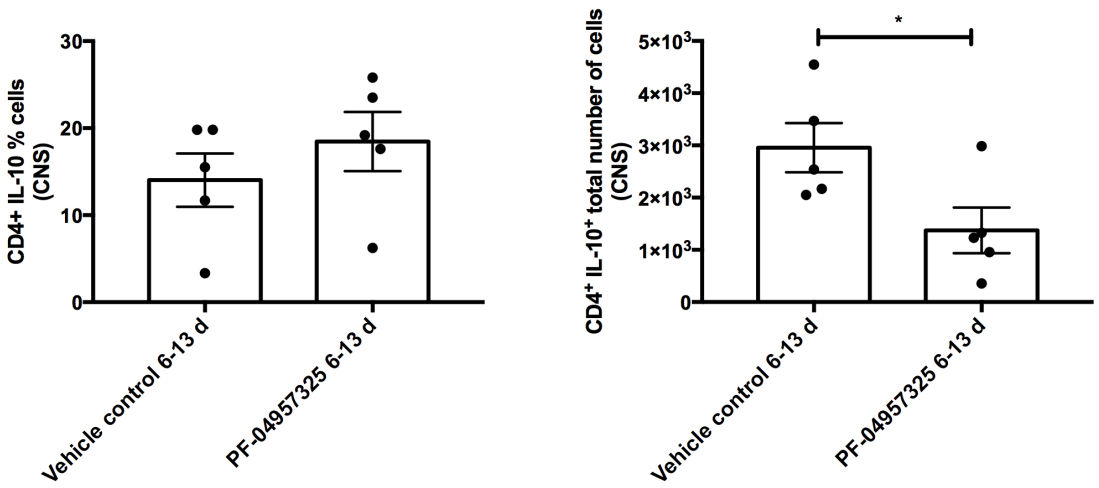

C

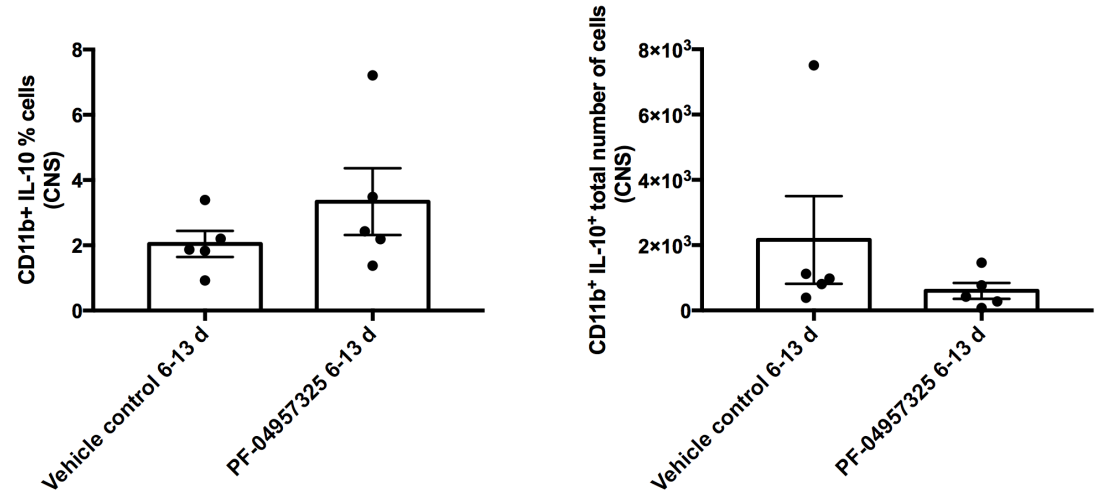

Figure 4.6. Treatment with PF-04957325 increases the IL-10 producing $CD4^+$ T cells in the spinal cord. (A) Detection of IL-10^+ $CD4^+$ cells after *ex vivo* restimulation with PMA/Ionomycin by flow cytometry in spinal cord mononuclear cells of EAE mice treated with vehicle control or PF-04957325. Data represents percent and total number of IL-10^+ $CD4^+$ T cells (B) and IL-10^+ $CD11b^+$ cells (C).

Figure 4.7

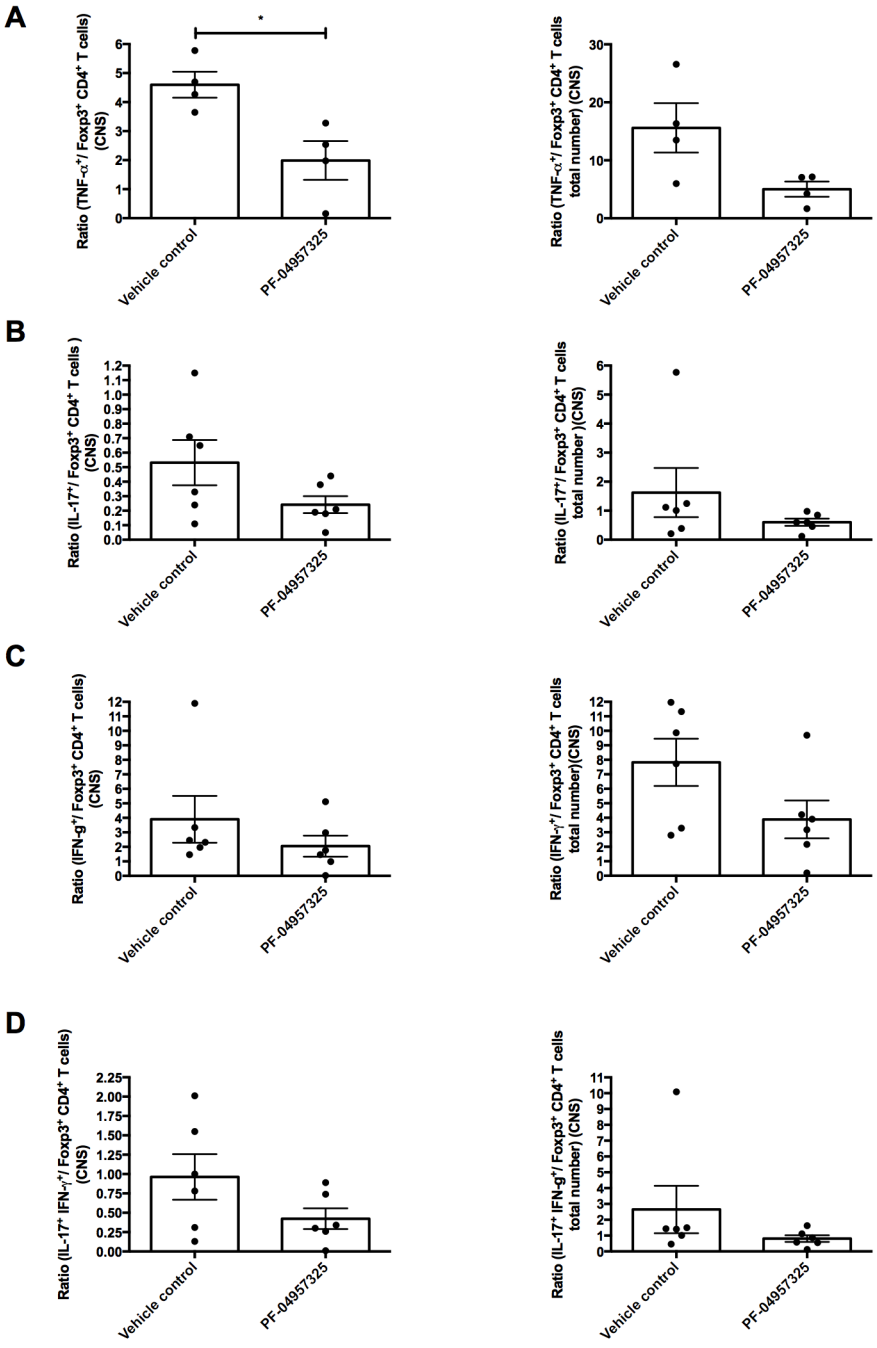
A
Ratio (TNF-α+/ Foxp3+ CD4+ T cells) (CNS)
Ratio (TNF-α+/ Foxp3+ CD4+ T cells total number) (CNS)
B
Ratio (IL-17+/ Foxp3+ CD4+ T cells) (CNS)
Ratio (IL-17+/ Foxp3+ CD4+ T cells total number)(CNS)
C
Ratio (IFN-g+/ Foxp3+ CD4+ T cells) (CNS)
Ratio (IFN-γ+/ Foxp3+ CD4+ T cells total number)(CNS)
D
Ratio (IL-17+ IFN-γ+/ Foxp3+ CD4+ T cells) (CNS)
Ratio (IL-17+ IFN-g+/ Foxp3+ CD4+ T cells total number) (CNS)
Vehicle control
PF-04957325

Figure 4.7. Relative decrease in pathogenic $CD4^+$ T cells and increase in Treg cells in the spinal cord after treatment with PF-04957325

The above graphs show the ratio of percent (left graphs) or total number (right graphs) TNF-α^+ (A), IL-17^+ (B) and IFN-γ^+ (C) and IL-17^+ IFN-γ^+ (D) $CD4^+$ cells to Treg cells in the spinal cord mononuclear cells of EAE mice treated with vehicle control or PF-04957325.

Figure 4.8

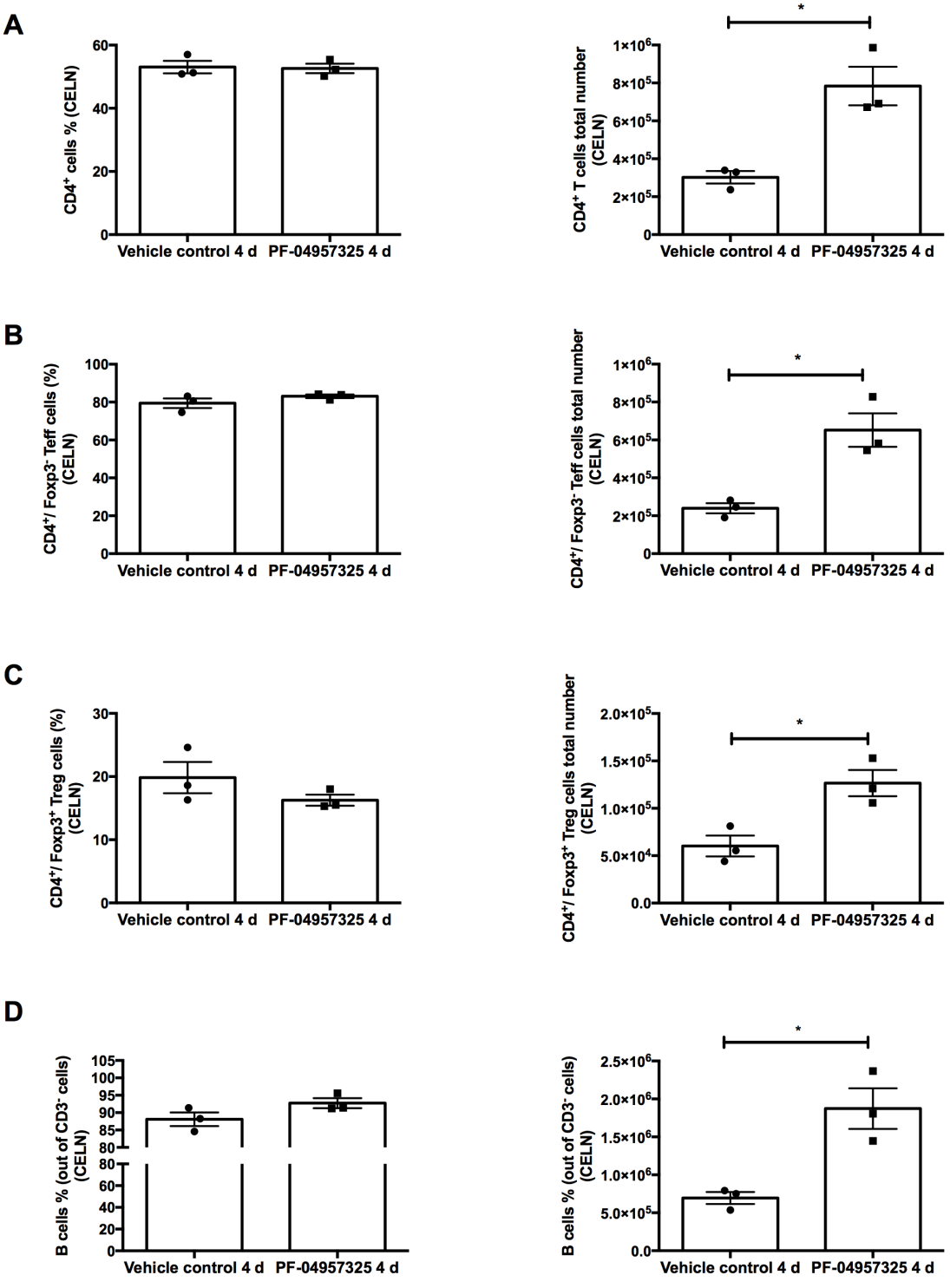
A
CD4+ cells % (CELN)
60
40
20
0
Vehicle control 4 d
PF-04957325 4 d
*
CD4+ T cells total number (CELN)
1×10^6
8×10^5
6×10^5
4×10^5
2×10^5
0
Vehicle control 4 d
PF-04957325 4 d
B
CD4+/ Foxp3- Teff cells (%) (CELN)
100
80
60
40
20
0
Vehicle control 4 d
PF-04957325 4 d
*
CD4+/ Foxp3- Teff cells total number (CELN)
1×10^6
8×10^5
6×10^5
4×10^5
2×10^5
0
Vehicle control 4 d
PF-04957325 4 d
C
CD4+/ Foxp3+ Treg cells (%) (CELN)
30
20
10
0
Vehicle control 4 d
PF-04957325 4 d
*
CD4+/ Foxp3+ Treg cells total number (CELN)
2.0×10^5
1.5×10^5
1.0×10^5
5.0×10^4
0.0
Vehicle control 4 d
PF-04957325 4 d
D
B cells % (out of CD3- cells) (CELN)
105
100
95
90
85
80
80
60
40
20
0
Vehicle control 4 d
PF-04957325 4 d
*
B cells % (out of CD3- cells) (CELN)
2.5×10^6
2.0×10^6
1.5×10^6
1.0×10^6
5.0×10^5
0.0
Vehicle control 4 d
PF-04957325 4 d

Figure 4.8

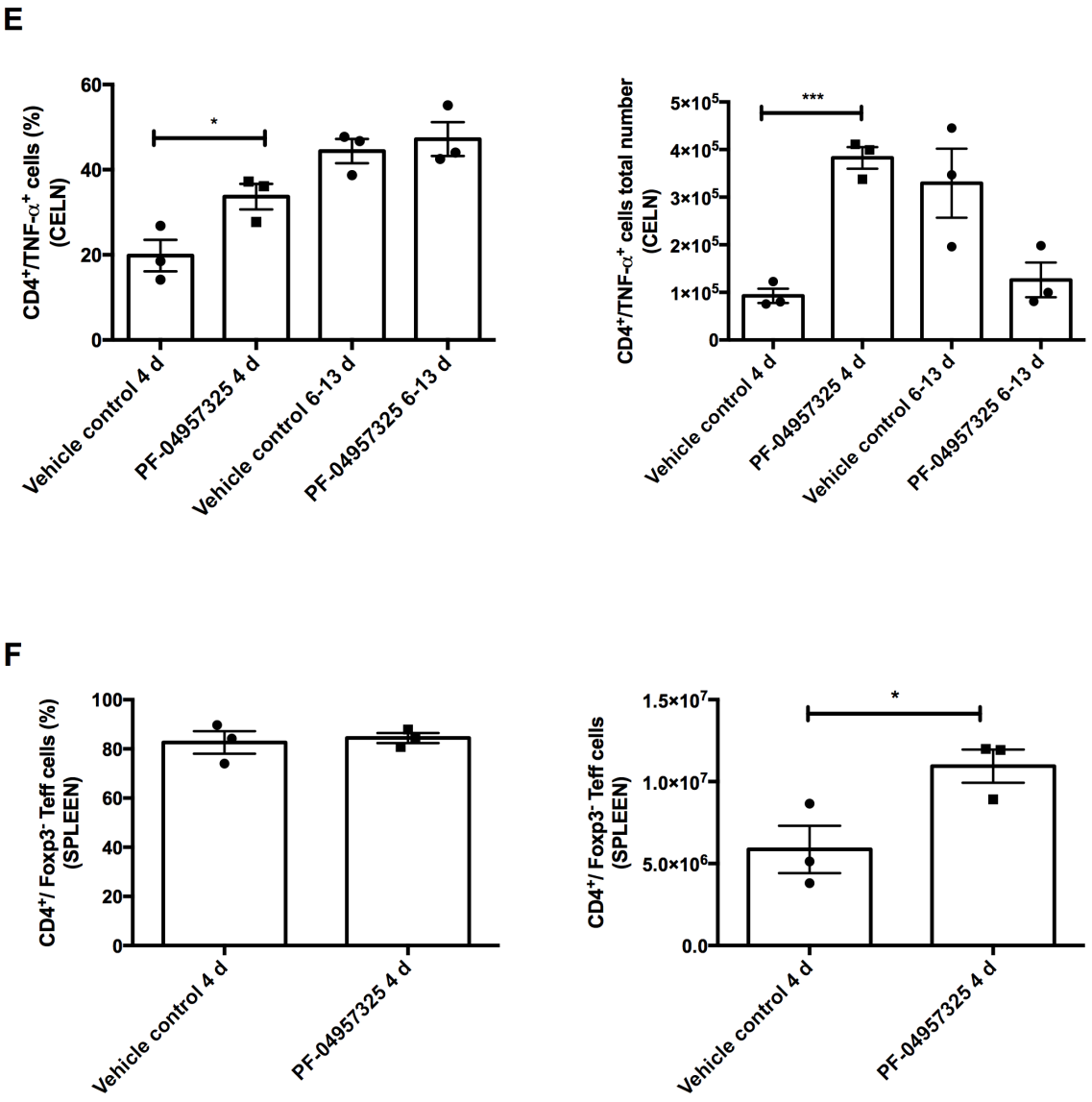

Figure 4.8. 4d treatment with PF-04957325 leads to accumulation of cells in the peripheral lymphoid organs

Data represents percent and total number of $CD4^+$ T cells (A), $Foxp3^-$/Teff cells (B), $Foxp3^+$/Treg cells (C), B cells (D), TNF-α^+ $CD4^+$ T cells (E) in the cervical lymph nodes and $Foxp3^-$/Teff cells in the spleen (F) of EAE mice treated with vehicle control or PF-04957325 for 4 d or 6-13 d analyzed by flow cytometry.

Figure 4.9

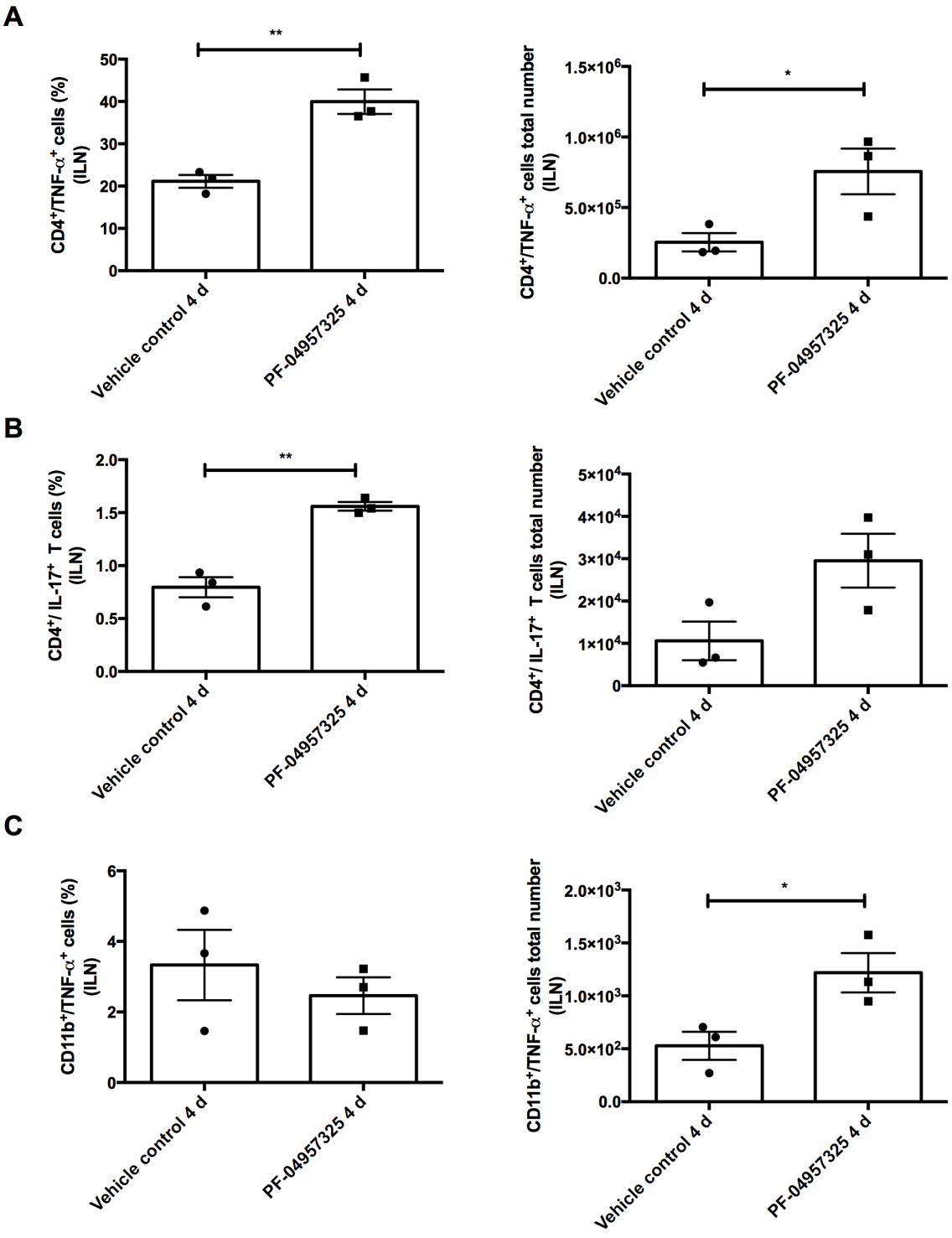

Figure 4.9. 4d treatment with PF-04957325 leads to accumulation of cells in the inguinal lymph nodes

Data represents percent and total number of TNF-α^+ (A), IL-17^+ $CD4^+$ T cells (B) and TNF-α^+ $CD11b^+$ cells in the draining inguinal lymph nodes of EAE mice treated with vehicle control or PF-04957325 for 4 d analyzed by flow cytometry.

Figure 4.10

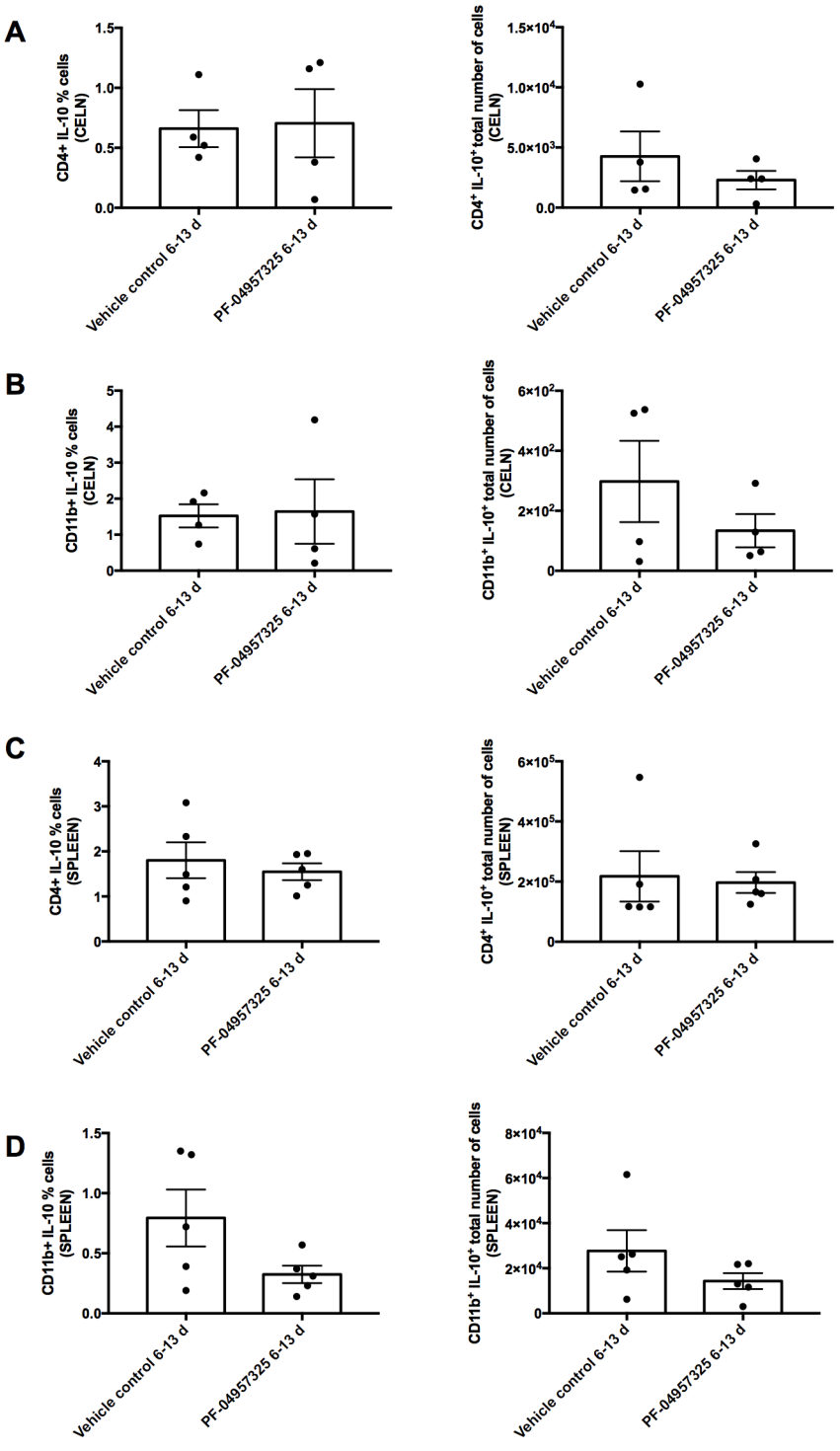
A
CD4+ IL-10 % cells (CELN)
1.5
1.0
0.5
0.0
Vehicle control 6-13 d
PF-04957325 6-13 d
CD4+ IL-10+ total number of cells (CELN)
1.5×10^4
1.0×10^4
5.0×10^3
0.0
Vehicle control 6-13 d
PF-04957325 6-13 d
B
CD11b+ IL-10 % cells (CELN)
5
4
3
2
1
0
Vehicle control 6-13 d
PF-04957325 6-13 d
CD11b+ IL-10+ total number of cells (CELN)
6×10^2
4×10^2
2×10^2
0
Vehicle control 6-13 d
PF-04957325 6-13 d
C
CD4+ IL-10 % cells (SPLEEN)
4
3
2
1
0
Vehicle control 6-13 d
PF-04957325 6-13 d
CD4+ IL-10+ total number of cells (SPLEEN)
6×10^5
4×10^5
2×10^5
0
Vehicle control 6-13 d
PF-04957325 6-13 d
D
CD11b+ IL-10 % cells (SPLEEN)
1.5
1.0
0.5
0.0
Vehicle control 6-13 d
PF-04957325 6-13 d
CD11b+ IL-10+ total number of cells (SPLEEN)
8×10^4
6×10^4
4×10^4
2×10^4
0
Vehicle control 6-13 d
PF-04957325 6-13 d

Figure 4.10. Treatment with PF-04957325 does not affect IL-10 producing $CD4^+$ T cells in the peripheral lymphoid organs. Data represents percent and total number of $IL\text{-}10^+$ $CD4^+$ T cells and $IL\text{-}10^+$ $CD11b^+$ monocytes in the cervical lymph node (A-B) and spleen (C-D) of EAE mice treated with vehicle control or PF-04957325 for 6-13 d and analyzed by flow cytometry.

Chapter 5

Final Discussion

cAMP signaling has been shown to be inhibitory to T cells activation, proliferation and cytokine production (*77*). Hence cAMP production via either using cAMP activators or inhibiting cAMP degradation through phosphodiesterase (PDE) inhibitors is a promising therapeutic approach for treatment of inflammatory diseases. Our research focuses on PDE8 gene family which is upregulated in T cells after anti-CD3/ anti-CD28 activation in vitro, as well as after *in vivo* activation with peptide. We have shown expression of PDE8 in $CD4^+$ T cells population in different disease models - lung draining hilar lymph nodes in ovalbumin induced allergic airway disease model (AAD) over the course of the acute inflammatory disease and to recede at the late tolerant non-inflammatory stage, in vivo myelin oligodendrocyte protein activated cells, breast cancer cell lines, human breast cancer patient tissue as well multiple sclerosis PBMCS (*33, 126*). Overexpression of PDE8 in these various inflammatory conditions necessitated exploring importance of PDE8 in maintaining homeostasis.

To evaluate PDE8A as a potential drug target, the selective and combined effects of the highly potent PDE8-selective inhibitor PF-04957325 was compared with the PDE4-selective inhibitor piclamilast (PICL). As previously shown, PF-04957325 suppressed T cell adhesion to endothelial cells. In contrast, PICL alone increased firm T cell adhesion to endothelial cells by ~20% and significantly abrogated the inhibitory effect of PF-04957325 on T cell adhesion by over 50% when cells were co-exposed to PICL and PF-04957325. Despite its robust effect on T cell adhesion, PF-04957325 was over two

orders of magnitude less efficient than PICL in suppressing polyclonal Teff cell proliferation, and showed no effect on cytokine gene expression in these cells. More importantly, PDE8 inhibition did not suppress proliferation and cytokine production of myelin-antigen reactive pro-inflammatory Teff cells *in vivo* and *in vitro*. Thus, targeting PDE8 through PF-04957325 selectively regulates Teff cell interactions with endothelial cells without marked immunosuppression of proliferation, while PDE4 inhibition has partially opposing effects. Collectively, these data identified PF-04957325 as a novel function-specific tool for the suppression of Teff cell adhesion and indicate that PDE4 and PDE8 play unique and non-redundant roles in the control of Teff cell functions.

We then analyzed the differential effect of PDE8 on Teff versus Treg cells adhesion and identified the role of a novel PDE8A-Raf-1 kinase signaling complex in these cell types. Inhibition of PDE8 using a highly specific PDE8 inhibitor PF-04957325 suppressed MOG activated $CD4^+$ effector T cells (Teff) mediated adhesion to inflamed brain endothelial cells under shear flow conditions by ~37%. However, the inhibition of PDE8 does not effect the motility of Treg cells, which are more motile even under naïve conditions compared to the Teff cells. This differential effect on both the cell populations is consistent with the observed differential expression of PDE8A in Teff cells versus Treg cells where it is considerably more highly expressed in Teff cells under naive and activated states (*135*). PDE8 acts partially via the inhibiting ERK-MAPK signaling pathway. Further we have explored the role of the PDE8A-Raf-1 kinase signaling complex in $CD4^+$ T cells. Disruption of this complex leads to ~87% suppression of total $CD4^+$ T cell adhesion, ~43% reduction in Teff cell adhesion and no significant effect of

Treg cell adhesion while interacting with activated brain endothelial cells. Mechanistically the PDE8A-Raf-1 kinase complex acts by suppressing the LFA-1 integrin mediated adhesion, spreading and locomotion while interacting with the endothelial ligand ICAM-1. Further we have shown that PDE8A-Raf-1 kinase acts via Raf-1 signaling independent of downstream ERK-MAPK pathway. This study demonstrates for the first time that T cell motility under physiological shear stress conditions is profoundly modulated by a pool of PDE8A. This effect is mediated by the interaction between PDE8A and Raf-1 kinase and constitutes a novel signaling axis for the investigation of T cell adhesion and migration.

To study targeting PDE8 in a T cell mediated disease, we tested efficacy of the treating with PDE8 inhibitor therapeutically, in a mice model of multiple sclerosis (MS) known as experimental autoimmune encephalomyelitis (EAE). Treatment of mice with active EAE or mice with adoptive transferred EAE with PDE8 inhibitor after disease onset leads to suppression of clinical symptoms of the disease compared to the vehicle control treated mice. This effect of the inhibitor lasts as long as the inhibitor is administered *in vivo*. PDE8 inhibition has an effect of immune cell infiltration into the sites of inflammation – brain and spinal cord. Specifically we found that there was a reduction in number of $CD4^+$ Teff cells accumulating in the spinal cord. These findings confirm our hypothesis that PDE8 plays a role in regulating migration of $CD4^+$ T cells. Further we observed there is a trend for increase in percent of Treg cells entering the CNS after PDE8 inhibition. This observation is similar to our finding that PDE8 does not suppress Treg

cell adhesion to brain endothelial cells *in vitro*. PDE8 inhibition *in vivo* leads to reduction in $CD4^+$ T cells with a pro-inflammatory phenotype (Th1 and Th17 cells).

These findings suggest that targeting PDE8 can be a beneficial treatment option in autoimmune diseases.

Figure 5.1

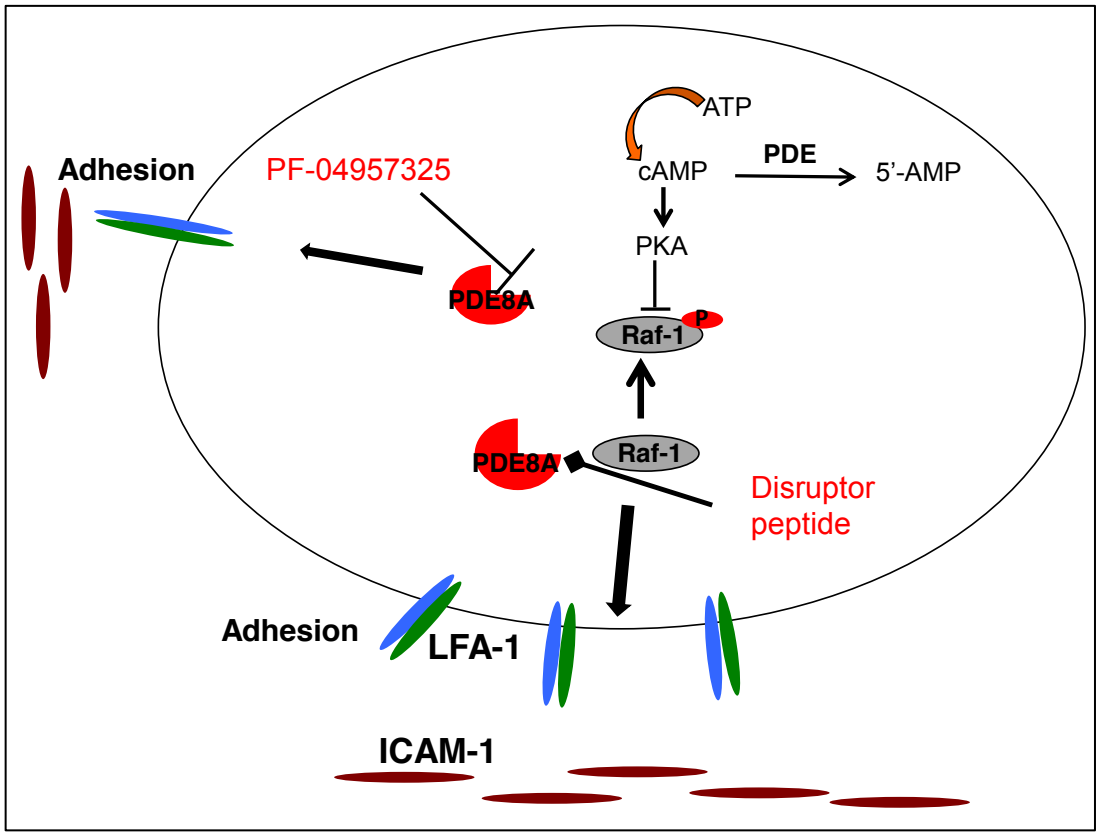

Figure 5.1: PDE8 and PDE8A-Raf-1 kinase complex regulate $CD4^+$ T cell motility

cAMP signaling leads to inhibitory phosphorylation of Raf-1 at serine 259 which then cannot activate downstream ERK-MAPK signaling. PDE8 has been recently shown to associate with Raf-1 kinase protein and create a compartment of low cAMP and protect Raf-1 from PKA medated inhibitory phosphorylation. The diagram describes the two approaches used to study CD4 T cells motility - Targeting PDE8 enzymatic activity with PF-04957325 and PDE8-Raf-1 kinase signaling complex using disruptor peptide. PDE8A-Raf-1 kinase regulates adhesion via the affecting the LFA-1-ICAM-1 interaction. PDE8 regulates adhesion in Teff cells via unknown mechanisms.

Chapter 6

Future directions

6.1 Role of PDE8 and PDE8A-Raf-1 kinase complex in regulating endothelial cells adhesion molecule expression and barrier functions

We have previously started to study the effect of the PDE8 inhibition on brain endothelial cells bEnd.3 cells using PDE inhibitor dypyridamole, which inhibits PDE8 with an IC_{50} in the range of 4-9 μM (*24*). PDE8A gene expression in endothelial was four fold lower than expression of PDE4B, which was the most abundant PDE gene expressed in bEnd.3 cells. There was significant reduction in expression of vascular recruitment molecules important in mediating interaction of T cells - VCAM-1 and ICAM-1, after treatment with dypyridamole. In addition there was a reduction in expression of claudin-5 tight junction protein important in regulating vascular permeability.

We now want to explore the effect of PDE8 selective inhibitor PF-04957325 on protein expression of vascular adhesion molecule and tight junction proteins.
PDE4 inhibitor Roflumilast suppressed the histamine- induced permeability rat mesenteric microvascular permeability *in vivo* and thrombin induced HUVEC (human vascular endothelial cells) permeability *in vitro* (*162*). The study also shows the inhibition of PDE4 inhibits LPS induced leukocyte endothelial interaction *in vivo*. Thus it would be interesting to test the effect of the dual PDE4/8 inhibitor on bEnd.3 cells.

6.1.1 PDE8A protein expression in brain endothelial cells

Since we used mouse brain ECs – bEnd.3 cells in our *in vitro* flow chamber motility assays, we assessed the effect of PDE8 and PDE8A-Raf-1 kinase complex on ERK signaling. We first analyzed expression of PDE8A in bEnd.3 cells and found 2 PDE8A transcripts robustly expressed in bEnd.3 cells with or without LPS stimulation (Fig. 6.1). The molecular weights of the transcripts were approximately 93 kDa and 88 kDa suggesting that they represent PDE8A1 and PDE8A2 splice variants.

6.1.2 Effect of PDE8 inhibition and disruption of the PDE8A-Raf-1 complex in brain endothelial cells

Next, we stimulated bEnd.3 cells with LPS for 18 h followed by treatment with PF-04957325 or disruptor peptide or RKIP inhibitor locostatin for 1 h western blot (Fig. 6.2A). There was a slight increase in ERK1/2 phosphorylation after treatment with PF-04957325. Treatment with disruptor peptide for 1 h did not show any effect on ERK1/2 phosphorylation (Fig 6.2B). This is preliminary data presented from one experiment. More experiments need to be done to test the effect on Raf-1 and ERK signaling pathway. Also, we need to test the effect of PDE8 and PDE8A-Raf-1 kinase on vascular permeability by analyzing expression of vascular adhesion molecules (ICAM-1, VCAM-1) and tight junction proteins (claudin-5) in endothelial cells by western blot and flow cytometry.

6.2 Exploring PDE8A expression in human samples

Recent studies have identified PDE8 as an important drug target in autoimmune, neurodegenerative disorders and cancer. PDE8A1 transcripts have been shown to be altered and elevated in systemic lupus erythematosus (SLE) (*163*). PDE8A expression is elevated in breast cancer patient tissue and highly recurrent AKAP13-PDE8A fusion transcripts have been observed in colorectal cancer patient samples and cell lines (*164*). In addition, PDE8B expression is increased in alzheimer disease brains (*165*).

In a collaborative blinded study using de-identified PBMC samples from MS patients at the Department of Neurology, Ohio State University (Lab of Dr. Lovett-Racke), we have analyzed PDE8A expression in PBMCs samples from MS patients (experiment performed by Dr. Hongli Dong). PDE8A is robustly expressed in these human PBMC samples (Fig. 6.3).

In order to look at PDE8A expression in other immune cell populations, we have also analyzed PDE8A expression in de-identified human B cell samples from Department of Internal Medicine-Rheumatology at University of Michigan Medical School (Lab of Dr. Steven Lundy). PDE8A is expressed in the human B cell samples (Fig. 6.4). Our goal is to test whether there is variation in PDE8 expression in patients with different forms of MS and in other autoimmune disorders. Further we want to test whether treating human $CD4^+$ T cells as well other immune cells with PF-04957325 and dual PDE4/8 inhibitor has an effect on motility of cells. We need to obtain $CD4^+$ T cells isolated from patients and healthy donors and treat them *in vitro* with the PDE8 enzymatic inhibitor and dual PDE4/8 inhibitor and test the effect on motility of the cells while interacting with HUVECs (human vascular endothelial cells) under shear flow conditions.

6.3 Combined treatment with PDE8 and PDE4 inhibitors

A previous study from the Beavo lab has shown that PDE4 and PDE8 act in conjunction to regulate cAMP pools that control testosterone production (*166*). This is an interesting concept put forward by Beavo and colleagues who suggested that cAMP dependent processes in Leydig cells may be regulated by signaling microdomains that include PDE4 and 8. Therefore, dual inhibition of PDE4 and 8 might be a suitable means to treat pathologies caused by defects in steroidogenesis and this may also apply to pro-inflammatory T cell functions (*166, 167*).

Demirbas D et al. discovered a dual PDE4/8 inhibitor BC8-15 using yeast high throughput screening assay (*97*). BC8-15 inhibits PDE8A and PDE4A with an IC_{50} of 0.28 μM and 0.22 μM respectively. They also identified two structural derivatives: 1] BC8-15A which has reduced potency against both PDE4 and PDE8 (IC_{50} 1.59 μM for both PDE8A and PDE4A) and 2] BC8-15C has reduced potency against PDE8A (59.32 μM) while retaining activity against PDE4A (IC_{50} 0.13 μM). They further tested effect of BC8-15 treatment testosterone production in leydig cells. They found that treatment with the dual PDE4/8 inhibitor leads to a more elevation of testosterone release from leydig cells compared to treatment with rolipram alone. Thus we need to test the effect of the dual PDE4/8 inhibitor on motility of activated $CD4^+$ T cells under flow. PF-04957325 treatment in EAE has a small effect on clinical suppression of disease and immune cell infiltration into the CNS (Basole C et al., unpublished). Testing the dual PDE4/8 inhibitor might be a better treatment option since PDE4 inhibitors lead to amelioration of disease and suppression of inflammatory cytokines in the EAE model (*28*).

Figure 6.1

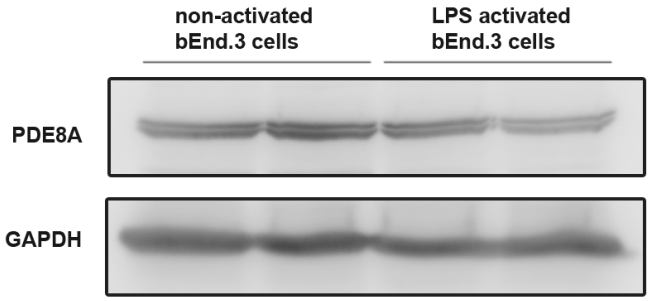

Figure 6.1: PDE8A expression in un-stimulated and LPS stimulated bEnd.3 cells. bEnd.3 cells activated with LPS (1.25 µg/ml) for 18 h. Cell lysates were then probed with PDE8A and GAPDH by western blot.

Figure 6.2

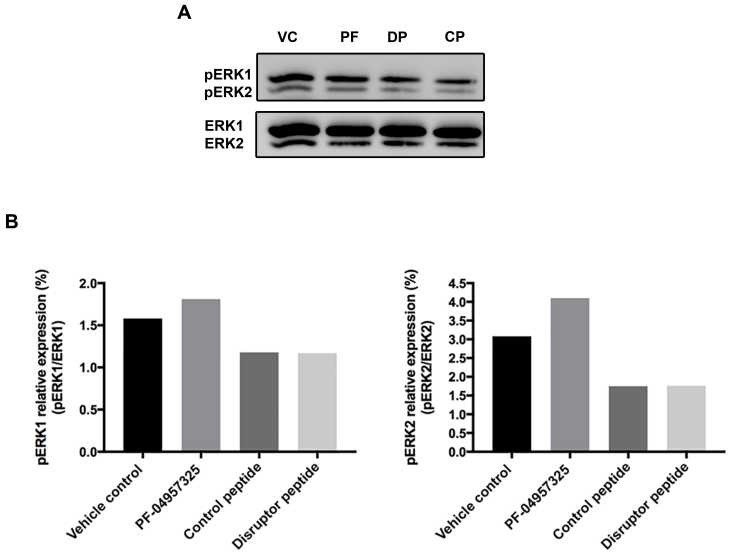

Fig 6.2. Effect of the PDE8 inhibitor and disruptor peptide on LPS activated brain endothelial cells.

(A) bEnd.3 cells activated with LPS (1.25 µg/ml) for 18 h followed by treatment with Vehicle control (VC)/ 1 µM PF-04957325 (PF) for 1 h or 10 µM control peptide (CP)/ disruptor peptide (DP) for 1 h. Cell lysates were then probed for phospho ERK1/2, ERK1/2 by Western blot. (B) Graph shows the level of phospho-ERK1/2 relative to ERK1/2.

Figure 6.3A

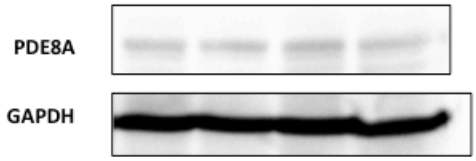

Figure 6.3 PDE8A expression in human PBMCs samples from MS patients

Cell lysates were probed with PDE8A and GAPDH by western blot. (Experiment performed by Dr. Hongli Dong.)

Figure 6.4

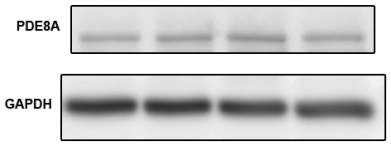

Figure 6.4 PDE8A expression in human B cell samples

Cell lysates were probed with PDE8A and GAPDH by western blot. (Experiment performed by Rebecca Nguyen.)

Chapter 7

References

1. K. Ley, C. Laudanna, M. I. Cybulsky, S. Nourshargh, Getting to the site of inflammation: the leukocyte adhesion cascade updated. *Nat Rev Immunol* **7**, 678-689 (2007).
2. P. Sundd, E. Gutierrez, E. K. Koltsova, Y. Kuwano, S. Fukuda, M. K. Pospieszalska, A. Groisman, K. Ley, 'Slings' enable neutrophil rolling at high shear. *Nature* **488**, 399-403 (2012).
3. R. Shamri, V. Grabovsky, J. M. Gauguet, S. Feigelson, E. Manevich, W. Kolanus, M. K. Robinson, D. E. Staunton, U. H. von Andrian, R. Alon, Lymphocyte arrest requires instantaneous induction of an extended LFA-1 conformation mediated by endothelium-bound chemokines. *Nat Immunol* **6**, 497-506 (2005).
4. F. Moazzam, F. A. DeLano, B. W. Zweifach, G. W. Schmid-Schonbein, The leukocyte response to fluid stress. *Proc Natl Acad Sci U S A* **94**, 5338-5343 (1997).
5. S. Nourshargh, R. Alon, Leukocyte migration into inflamed tissues. *Immunity* **41**, 694-707 (2014).
6. V. Grabovsky, S. Feigelson, C. Chen, D. A. Bleijs, A. Peled, G. Cinamon, F. Baleux, F. Arenzana-Seisdedos, T. Lapidot, Y. van Kooyk, R. R. Lobb, R. Alon, Subsecond induction of alpha4 integrin clustering by immobilized chemokines stimulates leukocyte tethering and rolling on endothelial vascular cell adhesion molecule 1 under flow conditions. *J Exp Med* **192**, 495-506 (2000).
7. Z. Shulman, V. Shinder, E. Klein, V. Grabovsky, O. Yeger, E. Geron, A. Montresor, M. Bolomini-Vittori, S. W. Feigelson, T. Kirchhausen, C. Laudanna, G. Shakhar, R. Alon, Lymphocyte crawling and transendothelial migration require chemokine triggering of high-affinity LFA-1 integrin. *Immunity* **30**, 384-396 (2009).
8. W. A. Muller, Mechanisms of leukocyte transendothelial migration. *Annu Rev Pathol* **6**, 323-344 (2011).
9. G. Cinamon, V. Shinder, R. Alon, Shear forces promote lymphocyte migration across vascular endothelium bearing apical chemokines. *Nat Immunol* **2**, 515-522 (2001).
10. S. Brocke, C. Piercy, L. Steinman, I. L. Weissman, T. Veromaa, Antibodies to CD44 and integrin alpha4, but not L-selectin, prevent central nervous system inflammation and experimental encephalomyelitis by blocking secondary leukocyte recruitment. *Proc Natl Acad Sci U S A* **96**, 6896-6901 (1999).
11. T. A. Yednock, C. Cannon, L. C. Fritz, F. Sanchez-Madrid, L. Steinman, N. Karin, Prevention of experimental autoimmune encephalomyelitis by antibodies against alpha 4 beta 1 integrin. *Nature* **356**, 63-66 (1992).
12. O. Stuve, B. C. Kieseier, B. Hemmer, H. P. Hartung, A. Awad, E. M. Frohman, B. M. Greenberg, M. K. Racke, S. S. Zamvil, J. T. Phillips, R. Gold, A. Chan, U. Zettl, R. Milo, E. Marder, O. Khan, T. N. Eagar, Translational research in neurology and neuroscience 2010: multiple sclerosis. *Arch Neurol* **67**, 1307-1315 (2010).

13. D. H. Miller, O. A. Khan, W. A. Sheremata, L. D. Blumhardt, G. P. Rice, M. A. Libonati, A. J. Willmer-Hulme, C. M. Dalton, K. A. Miszkiel, P. W. O'Connor, A controlled trial of natalizumab for relapsing multiple sclerosis. *N Engl J Med* **348**, 15-23 (2003).
14. S. Huang, S. Apasov, M. Koshiba, M. Sitkovsky, Role of A2a extracellular adenosine receptor-mediated signaling in adenosine-mediated inhibition of T-cell activation and expansion. *Blood* **90**, 1600-1610 (1997).
15. L. Li, C. Yee, J. A. Beavo, CD3- and CD28-dependent induction of PDE7 required for T cell activation. *Science* **283**, 848-851 (1999).
16. D. Peter, S. L. Jin, M. Conti, A. Hatzelmann, C. Zitt, Differential expression and function of phosphodiesterase 4 (PDE4) subtypes in human primary CD4+ T cells: predominant role of PDE4D. *J Immunol* **178**, 4820-4831 (2007).
17. J. F. Kinsel, M. V. Sitkovsky, Possible targeting of G protein coupled receptors to manipulate inflammation in vivo using synthetic and natural ligands. *Annals of the rheumatic diseases* **62 Suppl 2**, ii22-24 (2003).
18. M. V. Sitkovsky, A. Ohta, The 'danger' sensors that STOP the immune response: the A2 adenosine receptors? *Trends Immunol* **26**, 299-304 (2005).
19. G. S. Baillie, Compartmentalized signalling: spatial regulation of cAMP by the action of compartmentalized phosphodiesterases. *Febs J* **276**, 1790-1799 (2009).
20. G. S. Baillie, J. D. Scott, M. D. Houslay, Compartmentalisation of phosphodiesterases and protein kinase A: opposites attract. *FEBS letters* **579**, 3264-3270 (2005).
21. A. Lerner, P. M. Epstein, Cyclic nucleotide phosphodiesterases as targets for treatment of haematological malignancies. *Biochem J* **393**, 21-41 (2006).
22. P. M. Epstein, J. S. Mills, E. M. Hersh, S. J. Strada, W. J. Thompson, Activation of cyclic nucleotide phosphodiesterase from isolated human peripheral blood lymphocytes by mitogenic agents. *Cancer Res* **40**, 379-386 (1980).
23. N. A. Glavas, C. Ostenson, J. B. Schaefer, V. Vasta, J. A. Beavo, T cell activation up-regulates cyclic nucleotide phosphodiesterases 8A1 and 7A3. *Proc Natl Acad Sci U S A* **98**, 6319-6324 (2001).
24. A. G. Vang, S. Z. Ben-Sasson, H. Dong, B. Kream, M. P. DeNinno, M. M. Claffey, W. Housley, R. B. Clark, P. M. Epstein, S. Brocke, PDE8 regulates rapid Teff cell adhesion and proliferation independent of ICER. *PLoS One* **5**, e12011 (2010).
25. J. Seybold, R. Newton, L. Wright, P. A. Finney, N. Suttorp, P. J. Barnes, I. M. Adcock, M. A. Giembycz, Induction of phosphodiesterases 3B, 4A4, 4D1, 4D2, and 4D3 in Jurkat T-cells and in human peripheral blood T-lymphocytes by 8-bromo-cAMP and Gs-coupled receptor agonists. Potential role in beta2-adrenoreceptor desensitization. *J Biol Chem* **273**, 20575-20588 (1998).
26. B. Bielekova, A. Lincoln, H. McFarland, R. Martin, Therapeutic potential of phosphodiesterase-4 and -3 inhibitors in Th1-mediated autoimmune diseases. *J Immunol* **164**, 1117-1124 (2000).
27. N. Sommer, P. A. Loschmann, G. H. Northoff, M. Weller, A. Steinbrecher, J. P. Steinbach, R. Lichtenfels, R. Meyermann, A. Riethmuller, A. Fontana, et al., The

antidepressant rolipram suppresses cytokine production and prevents autoimmune encephalomyelitis. *Nat Med* **1**, 244-248 (1995).
28. N. Sommer, R. Martin, H. F. McFarland, L. Quigley, B. Cannella, C. S. Raine, D. E. Scott, P. A. Loschmann, M. K. Racke, Therapeutic potential of phosphodiesterase type 4 inhibition in chronic autoimmune demyelinating disease. *J Neuroimmunol* **79**, 54-61 (1997).
29. S. J. Smith, L. B. Cieslinski, R. Newton, L. E. Donnelly, P. S. Fenwick, A. G. Nicholson, P. J. Barnes, M. S. Barnette, M. A. Giembycz, Discovery of BRL 50481 [3-(N,N-dimethylsulfonamido)-4-methyl-nitrobenzene], a selective inhibitor of phosphodiesterase 7: in vitro studies in human monocytes, lung macrophages, and CD8+ T-lymphocytes. *Molecular pharmacology* **66**, 1679-1689 (2004).
30. G. Yang, K. W. McIntyre, R. M. Townsend, H. H. Shen, W. J. Pitts, J. H. Dodd, S. G. Nadler, M. McKinnon, A. J. Watson, Phosphodiesterase 7A-deficient mice have functional T cells. *J Immunol* **171**, 6414-6420 (2003).
31. A. Nakata, K. Ogawa, T. Sasaki, N. Koyama, K. Wada, J. Kotera, H. Kikkawa, K. Omori, O. Kaminuma, Potential role of phosphodiesterase 7 in human T cell function: comparative effects of two phosphodiesterase inhibitors. *Clin Exp Immunol* **128**, 460-466 (2002).
32. H. Dong, V. Osmanova, P. M. Epstein, S. Brocke, Phosphodiesterase 8 (PDE8) regulates chemotaxis of activated lymphocytes. *Biochem Biophys Res Commun* **345**, 713-719 (2006).
33. H. Dong, K. P. Claffey, S. Brocke, P. M. Epstein, Inhibition of breast cancer cell migration by activation of cAMP signaling. *Breast Cancer Res Treat* **152**, 17-28 (2015).
34. D. A. Fisher, J. F. Smith, J. S. Pillar, S. H. St Denis, J. B. Cheng, Isolation and characterization of PDE8A, a novel human cAMP-specific phosphodiesterase. *Biochem Biophys Res Commun* **246**, 570-577 (1998).
35. M. Conti, J. Beavo, Biochemistry and physiology of cyclic nucleotide phosphodiesterases: essential components in cyclic nucleotide signaling. *Annu Rev Biochem* **76**, 481-511 (2007).
36. S. H. Francis, I. V. Turko, J. D. Corbin, Cyclic nucleotide phosphodiesterases: relating structure and function. *Prog Nucleic Acid Res Mol Biol* **65**, 1-52 (2001).
37. B. Bielekova, N. Richert, T. Howard, A. N. Packer, G. Blevins, J. Ohayon, H. F. McFarland, C. S. Sturzebecher, R. Martin, Treatment with the phosphodiesterase type-4 inhibitor rolipram fails to inhibit blood--brain barrier disruption in multiple sclerosis. *Mult Scler* **15**, 1206-1214 (2009).
38. S. H. Soderling, S. J. Bayuga, J. A. Beavo, Cloning and characterization of a cAMP-specific cyclic nucleotide phosphodiesterase. *Proc Natl Acad Sci U S A* **95**, 8991-8996 (1998).
39. M. Hayashi, K. Matsushima, H. Ohashi, H. Tsunoda, S. Murase, Y. Kawarada, T. Tanaka, Molecular cloning and characterization of human PDE8B, a novel thyroid-specific isozyme of 3',5'-cyclic nucleotide phosphodiesterase. *Biochem Biophys Res Commun* **250**, 751-756 (1998).
40. P. Wang, P. Wu, R. W. Egan, M. M. Billah, Human phosphodiesterase 8A splice variants: cloning, gene organization, and tissue distribution. *Gene* **280**, 183-194 (2001).

41. M. Gamanuma, K. Yuasa, T. Sasaki, N. Sakurai, J. Kotera, K. Omori, Comparison of enzymatic characterization and gene organization of cyclic nucleotide phosphodiesterase 8 family in humans. *Cell Signal* **15**, 565-574 (2003).
42. P. Wu, P. Wang, Per-Arnt-Sim domain-dependent association of cAMP-phosphodiesterase 8A1 with IkappaB proteins. *Proc Natl Acad Sci U S A* **101**, 17634-17639 (2004).
43. K. M. Brown, L. C. Lee, J. E. Findlay, J. P. Day, G. S. Baillie, Cyclic AMP-specific phosphodiesterase, PDE8A1, is activated by protein kinase A-mediated phosphorylation. *FEBS letters* **586**, 1631-1637 (2012).
44. M. A. Giembycz, C. J. Corrigan, J. Seybold, R. Newton, P. J. Barnes, Identification of cyclic AMP phosphodiesterases 3, 4 and 7 in human CD4+ and CD8+ T-lymphocytes: role in regulating proliferation and the biosynthesis of interleukin-2. *Br J Pharmacol* **118**, 1945-1958 (1996).
45. B. Serrels, E. Sandilands, A. Serrels, G. Baillie, M. D. Houslay, V. G. Brunton, M. Canel, L. M. Machesky, K. I. Anderson, M. C. Frame, A complex between FAK, RACK1, and PDE4D5 controls spreading initiation and cancer cell polarity. *Curr Biol* **20**, 1086-1092 (2010).
46. K. M. Brown, J. P. Day, E. Huston, B. Zimmermann, K. Hampel, F. Christian, D. Romano, S. Terhzaz, L. C. Lee, M. J. Willis, D. B. Morton, J. A. Beavo, M. Shimizu-Albergine, S. A. Davies, W. Kolch, M. D. Houslay, G. S. Baillie, Phosphodiesterase-8A binds to and regulates Raf-1 kinase. *Proc Natl Acad Sci U S A* **110**, E1533-1542 (2013).
47. J. W. Ramos, The regulation of extracellular signal-regulated kinase (ERK) in mammalian cells. *Int J Biochem Cell Biol* **40**, 2707-2719 (2008).
48. R. L. Klemke, S. Cai, A. L. Giannini, P. J. Gallagher, P. de Lanerolle, D. A. Cheresh, Regulation of cell motility by mitogen-activated protein kinase. *J Cell Biol* **137**, 481-492 (1997).
49. E. Viala, J. Pouyssegur, Regulation of tumor cell motility by ERK mitogen-activated protein kinases. *Ann N Y Acad Sci* **1030**, 208-218 (2004).
50. M. D. Houslay, G. S. Baillie, The role of ERK2 docking and phosphorylation of PDE4 cAMP phosphodiesterase isoforms in mediating cross-talk between the cAMP and ERK signalling pathways. *Biochem Soc Trans* **31**, 1186-1190 (2003).
51. A. S. Dhillon, C. Pollock, H. Steen, P. E. Shaw, H. Mischak, W. Kolch, Cyclic AMP-dependent kinase regulates Raf-1 kinase mainly by phosphorylation of serine 259. *Mol Cell Biol* **22**, 3237-3246 (2002).
52. P. M. Epstein, R. Hachisu, Cyclic nucleotide phosphodiesterase in normal and leukemic human lymphocytes and lymphoblasts. *Adv Cyclic Nucleotide Protein Phosphorylation Res* **16**, 303-324 (1984).
53. H. Dong, C. Zitt, C. Auriga, A. Hatzelmann, P. M. Epstein, Inhibition of PDE3, PDE4 and PDE7 potentiates glucocorticoid-induced apoptosis and overcomes glucocorticoid resistance in CEM T leukemic cells. *Biochem Pharmacol* **79**, 321-329 (2010).
54. A. Hatzelmann, E. J. Morcillo, G. Lungarella, S. Adnot, S. Sanjar, R. Beume, C. Schudt, H. Tenor, The preclinical pharmacology of roflumilast--a selective, oral

phosphodiesterase 4 inhibitor in development for chronic obstructive pulmonary disease. *Pulm Pharmacol Ther* **23**, 235-256 (2010).
55. O. FitzGerald, Spondyloarthropathies: Apremilast: welcome advance in treatment of psoriatic arthritis. *Nature reviews. Rheumatology*, (2014).
56. M. C. Genovese, K. Jarosova, D. Cieslak, J. Alper, A. Kivitz, D. R. Hough, P. Maes, L. Pineda, M. Chen, F. Zaidi, Apremilast in patients with active rheumatoid arthritis: A phase II, multicenter, randomized, double-blind, placebo-controlled, parallel-group study. *Arthritis & rheumatology*, (2015).
57. A. Kavanaugh, P. J. Mease, J. J. Gomez-Reino, A. O. Adebajo, J. Wollenhaupt, D. D. Gladman, E. Lespessailles, S. Hall, M. Hochfeld, C. Hu, D. Hough, R. M. Stevens, G. Schett, Treatment of psoriatic arthritis in a phase 3 randomised, placebo-controlled trial with apremilast, an oral phosphodiesterase 4 inhibitor. *Annals of the rheumatic diseases* **73**, 1020-1026 (2014).
58. A. C. Palfreeman, K. E. McNamee, F. E. McCann, New developments in the management of psoriasis and psoriatic arthritis: a focus on apremilast. *Drug design, development and therapy* **7**, 201-210 (2013).
59. R. M. Poole, A. D. Ballantyne, Apremilast: first global approval. *Drugs* **74**, 825-837 (2014).
60. P. Schafer, Apremilast mechanism of action and application to psoriasis and psoriatic arthritis. *Biochem Pharmacol* **83**, 1583-1590 (2012).
61. P. H. Schafer, A. Parton, L. Capone, D. Cedzik, H. Brady, J. F. Evans, H. W. Man, G. W. Muller, D. I. Stirling, R. Chopra, Apremilast is a selective PDE4 inhibitor with regulatory effects on innate immunity. *Cell Signal* **26**, 2016-2029 (2014).
62. G. Schett, V. S. Sloan, R. M. Stevens, P. Schafer, Apremilast: a novel PDE4 inhibitor in the treatment of autoimmune and inflammatory diseases. *Therapeutic advances in musculoskeletal disease* **2**, 271-278 (2010).
63. G. Schett, J. Wollenhaupt, K. Papp, R. Joos, J. F. Rodrigues, A. R. Vessey, C. Hu, R. Stevens, K. L. de Vlam, Oral apremilast in the treatment of active psoriatic arthritis: results of a multicenter, randomized, double-blind, placebo-controlled study. *Arthritis and rheumatism* **64**, 3156-3167 (2012).
64. Z. D. Draelos, L. F. Stein Gold, D. F. Murrell, M. H. Hughes, L. T. Zane, Post Hoc Analyses of the Effect of Crisaborole Topical Ointment, 2% on Atopic Dermatitis: Associated Pruritus from Phase 1 and 2 Clinical Studies. *J Drugs Dermatol* **15**, 172-176 (2016).
65. K. Jarnagin, S. Chanda, D. Coronado, V. Ciaravino, L. T. Zane, E. Guttman-Yassky, M. G. Lebwohl, Crisaborole Topical Ointment, 2%: A Nonsteroidal, Topical, Anti-Inflammatory Phosphodiesterase 4 Inhibitor in Clinical Development for the Treatment of Atopic Dermatitis. *J Drugs Dermatol* **15**, 390-396 (2016).
66. A. S. Paller, W. L. Tom, M. G. Lebwohl, R. L. Blumenthal, M. Boguniewicz, R. S. Call, L. F. Eichenfield, D. W. Forsha, W. C. Rees, E. L. Simpson, M. C. Spellman, L. F. Stein Gold, A. L. Zaenglein, M. H. Hughes, L. T. Zane, A. A. Hebert, Efficacy and safety of crisaborole ointment, a novel, nonsteroidal phosphodiesterase 4 (PDE4) inhibitor for the topical treatment of atopic dermatitis (AD) in children and adults. *J Am Acad Dermatol* **75**, 494-503 e494 (2016).

67. L. F. Stein Gold, L. Spelman, M. C. Spellman, M. H. Hughes, L. T. Zane, A Phase 2, Randomized, Controlled, Dose-Ranging Study Evaluating Crisaborole Topical Ointment, 0.5% and 2% in Adolescents With Mild to Moderate Atopic Dermatitis. *J Drugs Dermatol* **14**, 1394-1399 (2015).
68. W. L. Tom, M. Van Syoc, S. Chanda, L. T. Zane, Pharmacokinetic Profile, Safety, and Tolerability of Crisaborole Topical Ointment, 2% in Adolescents with Atopic Dermatitis: An Open-Label Phase 2a Study. *Pediatr Dermatol* **33**, 150-159 (2016).
69. L. T. Zane, S. Chanda, K. Jarnagin, D. B. Nelson, L. Spelman, L. S. Gold, Crisaborole and its potential role in treating atopic dermatitis: overview of early clinical studies. *Immunotherapy* **8**, 853-866 (2016).
70. L. T. Zane, M. H. Hughes, S. Shakib, Tolerability of Crisaborole Ointment for Application on Sensitive Skin Areas: A Randomized, Double-Blind, Vehicle-Controlled Study in Healthy Volunteers. *Am J Clin Dermatol* **17**, 519-526 (2016).
71. E. Bettelli, Y. Carrier, W. Gao, T. Korn, T. B. Strom, M. Oukka, H. L. Weiner, V. K. Kuchroo, Reciprocal developmental pathways for the generation of pathogenic effector TH17 and regulatory T cells. *Nature* **441**, 235-238 (2006).
72. W. Bruck, R. Gold, B. T. Lund, C. Oreja-Guevara, A. Prat, C. M. Spencer, L. Steinman, M. Tintore, T. L. Vollmer, M. S. Weber, L. P. Weiner, T. Ziemssen, S. S. Zamvil, Therapeutic Decisions in Multiple Sclerosis: Moving Beyond Efficacy. *JAMA Neurol*, (2013).
73. H. F. McFarland, R. Martin, Multiple sclerosis: a complicated picture of autoimmunity. *Nat Immunol* **8**, 913-919 (2007).
74. B. Rossi, S. Angiari, E. Zenaro, S. L. Budui, G. Constantin, Vascular inflammation in central nervous system diseases: adhesion receptors controlling leukocyte-endothelial interactions. *J Leukoc Biol* **89**, 539-556 (2011).
75. L. Steinman, S. S. Zamvil, Virtues and pitfalls of EAE for the development of therapies for multiple sclerosis. *Trends Immunol* **26**, 565-571 (2005).
76. M. Rangachari, V. K. Kuchroo, Using EAE to better understand principles of immune function and autoimmune pathology. *J Autoimmun* **45**, 31-39 (2013).
77. H. R. Bourne, L. M. Lichtenstein, K. L. Melmon, C. S. Henney, Y. Weinstein, G. M. Shearer, Modulation of inflammation and immunity by cyclic AMP. *Science* **184**, 19-28 (1974).
78. A. T. Bender, J. A. Beavo, Cyclic nucleotide phosphodiesterases: molecular regulation to clinical use. *Pharmacol Rev* **58**, 488-520 (2006).
79. A. G. Vang, W. Housley, H. Dong, C. Basole, S. Z. Ben-Sasson, B. E. Kream, P. M. Epstein, R. B. Clark, S. Brocke, Regulatory T-cells and cAMP suppress effector T-cells independently of PKA-CREM/ICER: a potential role for Epac. *Biochem J* **456**, 463-473 (2013).
80. M. Almahariq, F. C. Mei, H. Wang, A. T. Cao, S. Yao, L. Soong, J. Sun, Y. Cong, J. Chen, X. Cheng, Exchange protein directly activated by cAMP modulates regulatory T-cell-mediated immunosuppression. *Biochem J* **465**, 295-303 (2015).
81. M. D. Houslay, Underpinning compartmentalised cAMP signalling through targeted cAMP breakdown. *Trends Biochem Sci* **35**, 91-100 (2010).

82. O. Lomas, M. Zaccolo, Phosphodiesterases maintain signaling fidelity via compartmentalization of cyclic nucleotides. *Physiology (Bethesda)* **29**, 141-149 (2014).
83. M. Conti, D. Mika, W. Richter, Cyclic AMP compartments and signaling specificity: role of cyclic nucleotide phosphodiesterases. *J Gen Physiol* **143**, 29-38 (2014).
84. S. H. Francis, M. A. Blount, J. D. Corbin, Mammalian cyclic nucleotide phosphodiesterases: molecular mechanisms and physiological functions. *Physiol Rev* **91**, 651-690 (2011).
85. D. H. Maurice, H. Ke, F. Ahmad, Y. Wang, J. Chung, V. C. Manganiello, Advances in targeting cyclic nucleotide phosphodiesterases. *Nat Rev Drug Discov* **13**, 290-314 (2014).
86. F. Ahmad, T. Murata, K. Shimizu, E. Degerman, D. Maurice, V. Manganiello, Cyclic nucleotide phosphodiesterases: important signaling modulators and therapeutic targets. *Oral Dis* **21**, e25-50 (2015).
87. M. F. Azevedo, F. R. Faucz, E. Bimpaki, A. Horvath, I. Levy, R. B. de Alexandre, F. Ahmad, V. Manganiello, C. A. Stratakis, Clinical and molecular genetics of the phosphodiesterases (PDEs). *Endocr Rev* **35**, 195-233 (2014).
88. A. Castro, M. J. Jerez, C. Gil, A. Martinez, Cyclic nucleotide phosphodiesterases and their role in immunomodulatory responses: advances in the development of specific phosphodiesterase inhibitors. *Med Res Rev* **25**, 229-244 (2005).
89. C. Burnouf, M. P. Pruniaux, Recent advances in PDE4 inhibitors as immunoregulators and anti-inflammatory drugs. *Curr Pharm Des* **8**, 1255-1296 (2002).
90. J. E. Souness, D. Aldous, C. Sargent, Immunosuppressive and anti-inflammatory effects of cyclic AMP phosphodiesterase (PDE) type 4 inhibitors. *Immunopharmacology* **47**, 127-162 (2000).
91. A. Martinez, C. Gil, cAMP-specific phosphodiesterase inhibitors: promising drugs for inflammatory and neurological diseases. *Expert opinion on therapeutic patents* **24**, 1311-1321 (2014).
92. M. A. Giembycz, Can the anti-inflammatory potential of PDE4 inhibitors be realized: guarded optimism or wishful thinking? *Br J Pharmacol*, (2008).
93. D. Spina, PDE4 inhibitors: current status. *Br J Pharmacol*, (2008).
94. H. Tenor, A. Hatzelmann, R. Beume, G. Lahu, K. Zech, T. D. Bethke, Pharmacology, clinical efficacy, and tolerability of phosphodiesterase-4 inhibitors: impact of human pharmacokinetics. *Handbook of experimental pharmacology*, 85-119 (2011).
95. L. C. Tsai, M. Shimizu-Albergine, J. A. Beavo, The high-affinity cAMP-specific phosphodiesterase 8B controls steroidogenesis in the mouse adrenal gland. *Molecular pharmacology* **79**, 639-648 (2011).
96. L. C. Tsai, J. A. Beavo, Regulation of adrenal steroidogenesis by the high-affinity phosphodiesterase 8 family. *Hormone and metabolic research = Hormon- und Stoffwechselforschung = Hormones et metabolisme* **44**, 790-794 (2012).
97. D. Demirbas, A. R. Wyman, M. Shimizu-Albergine, O. Cakici, J. A. Beavo, C. S. Hoffman, A yeast-based chemical screen identifies a PDE inhibitor that elevates

steroidogenesis in mouse Leydig cells via PDE8 and PDE4 inhibition. *PLoS One* **8**, e71279 (2013).
98. W. F. t. Carson, L. A. Guernsey, A. Singh, A. T. Vella, C. M. Schramm, R. S. Thrall, Accumulation of regulatory T cells in local draining lymph nodes of the lung correlates with spontaneous resolution of chronic asthma in a murine model. *International archives of allergy and immunology* **145**, 231-243 (2008).
99. V. Preller, A. Gerber, S. Wrenger, M. Togni, D. Marguet, J. Tadje, U. Lendeckel, C. Rocken, J. Faust, K. Neubert, B. Schraven, R. Martin, S. Ansorge, S. Brocke, D. Reinhold, TGF-beta1-mediated control of central nervous system inflammation and autoimmunity through the inhibitory receptor CD26. *J Immunol* **178**, 4632-4640 (2007).
100. S. Brocke, L. Quigley, H. F. McFarland, L. Steinman, Isolation and Characterization of Autoreactive T Cells in Experimental Autoimmune Encephalomyelitis of the Mouse. *Methods* **9**, 458-462 (1996).
101. D. Ekholm, B. Hemmer, G. Gao, M. Vergelli, R. Martin, V. Manganiello, Differential expression of cyclic nucleotide phosphodiesterase 3 and 4 activities in human T cell clones specific for myelin basic protein. *J Immunol* **159**, 1520-1529 (1997).
102. C. Lugnier, Cyclic nucleotide phosphodiesterase (PDE) superfamily: a new target for the development of specific therapeutic agents. *Pharmacol Ther* **109**, 366-398 (2006).
103. S. B. Zhuplatov, T. Masaki, D. K. Blumenthal, A. K. Cheung, Mechanism of dipyridamole's action in inhibition of venous and arterial smooth muscle cell proliferation. *Basic Clin Pharmacol Toxicol* **99**, 431-439 (2006).
104. V. Vasta, in *Cyclic Nucleotide Phosphodiesterases in Health and Disease,* J. A. Beavo, S. H. Francis, M. D. Houslay, Eds. (CRC press, New York, NY, 2007), pp. 205-219.
105. W. S. Brown, J. S. Khalili, T. G. Rodriguez-Cruz, G. Lizee, B. W. McIntyre, B-Raf regulation of integrin alpha4beta1-mediated resistance to shear stress through changes in cell spreading and cytoskeletal association in T cells. *J Biol Chem* **289**, 23141-23153 (2014).
106. L. Steinman, Multiple sclerosis: a coordinated immunological attack against myelin in the central nervous system. *Cell* **85**, 299-302 (1996).
107. M. L. Ford, T. M. Onami, A. I. Sperling, R. Ahmed, B. D. Evavold, CD43 modulates severity and onset of experimental autoimmune encephalomyelitis. *J Immunol* **171**, 6527-6533 (2003).
108. M. Li, R. M. Ransohoff, Multiple roles of chemokine CXCL12 in the central nervous system: a migration from immunology to neurobiology. *Prog Neurobiol* **84**, 116-131 (2008).
109. R. M. Ransohoff, Natalizumab for multiple sclerosis. *N Engl J Med* **356**, 2622-2629 (2007).
110. L. Steinman, Immune therapy for autoimmune diseases. *Science* **305**, 212-216 (2004).
111. A. Singh, R. S. Thrall, L. A. Guernsey, W. F. t. Carson, E. R. Secor, Jr., R. E. Cone, T. V. Rajan, C. M. Schramm, Subcutaneous late phase responses are

augmented during local inhalational tolerance in a murine asthma model. *Immunol Cell Biol* **86**, 535-538 (2008).
112. D. Reinhold, A. Biton, S. Pieper, U. Lendeckel, J. Faust, K. Neubert, U. Bank, M. Tager, S. Ansorge, S. Brocke, Dipeptidyl peptidase IV (DP IV, CD26) and aminopeptidase N (APN, CD13) as regulators of T cell function and targets of immunotherapy in CNS inflammation. *Int Immunopharmacol* **6**, 1935-1942 (2006).
113. C. M. Schramm, L. Puddington, C. Wu, L. Guernsey, M. Gharaee-Kermani, S. H. Phan, R. S. Thrall, Chronic inhaled ovalbumin exposure induces antigen-dependent but not antigen-specific inhalational tolerance in a murine model of allergic airway disease. *Am J Pathol* **164**, 295-304 (2004).
114. C. A. Yiamouyiannis, C. M. Schramm, L. Puddington, P. Stengel, E. Baradaran-Hosseini, W. W. Wolyniec, H. E. Whiteley, R. S. Thrall, Shifts in lung lymphocyte profiles correlate with the sequential development of acute allergic and chronic tolerant stages in a murine asthma model. *Am J Pathol* **154**, 1911-1921 (1999).
115. J. A. Ledbetter, M. Parsons, P. J. Martin, J. A. Hansen, P. S. Rabinovitch, C. H. June, Antibody binding to CD5 (Tp67) and Tp44 T cell surface molecules: effects on cyclic nucleotides, cytoplasmic free calcium, and cAMP-mediated suppression. *J Immunol* **137**, 3299-3305 (1986).
116. B. S. Skalhegg, B. F. Landmark, S. O. Doskeland, V. Hansson, T. Lea, T. Jahnsen, Cyclic AMP-dependent protein kinase type I mediates the inhibitory effects of 3',5'-cyclic adenosine monophosphate on cell replication in human T lymphocytes. *J Biol Chem* **267**, 15707-15714 (1992).
117. S. Yoon, R. Seger, The extracellular signal-regulated kinase: multiple substrates regulate diverse cellular functions. *Growth Factors* **24**, 21-44 (2006).
118. S. Vallabhapurapu, M. Karin, Regulation and function of NF-kappaB transcription factors in the immune system. *Annu Rev Immunol* **27**, 693-733 (2009).
119. L. Chang, M. Karin, Mammalian MAP kinase signalling cascades. *Nature* **410**, 37-40 (2001).
120. M. Cargnello, P. P. Roux, Activation and function of the MAPKs and their substrates, the MAPK-activated protein kinases. *Microbiol Mol Biol Rev* **75**, 50-83 (2011).
121. I. Merida, E. Andrada, S. I. Gharbi, A. Avila-Flores, Redundant and specialized roles for diacylglycerol kinases alpha and zeta in the control of T cell functions. *Sci Signal* **8**, re6 (2015).
122. H. Lavoie, M. Therrien, Regulation of RAF protein kinases in ERK signalling. *Nat Rev Mol Cell Biol* **16**, 281-298 (2015).
123. N. Dumaz, R. Marais, Protein kinase A blocks Raf-1 activity by stimulating 14-3-3 binding and blocking Raf-1 interaction with Ras. *J Biol Chem* **278**, 29819-29823 (2003).
124. A. S. Dhillon, W. Kolch, Untying the regulation of the Raf-1 kinase. *Arch Biochem Biophys* **404**, 3-9 (2002).
125. D. H. Maurice, PDE8A runs interference to limit PKA inhibition of Raf-1. *Proc Natl Acad Sci U S A* **110**, 6248-6249 (2013).
126. A. G. Vang, C. Basole, H. Dong, R. K. Nguyen, W. Housley, L. Guernsey, A. J. Adami, R. S. Thrall, R. B. Clark, P. M. Epstein, S. Brocke, Differential Expression

and Function of PDE8 and PDE4 in Effector T cells: Implications for PDE8 as a Drug Target in Inflammation. *Frontiers in Pharmacology* **7**, (2016).
127. H. Wang, Z. Yan, S. Yang, J. Cai, H. Robinson, H. Ke, Kinetic and structural studies of phosphodiesterase-8A and implication on the inhibitor selectivity. *Biochemistry* **47**, 12760-12768 (2008).
128. M. A. Gavin, J. P. Rasmussen, J. D. Fontenot, V. Vasta, V. C. Manganiello, J. A. Beavo, A. Y. Rudensky, Foxp3-dependent programme of regulatory T-cell differentiation. *Nature* **445**, 771-775 (2007).
129. E. Maganto-Garcia, D. X. Bu, M. L. Tarrio, P. Alcaide, G. Newton, G. K. Griffin, K. J. Croce, F. W. Luscinskas, A. H. Lichtman, N. Grabie, Foxp3+-inducible regulatory T cells suppress endothelial activation and leukocyte recruitment. *J Immunol* **187**, 3521-3529 (2011).
130. E. Manevich-Mendelson, S. W. Feigelson, R. Pasvolsky, M. Aker, V. Grabovsky, Z. Shulman, S. S. Kilic, M. A. Rosenthal-Allieri, S. Ben-Dor, A. Mory, A. Bernard, M. Moser, A. Etzioni, R. Alon, Loss of Kindlin-3 in LAD-III eliminates LFA-1 but not VLA-4 adhesiveness developed under shear flow conditions. *Blood* **114**, 2344-2353 (2009).
131. L. Steinman, The discovery of natalizumab, a potent therapeutic for multiple sclerosis. *J Cell Biol* **199**, 413-416 (2012).
132. R. Lee, S. Wolda, E. Moon, J. Esselstyn, C. Hertel, A. Lerner, PDE7A is expressed in human B-lymphocytes and is up-regulated by elevation of intracellular cAMP. *Cell Signal* **14**, 277-284 (2002).
133. E. Moon, R. Lee, R. Near, L. Weintraub, S. Wolda, A. Lerner, Inhibition of PDE3B augments PDE4 inhibitor-induced apoptosis in a subset of patients with chronic lymphocytic leukemia. *Clin Cancer Res* **8**, 589-595 (2002).
134. R. L. Kortum, A. K. Rouquette-Jazdanian, L. E. Samelson, Ras and extracellular signal-regulated kinase signaling in thymocytes and T cells. *Trends Immunol* **34**, 259-268 (2013).
135. A. G. Vang, W. Housley, H. Dong, C. Basole, S. Z. Ben-Sasson, B. E. Kream, P. M. Epstein, R. B. Clark, S. Brocke, Regulatory T cells and cAMP suppress effector T cells independently of PKA-CREM/ICER: a potential role for Epac. *Biochem J*, (2013).
136. H. Abrahamsen, G. Baillie, J. Ngai, T. Vang, K. Nika, A. Ruppelt, T. Mustelin, M. Zaccolo, M. Houslay, K. Tasken, TCR- and CD28-mediated recruitment of phosphodiesterase 4 to lipid rafts potentiates TCR signaling. *J Immunol* **173**, 4847-4858 (2004).
137. S. Yun, M. Budatha, J. E. Dahlman, B. G. Coon, R. T. Cameron, R. Langer, D. G. Anderson, G. Baillie, M. A. Schwartz, Interaction between integrin alpha5 and PDE4D regulates endothelial inflammatory signalling. *Nat Cell Biol* **18**, 1043-1053 (2016).
138. S. W. Feigelson, R. Pasvolsky, S. Cemerski, Z. Shulman, V. Grabovsky, T. Ilani, A. Sagiv, F. Lemaitre, C. Laudanna, A. S. Shaw, R. Alon, Occupancy of lymphocyte LFA-1 by surface-immobilized ICAM-1 is critical for TCR- but not for chemokine-triggered LFA-1 conversion to an open headpiece high-affinity state. *J Immunol* **185**, 7394-7404 (2010).

139. Z. Shulman, R. Alon, Chapter 14. Real-time in vitro assays for studying the role of chemokines in lymphocyte transendothelial migration under physiologic flow conditions. *Methods Enzymol* **461**, 311-332 (2009).
140. R. M. Klein, L. S. Spofford, E. V. Abel, A. Ortiz, A. E. Aplin, B-RAF regulation of Rnd3 participates in actin cytoskeletal and focal adhesion organization. *Mol Biol Cell* **19**, 498-508 (2008).
141. K. Ehrenreiter, D. Piazzolla, V. Velamoor, I. Sobczak, J. V. Small, J. Takeda, T. Leung, M. Baccarini, Raf-1 regulates Rho signaling and cell migration. *J Cell Biol* **168**, 955-964 (2005).
142. R. Marais, Y. Light, H. F. Paterson, C. S. Mason, C. J. Marshall, Differential regulation of Raf-1, A-Raf, and B-Raf by oncogenic ras and tyrosine kinases. *J Biol Chem* **272**, 4378-4383 (1997).
143. C. K. Weber, J. R. Slupsky, C. Herrmann, M. Schuler, U. R. Rapp, C. Block, Mitogenic signaling of Ras is regulated by differential interaction with Raf isozymes. *Oncogene* **19**, 169-176 (2000).
144. C. A. Pritchard, L. Hayes, L. Wojnowski, A. Zimmer, R. M. Marais, J. C. Norman, B-Raf acts via the ROCKII/LIMK/cofilin pathway to maintain actin stress fibers in fibroblasts. *Mol Cell Biol* **24**, 5937-5952 (2004).
145. C. A. Pritchard, M. L. Samuels, E. Bosch, M. McMahon, Conditionally oncogenic forms of the A-Raf and B-Raf protein kinases display different biological and biochemical properties in NIH 3T3 cells. *Mol Cell Biol* **15**, 6430-6442 (1995).
146. L. Wojnowski, L. F. Stancato, A. C. Larner, U. R. Rapp, A. Zimmer, Overlapping and specific functions of Braf and Craf-1 proto-oncogenes during mouse embryogenesis. *Mech Dev* **91**, 97-104 (2000).
147. A. Norambuena, C. Metz, L. Vicuna, A. Silva, E. Pardo, C. Oyanadel, L. Massardo, A. Gonzalez, A. Soza, Galectin-8 induces apoptosis in Jurkat T cells by phosphatidic acid-mediated ERK1/2 activation supported by protein kinase A down-regulation. *J Biol Chem* **284**, 12670-12679 (2009).
148. T. Korn, J. Reddy, W. Gao, E. Bettelli, A. Awasthi, T. R. Petersen, B. T. Backstrom, R. A. Sobel, K. W. Wucherpfennig, T. B. Strom, M. Oukka, V. K. Kuchroo, Myelin-specific regulatory T cells accumulate in the CNS but fail to control autoimmune inflammation. *Nat Med* **13**, 423-431 (2007).
149. S. W. Feigelson, V. Grabovsky, E. Manevich-Mendelson, R. Pasvolsky, Z. Shulman, V. Shinder, E. Klein, A. Etzioni, M. Aker, R. Alon, Kindlin-3 is required for the stabilization of TCR-stimulated LFA-1:ICAM-1 bonds critical for lymphocyte arrest and spreading on dendritic cells. *Blood* **117**, 7042-7052 (2011).
150. T. Wang, J. R. Sheppard, J. E. Foker, Rise and fall of cyclic AMP required for onset of lymphocyte DNA synthesis. *Science* **201**, 155-157 (1978).
151. S. Sloka, L. M. Metz, W. Hader, Y. Starreveld, V. W. Yong, Reduction of microglial activity in a model of multiple sclerosis by dipyridamole. *J Neuroinflammation* **10**, 89 (2013).
152. L. T. Zane, L. Kircik, R. Call, E. Tschen, Z. D. Draelos, S. Chanda, M. Van Syoc, A. A. Hebert, Crisaborole Topical Ointment, 2% in Patients Ages 2 to 17 Years with Atopic Dermatitis: A Phase 1b, Open-Label, Maximal-Use Systemic Exposure Study. *Pediatr Dermatol* **33**, 380-387 (2016).

153. E. Bjorgo, K. Moltu, K. Tasken, Phosphodiesterases as targets for modulating T-cell responses. *Handbook of experimental pharmacology*, 345-363 (2011).
154. C. Warnke, T. Menge, H. P. Hartung, M. K. Racke, P. D. Cravens, J. L. Bennett, E. M. Frohman, B. M. Greenberg, S. S. Zamvil, R. Gold, B. Hemmer, B. C. Kieseier, O. Stuve, Natalizumab and progressive multifocal leukoencephalopathy: what are the causal factors and can it be avoided? *Arch Neurol* **67**, 923-930 (2010).
155. T. Bopp, N. Dehzad, S. Reuter, M. Klein, N. Ullrich, M. Stassen, H. Schild, R. Buhl, E. Schmitt, C. Taube, Inhibition of cAMP degradation improves regulatory T cell-mediated suppression. *J Immunol* **182**, 4017-4024 (2009).
156. A. Biton, S. Ansorge, U. Bank, M. Tager, D. Reinhold, S. Brocke, Divergent actions by inhibitors of DP IV and APN family enzymes on CD4+ Teff cell motility and functions. *Immunobiology* **216**, 1295-1301 (2011).
157. A. Steinbrecher, D. Reinhold, L. Quigley, A. Gado, N. Tresser, L. Izikson, I. Born, J. Faust, K. Neubert, R. Martin, S. Ansorge, S. Brocke, Targeting dipeptidyl peptidase IV (CD26) suppresses autoimmune encephalomyelitis and up-regulates TGF-beta 1 secretion in vivo. *J Immunol* **166**, 2041-2048 (2001).
158. R. S. Blumberg, B. Dittel, D. Hafler, M. von Herrath, F. O. Nestle, Unraveling the autoimmune translational research process layer by layer. *Nat Med* **18**, 35-41 (2012).
159. Y. Lee, A. Awasthi, N. Yosef, F. J. Quintana, S. Xiao, A. Peters, C. Wu, M. Kleinewietfeld, S. Kunder, D. A. Hafler, R. A. Sobel, A. Regev, V. K. Kuchroo, Induction and molecular signature of pathogenic TH17 cells. *Nat Immunol* **13**, 991-999 (2012).
160. F. C. Nichols, W. J. Housley, C. A. O'Conor, T. Manning, S. Wu, R. B. Clark, Unique lipids from a common human bacterium represent a new class of Toll-like receptor 2 ligands capable of enhancing autoimmunity. *Am J Pathol* **175**, 2430-2438 (2009).
161. W. J. Housley, C. O. Adams, F. C. Nichols, L. Puddington, E. G. Lingenheld, L. Zhu, T. V. Rajan, R. B. Clark, Natural but not inducible regulatory T cells require TNF-alpha signaling for in vivo function. *J Immunol* **186**, 6779-6787 (2011).
162. M. J. Sanz, J. Cortijo, M. A. Taha, M. Cerda-Nicolas, E. Schatton, B. Burgbacher, J. Klar, H. Tenor, C. Schudt, A. C. Issekutz, A. Hatzelmann, E. J. Morcillo, Roflumilast inhibits leukocyte-endothelial cell interactions, expression of adhesion molecules and microvascular permeability. *Br J Pharmacol* **152**, 481-492 (2007).
163. R. J. Orlowski, K. S. O'Rourke, I. Olorenshaw, G. A. Hawkins, S. Maas, D. Laxminarayana, Altered editing in cyclic nucleotide phosphodiesterase 8A1 gene transcripts of systemic lupus erythematosus T lymphocytes. *Immunology* **125**, 408-419 (2008).
164. T. Nome, G. O. Thomassen, J. Bruun, T. Ahlquist, A. C. Bakken, A. M. Hoff, T. Rognum, A. Nesbakken, S. Lorenz, J. Sun, J. D. Barros-Silva, G. E. Lind, O. Myklebost, M. R. Teixeira, L. A. Meza-Zepeda, R. A. Lothe, R. I. Skotheim, Common fusion transcripts identified in colorectal cancer cell lines by high-throughput RNA sequencing. *Transl Oncol* **6**, 546-553 (2013).

165. S. Perez-Torres, R. Cortes, M. Tolnay, A. Probst, J. M. Palacios, G. Mengod, Alterations on phosphodiesterase type 7 and 8 isozyme mRNA expression in Alzheimer's disease brains examined by in situ hybridization. *Exp Neurol* **182**, 322-334 (2003).
166. M. Shimizu-Albergine, L. C. Tsai, E. Patrucco, J. A. Beavo, cAMP-specific phosphodiesterases 8A and 8B, essential regulators of Leydig cell steroidogenesis. *Molecular pharmacology* **81**, 556-566 (2012).
167. M. Golkowski, M. Shimizu-Albergine, H. W. Suh, J. A. Beavo, S. E. Ong, Studying mechanisms of cAMP and cyclic nucleotide phosphodiesterase signaling in Leydig cell function with phosphoproteomics. *Cell Signal* **28**, 764-778 (2016).